



Post-Flight Characterization of Samples for the MISSE–7 Spacesuit Fabric Exposure Experiment

*James R. Gaier, Deborah L. Waters, and Donald A. Jaworske
Glenn Research Center, Cleveland, Ohio*

*Terry R. McCue
Arctic Slope Research Corporation, Cleveland, Ohio*

*Angela Folz and Sammantha Baldwin
Glenn Research Center, Cleveland, Ohio*

*Gregory W. Clark, Brittany Batman, and John Bruce
Manchester College, North Manchester, Indiana*

NASA STI Program . . . in Profile

Since its founding, NASA has been dedicated to the advancement of aeronautics and space science. The NASA Scientific and Technical Information (STI) program plays a key part in helping NASA maintain this important role.

The NASA STI Program operates under the auspices of the Agency Chief Information Officer. It collects, organizes, provides for archiving, and disseminates NASA's STI. The NASA STI program provides access to the NASA Aeronautics and Space Database and its public interface, the NASA Technical Reports Server, thus providing one of the largest collections of aeronautical and space science STI in the world. Results are published in both non-NASA channels and by NASA in the NASA STI Report Series, which includes the following report types:

- **TECHNICAL PUBLICATION.** Reports of completed research or a major significant phase of research that present the results of NASA programs and include extensive data or theoretical analysis. Includes compilations of significant scientific and technical data and information deemed to be of continuing reference value. NASA counterpart of peer-reviewed formal professional papers but has less stringent limitations on manuscript length and extent of graphic presentations.
- **TECHNICAL MEMORANDUM.** Scientific and technical findings that are preliminary or of specialized interest, e.g., quick release reports, working papers, and bibliographies that contain minimal annotation. Does not contain extensive analysis.
- **CONTRACTOR REPORT.** Scientific and technical findings by NASA-sponsored contractors and grantees.

- **CONFERENCE PUBLICATION.** Collected papers from scientific and technical conferences, symposia, seminars, or other meetings sponsored or cosponsored by NASA.
- **SPECIAL PUBLICATION.** Scientific, technical, or historical information from NASA programs, projects, and missions, often concerned with subjects having substantial public interest.
- **TECHNICAL TRANSLATION.** English-language translations of foreign scientific and technical material pertinent to NASA's mission.

Specialized services also include creating custom thesauri, building customized databases, organizing and publishing research results.

For more information about the NASA STI program, see the following:

- Access the NASA STI program home page at <http://www.sti.nasa.gov>
- E-mail your question to help@sti.nasa.gov
- Fax your question to the NASA STI Information Desk at 443-757-5803
- Phone the NASA STI Information Desk at 443-757-5802
- Write to:
STI Information Desk
NASA Center for AeroSpace Information
7115 Standard Drive
Hanover, MD 21076-1320



Post-Flight Characterization of Samples for the MISSE-7 Spacesuit Fabric Exposure Experiment

*James R. Gaier, Deborah L. Waters, and Donald A. Jaworske
Glenn Research Center, Cleveland, Ohio*

*Terry R. McCue
Arctic Slope Research Corporation, Cleveland, Ohio*

*Angela Folz and Sammantha Baldwin
Glenn Research Center, Cleveland, Ohio*

*Gregory W. Clark, Brittany Batman, and John Bruce
Manchester College, North Manchester, Indiana*

National Aeronautics and
Space Administration

Glenn Research Center
Cleveland, Ohio 44135

Acknowledgments

This work is the result of a great deal of effort by a sizable team of dedicated professionals from many organizations, all of whom the author would like to thank. Samples were provided by M.A.B. Meador of the NASA Glenn Research Center (GRC), J. J. Kosmo of the NASA Johnson Space Center, and J. Ware of ILC Dover. E.A. Sechkar (Arctic Slope Regional Corporation) and F.P. Lam (Jacobs Sverdrup) provided engineering and fabrication for the flight and analysis hardware. Financial support was provided by the Exploration Technology Development Program's Dust Mitigation Project (M.J. Hyatt, GRC).

Trade names and trademarks are used in this report for identification only. Their usage does not constitute an official endorsement, either expressed or implied, by the National Aeronautics and Space Administration.

Level of Review: This material has been technically reviewed by technical management.

Available from

NASA Center for Aerospace Information
7115 Standard Drive
Hanover, MD 21076-1320

National Technical Information Service
5301 Shawnee Road
Alexandria, VA 22312

Available electronically at <http://www.sti.nasa.gov>

Contents

Abstract.....	1
Nomenclature.....	1
1.0 Introduction.....	2
2.0 Methods and Materials.....	4
2.1 Materials.....	4
2.2 Photography and Microscopy.....	5
2.3 Total Reflectance Spectroscopy.....	5
2.4 Mechanical Properties.....	6
3.0 Results and Discussion.....	7
3.1 Survey Photography.....	7
3.2 Microscopic Imaging.....	10
3.2.1 Pristine FEP Fabric.....	10
3.2.2 Dust Abraded FEP Fabric.....	12
3.2.3 Alan Bean Apollo FEP Fabric.....	12
3.2.4 Pristine Ortho-Fabric.....	14
3.2.5 Abraded Ortho-Fabric.....	14
3.2.6 Twice Abraded Ortho-Fabric.....	15
3.3 Energy Dispersive X-Ray Spectroscopy (EDS).....	15
3.4 Total Reflectance Spectroscopy.....	15
3.5 Tensile Test.....	19
4.0 Conclusions.....	20
Appendix A.—Post-Flight Pristine Apollo Fabric.....	21
A.1 B1f-1.....	21
A.1.1 Optical Microscopy.....	21
A.1.2 Electron Microscopy.....	21
A.1.3 Atomic Force Microscopy.....	22
A.2 B1f-2.....	22
A.2.1 Optical Microscopy.....	22
A.2.2 Electron Microscopy.....	22
A.2.3 Atomic Force Microscopy.....	23
A.3 B1f-3.....	23
A.3.1 Optical Microscopy.....	23
A.3.2 Electron Microscopy.....	23
A.4 B1f-4.....	24
A.4.1 Optical Microscopy.....	24
A.4.2 Electron Microscopy.....	24
A.5 B1f-5.....	24
A.5.1 Optical Microscopy.....	24
A.5.2 Electron Microscopy.....	24
A.5.3 Atomic Force Microscopy.....	25
A.6 B1f-6.....	25
A.6.1 Electron Microscopy.....	25
Appendix B.—Post-Flight Abraded Apollo Fabric.....	27
B.1 BA1f-1.....	27
B.1.1 Optical Microscopy.....	27
B.1.2 Electron Microscopy.....	27
B.2 BA1f-2.....	28
B.2.1 Optical Microscopy.....	28
B.2.2 Electron Microscopy.....	28

B.3	BA1f-3	28
	B.3.1 Optical Microscopy.....	28
	B.3.2 Electron Microscopy.....	29
B.4	BA1f-4	29
	B.4.1 Optical Microscopy.....	29
	B.4.2 Electron Microscopy.....	29
B.5	BA1f-5	29
	B.5.1 Optical Microscopy.....	29
	B.5.2 Electron Microscopy.....	30
B.6	BA1f-6 (Edge Under Holder)	30
	B.6.1 Electron Microscopy.....	30
B.7	BA1f-7 (Streak—Upper Left).....	30
	B.7.1 Electron Microscopy.....	30
B.8	BA1f-8 (Streak—Lower Right)	31
	B.8.1 Electron Microscopy.....	31
Appendix C.—Post-Flight Alan Bean Apollo 12 Fabric		33
C.1	AB1f-1	33
	C.1.1 Optical Microscopy.....	33
	C.1.2 Electron Microscopy.....	33
C.2	AB1f-2	35
	C.2.1 Optical Microscopy.....	35
	C.2.2 Electron Microscopy.....	35
C.3	AB1f-3	35
	C.3.1 Optical Microscopy.....	35
	C.3.2 Electron Microscopy.....	35
C.4	AB1f-4	36
	C.4.1 Optical Microscopy.....	36
	C.4.2 Electron Microscopy.....	36
C.5	AB1f-5	36
	C.5.1 Optical Microscopy.....	36
	C.5.2 Electron Microscopy.....	36
C.6	AB1f-6 (Edge Under Holder)	37
	C.6.1 Electron Microscopy.....	37
Appendix D.—Post-Flight Pristine Ortho-Fabric		39
D.1	O1f-1	39
	D.1.1 Optical Microscopy.....	39
	D.1.2 Electron Microscopy.....	39
	D.1.3 Atomic Force Microscopy	40
D.2	O1f-2	40
	D.2.1 Optical Microscopy.....	40
	D.2.2 Electron Microscopy.....	40
D.3	O1f-3	41
	D.3.1 Optical Microscopy.....	41
	D.3.2 Electron Microscopy.....	41
D.4	O1f-4	41
	D.4.1 Optical Microscopy.....	41
	D.4.2 Electron Microscopy.....	41
	D.4.3 Atomic Force Microscopy	42
D.5	O1f-5	42
	D.5.1 Optical Microscopy.....	42
	D.5.2 Electron Microscopy.....	42

D.6	O1f-6 (Edge Under Holder).....	42
	D.6.1 Electron Microscopy.....	42
Appendix E.—	Post-Flight Abraded Ortho-Fabric	45
E.1	OA1f-1	45
	E.1.1 Optical Microscopy.....	45
	E.1.2 Electron Microscopy.....	45
	E.1.3 Atomic Force Microscopy	47
E.2	OA1f-2	48
	E.2.1 Optical Microscopy.....	48
	E.2.2 Electron Microscopy.....	48
	E.2.3 Atomic Force Microscopy	48
E.3	OA1f-3	48
	E.3.1 Optical Microscopy.....	48
	E.3.2 Electron Microscopy.....	49
E.4	OA1f-4	49
	E.4.1 Optical Microscopy.....	49
	E.4.2 Electron Microscopy.....	49
	E.4.3 Atomic Force Microscopy	50
E.5	OA1f-5	50
	E.5.1 Optical Microscopy.....	50
	E.5.2 Electron Microscopy.....	50
	E.5.3 Atomic Force Microscopy	51
E.6	OA1f-6 (Edge Under Holder).....	51
	E.6.1 Electron Microscopy.....	51
Appendix F.—	Post-Flight Doubly Abraded Ortho-Fabric	53
F.1	OAA1f-1	53
	F.1.1 Optical Microscopy.....	53
	F.1.2 Electron Microscopy.....	53
	F.1.3 Atomic Force Microscopy	54
F.2	OAA1f-2	55
	F.2.1 Optical Microscopy.....	55
	F.2.2 Electron Microscopy.....	55
	F.2.3 Atomic Force Microscopy	56
F.3	OAA1f-3	57
	F.3.1 Optical Microscopy.....	57
	F.3.2 Electron Microscopy.....	57
F.4	OAA1f-4	57
	F.4.1 Optical Microscopy.....	57
	F.4.2 Electron Microscopy.....	57
F.5	OAA1f-5	58
	F.5.1 Optical Microscopy.....	58
	F.5.2 Electron Microscopy.....	58
F.6	OAA1f-6 (Edge Under Holder)	58
	F.6.1 Electron Microscopy.....	58
References.....		59

Post-Flight Characterization of Samples for the MISSE-7 Spacesuit Fabric Exposure Experiment

James R. Gaier, Deborah L. Waters, and Donald A. Jaworske
National Aeronautics and Space Administration
Glenn Research Center
Cleveland, Ohio 44135

Terry R. McCue
Arctic Slope Research Corporation
Cleveland, Ohio 44135

Angela Folz* and Sammantha Baldwin*
National Aeronautics and Space Administration
Glenn Research Center
Cleveland, Ohio 44135

Gregory W. Clark, Brittany Batman, and John Bruce
Manchester College
North Manchester, Indiana 46962

Abstract

Six samples of pristine and dust-abraded outer layer spacesuit fabrics were included in the Materials International Space Station Experiment-7, in which they were exposed to the wake side low Earth orbit environment (LEO) on the International Space Station (ISS) for 18 months in order to determine whether abrasion by lunar dust increases radiation degradation. The fabric samples were characterized using optical microscopy, field emission scanning electron microscopy, and tensile testing before and after exposure on the ISS. Comparison of pre- and post-flight characterizations showed that wake side LEO environment darkened and reddened all six fabrics, increasing their integrated solar absorptance by 7 to 38 percent. There was a decrease in the ultimate tensile strength and elongation to failure of lunar dust abraded Apollo spacesuit fibers by a factor of four and increased the elastic modulus by a factor of two. The severity of the degradation of the fabric samples over this short exposure time demonstrates the necessity to find ways to prevent or mitigate radiation damage to spacesuits when planning extended missions to the Moon.

Nomenclature

AFM	atomic force microscope
AO	atomic oxygen
AlFEP	vapor-deposited aluminum backed FEP film
EDS	Energy-Dispersive X-ray Spectroscopy
EM	electromagnetic
FEP	fluorinated ethylene propylene
FESEM	Field Emission Scanning Electron Microscopy
ISS	International Space Station
JSC-1A	lunar simulant
LEO	low Earth orbit

*Undergraduate Student Research Program

MISSE	Materials International Space Station Experiment
PEC	Passive Experiment Container
PGA	pressure garment assembly
PTFE	polytetrafluoroethylene
UV	ultraviolet
α	integrated solar absorptance
$\alpha(\lambda)$	wavelength-dependent absorptivity
λ	wavelength
$\rho(\lambda)$	wavelength-dependent total reflectivity

1.0 Introduction

During the Apollo missions, lunar dust was more problematic than anticipated. Post-mission documents reveal that there were difficulties with contaminated surfaces, clogged mechanisms, compromised seals, confusion of navigation equipment, degrading of radiators, irritation of eyes and lungs, and the abrasion of surfaces, including the spacesuits (Ref. 1) The Apollo astronauts were on the lunar surface for less than 24 hr, but even in this short period of time the suits showed appreciable wear. Apollo 12 astronaut Pete Conrad remarked, “*We must have had more than a hundred hours suited work with the same equipment, and the wear was not as bad on the training suits as it is on these flight suits in just the eight hours we were out.*” (Ref. 2) For example, Figure 1 shows a hole abraded through the outer layer of Harrison Schmitt’s Apollo 17 suit above the boot. If long term missions to the Moon or other extraterrestrial surfaces are going to be undertaken, the mechanisms of this degradation must be understood and mitigated.

The outer layer of both Apollo era and modern space suits is made from fluorinated ethylene propylene (FEP) or the closely related polytetrafluoroethylene (PTFE) Teflon. FEP was also used as a thermal control material on the Hubble Space Telescope. This was found to degrade with severe cracking after 6.8 years exposure to the space environment (Ref. 3). The primary cause of the degradation was concluded to have been polymer chain scission by particle and electromagnetic (EM) radiation combined with thermal cycling which facilitated a crystallization of the shorter chains, resulting in a far more brittle material (Refs. 3 and 4). Since radiation degrades primarily the surface of a material, and dust abrasion increases the surface area of a material, there is concern that abrasion may increase radiation degradation.



Figure 1.—Hole worn through the outer layer of Harrison Schmitt’s Apollo 17 space suit above the boot.

This concern about the synergistic effects of abrasion and radiation prompted the inclusion of the Spacesuit Fabrics Exposure Experiment on the Materials International Space Station Experiment-7 (MISSE-7). In this experiment, pristine and dust-abraded samples of outer layer spacesuit fabrics were flown on the wake-side PEC on the International Space Station (ISS) for approximately 18 months, from November 2009 to May 2011. They were exposed to the space radiation environment of low Earth orbit (LEO), which is similar to that of the Moon, though reduced in particle radiation because many of the solar wind ions are captured by the van Allen radiation belts, well above ISS orbit. The long-term exposure in LEO will shed light on the extent to which spacesuit fabrics will degrade in long-term exposure on the Moon, and how dust abrasion affects it.

The preparation and pre-flight characterization of the six fabric samples have been described previously (Ref. 5), and these data will be introduced as they relate to the post-flight data, which is the focus of this study.

The Spacesuit Fabric Exposure Experiment was integrated into the wake side of the ram/wake MISSE-7 Passive Experiment Container 7B (PEC-7B) at the NASA Langley Research Center. It was launched from the NASA Kennedy Space Center aboard the Space Shuttle Atlantis (STS-129) on November 16, 2009. On November 23, astronaut Randolph Bresnik removed MISSE-7 from the cargo bay and installed it on ELC-2. Figure 2 shows MISSE-7 as mounted on the ISS.

After 554 days in orbit, on May 20, 2011, astronauts Drew Feustel and Greg Chamitoff retrieved MISSE-7 and mounted it into the payload bay of Space Shuttle Endeavor. This was STS-134, the 25th and final flight of Endeavor, which returned MISSE-7 to Earth on June 1. MISSE-7 was transferred to the NASA Langley Research Center, and on July 12 the experiment was first recovered and photographed (Figure 3). De-integration occurred on July 21 and the experiment was returned to the NASA Glenn Research Center on July 26. Analysis was started almost immediately, in case reactions with air or laboratory humidity would induce further changes. No evidence of any such changes was found. All analyses were completed by mid-December 2011.

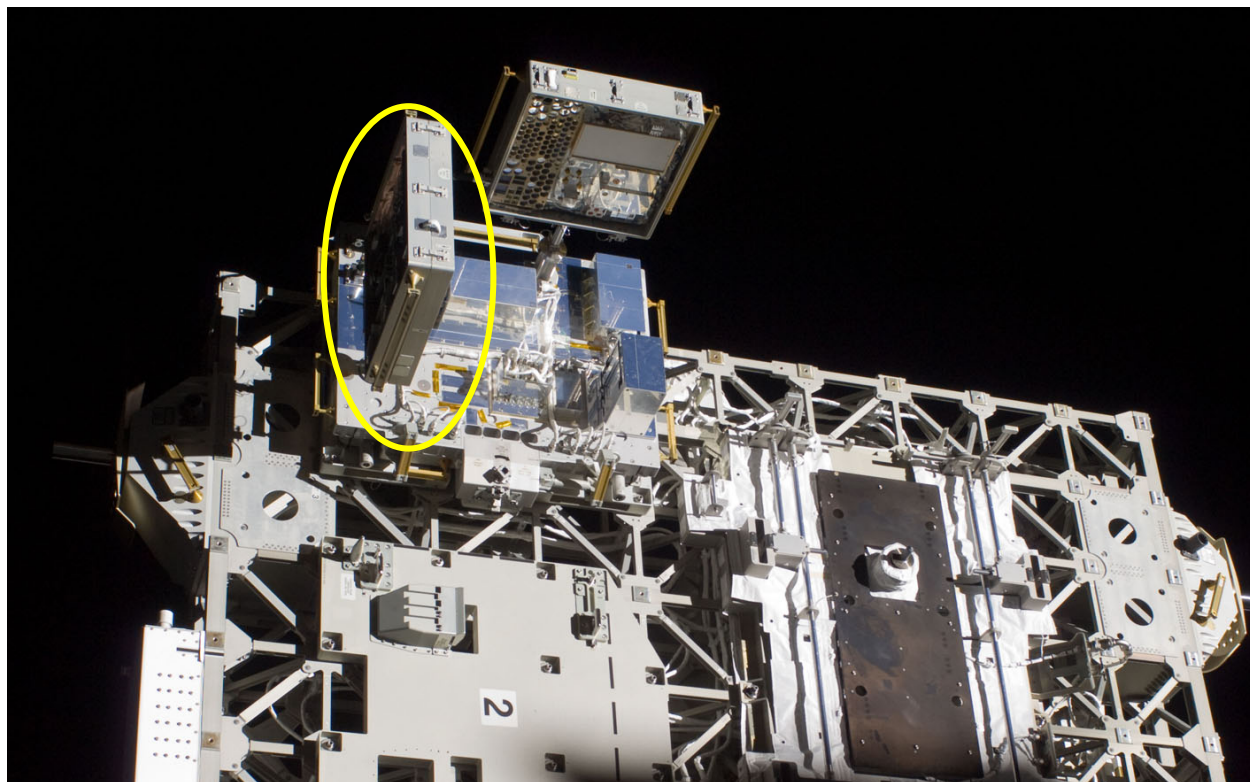


Figure 2.—MISSE-7 as mounted to ELC-2 on the ISS, with the PEC 7B circled. The direction of motion in orbit is right to left, so the wake side is on the right.

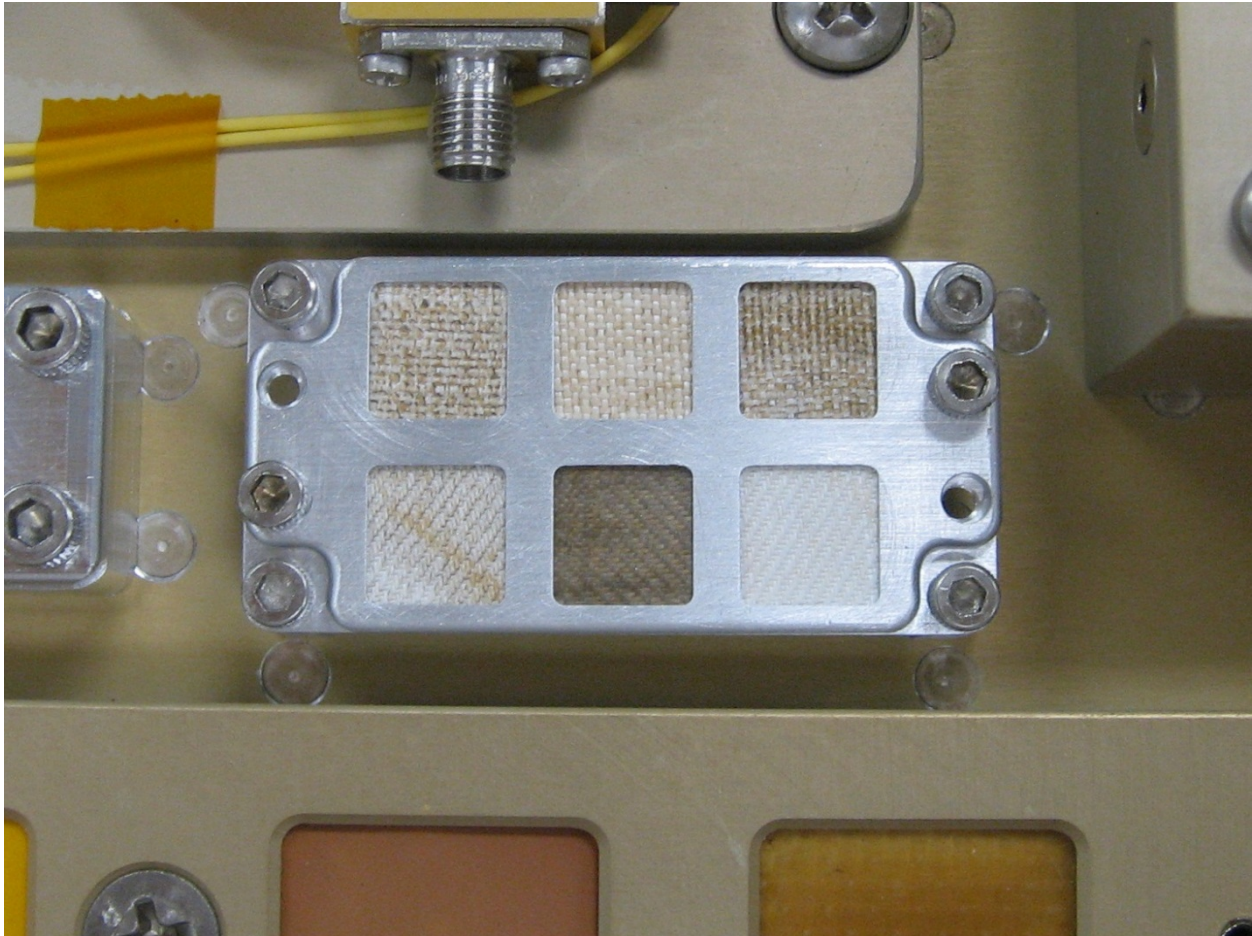


Figure 3.—The Spacesuit Fabric Exposure Experiment after recovery in the lab, before being removed from MISSE-7, showing in its local flight environment.

2.0 Methods and Materials

2.1 Materials

The MISSE-7 Spacesuit Fabrics Exposure Experiment consists of six samples of spacesuit fabric. During the Apollo program, the outer surface of the pressure garment assembly (PGA) was made of woven fluorinated ethylene-propylene (FEP) fabric. Although most of the PGAs were made with a plain-weave FEP, in some cases a twill-weave FEP was used. A small piece from the left knee region of the PGA worn on the lunar surface for 7.8 hr by Alan Bean during Apollo 12 was obtained and included in this experiment. This was one of the most heavily soiled portions of the Bean PGA. For comparison, a sample of the same twill weave FEP was flown as a control. In addition, a sample of control fabric that was ground-test abraded with the lunar soil simulant JSC-1A prior to flight was flown as well. The method of dust abrasion is detailed in the pre-flight report (Ref. 5).

PGA design has progressed since the Apollo era, and the suits worn by astronauts in their return to the Moon will probably not have an outer layer of woven FEP. The current PGAs used in Space Shuttle and International Space Station EVAs use Ortho-fabric (Fabric Development) as the outermost layer. Ortho-fabric is a two layer plain weave face tied to the back of 400 denier Gortex (W.L. Gore & Associates), 200 denier Nomex (DuPont) and 400 denier Kevlar (DuPont). The yarn count is 51×41 on the face, and 39×33 on the back. The fabric weight is 15.0 oz/yd² (0.355 kg/m²), with a thickness of 0.027 in (0.69 mm) (Ref. 6). The outer Gortex layer is made from expanded PTFE, so although the two fabric types are very

different, they both have fluorinated hydrocarbons as the outermost material. Three samples of Ortho-fabric were flown as part of the MISSE-7 Spacesuit Fabrics Exposure Experiment as well, with one being pristine (as received), a second abraded with JSC-1A to the same level as the FEP, and the third being abraded with JSC-1A for twice as long.

2.2 Photography and Microscopy

To the extent possible, all analyses were done using the same protocols that were used for the pre-flight samples. The instruments and procedures detailed in the pre-flight analysis paper for the optical microscopy, the field emission electron microscopy (FESEM) and the atomic force microscopy (AFM) were for the most part, unchanged. The one aspect that was different was the sampling areas. Whereas one of the goals of the preflight characterization was to establish the baseline structure, in the post-flight analysis changes and anomalies were the target. So in the FESEM and the AFM only two major regions were surveyed, that exposed and that shielded by the sample holder. Within those regions images were taken that were characteristic of the whole, and images of areas that appear to be anomalous.

In addition to survey photos taken of the entire sample holder such as shown in Figure 3, photographs were taken with the samples illuminated by a UV lamp. Fluorescence under UV illumination can indicate the presence of contamination or sample degradation. Energy dispersive x-ray spectroscopy (EDS) was also used to examine the samples for contamination. This was done in conjunction with the FESEM such that the elemental composition of specific microscopic areas of the samples could be determined.

2.3 Total Reflectance Spectroscopy

Optical spectroscopy was performed on the fabrics to look for signs of degradation. Of particular concern was whether the thermal properties, primarily the integrated solar absorptance, α , would increase as this would impose an additional heat load on the suit. In order to determine the α of a fabric, the wavelength-dependent absorptivity, $\alpha(\lambda)$, over the solar spectrum must be determined. This was done by measuring its wavelength-dependent reflectivity, $\rho(\lambda)$, and calculating $\alpha(\lambda)$ from conservation of energy. Each photon striking the fabric must be either absorbed, reflected, or transmitted, so if $T(\lambda)$ is the wavelength-dependent transmissivity, these three properties are related by Eq. (1):

$$\alpha(\lambda) + \rho(\lambda) + T(\lambda) = 1 \quad (1)$$

If the fabric can be considered opaque ($T = 0$), Eq. (1) can be expressed as Eq. (2):

$$\alpha(\lambda) = 1 - \rho(\lambda) \quad (2)$$

Although solar radiation will primarily impinge on the fabric directly from the solar disk, it will be reflected both specularly and diffusely, so the total $\rho(\lambda)$, including the specular and diffuse components is the quantity of interest. This was measured using a spectrophotometer equipped with an integrating sphere. The reflectance spectra reported here were collected on a Cary 5000 spectrophotometer (Varian) equipped with a DRA 2500, 150 mm diameter integrating sphere over the wavelength range of 250 to 2500 nm.

Data were collected from 250 to 2500 nm in increments of 1 nm, at a scan rate of 600 nm/min. A deuterium lamp was used to measure the 250 to 350 nm data, and a halogen lamp to measure the 350 to 2500 nm data. Immediately prior to running each sample, a spectrum of the Spectralon was collected as a sample, to determine whether the baseline was still valid. In all instances the deviations in the baseline were less than 1 percent. The integrated solar α of each sample was determined by calculating the convolution of the scaled $\rho(\lambda)$ of the simulant with the ASTM air mass zero solar spectrum E-490-00 and expressed as a fraction of the solar spectrum.

2.4 Mechanical Properties

Individual filaments from the Alan Bean sample were tensile tested to measure the ultimate tensile strength, elongation to failure, and Young's modulus of fibers. Pre- and post-flight values were compared to measure mechanical degradation. Only the Alan Bean fibers were tested because the FEP fabric used for the pristine and abraded FEP samples was constructed of thicker fibers (on the order of 300 μm in diameter, as opposed to an average of 23 μm for the Bean fibers). The Ortho-fabric outer layer PTFE fibers are much thicker (on the order of 500 μm in diameter). The protocol described below was not effective for these thicker fibers because they would slip out of the adhesive before breaking. Future testing should include developing a method to tensile test these thicker fibers.

The ASTM Standard Test Method for Tensile Strength and Young's Modulus of Fibers (Ref. 7) was used to develop the tensile test protocol. Each fiber was mounted on a 53 mm \times 15 mm tab cut from an index card. A 1/8 in. (3.1 mm) diameter hole punch was used to punch three holes in the center of the tab, as shown in Figure 4. After the tab was mounted in the instrument, the index card was cut along the dotted line such that only the fiber connected the two ends of the tab.

To obtain individual fibers, it was necessary to first separate fiber tows from the sample weave. Fiber tows were separated from the sample by gently grasping the end (to avoid touching the gauge length of the fiber and affecting the results) of an outside tow with one pair of forceps and the edge of the sample with another pair and gently pulling the tow out of the fabric weave. Individual fibers were separated from tows by grasping the end of the tow in one pair of forceps and the end of a fiber in another pair and gently pulling the fiber from the tow. The fibers were stored in a covered polystyrene Petri dish until they were adhered to tabs.

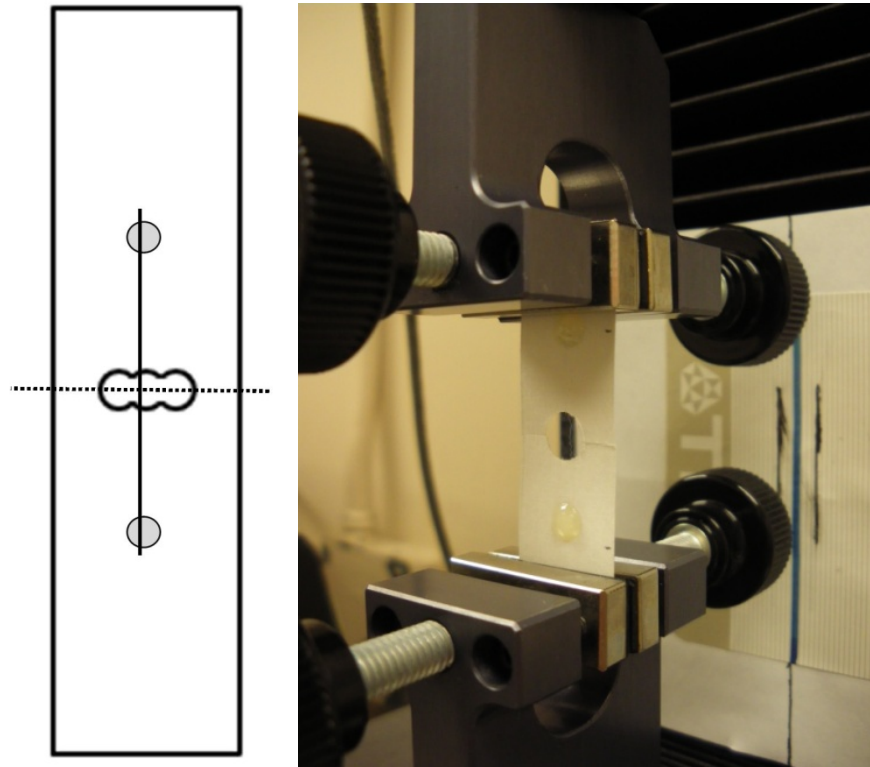


Figure 4.—Geometry of a tab and fiber mounted in adhesive (shown as grey circles) for the tensile test. After mounting the tab in the tensile tester, the tab was cut along the dotted line so that the resulting halves were connected only by the fiber.

Two tows from both the warp and the weft directions were separated from the scraps that had been cut from the Alan Bean sample prior to mounting it in the sample holder for flight. For simplicity, since the scraps were not exposed on the ISS they will be referred to as the “preflight” Alan Bean fibers. Six tows were separated from the warp direction of the post-flight Alan Bean sample: four tows that had been shielded under the sample holder (stored in covered polystyrene Petri dishes for possible future tests), and two tows that had been in the exposed area of the sample. The same number of tows were separated from the weft direction of the sample. Fibers from the exposed tows were used for tensile testing. Twenty individual preflight fibers and 20 individual post-flight fibers were adhered to tabs for tensile testing.

To adhere an individual fiber to a tab, two drops of adhesive were applied to a tab on both sides of the center hole. Both ends of a single fiber were grasped with forceps and the fiber was placed over the center hole, in the adhesive drops. Care was taken to not stretch the fiber. Then both ends of the fiber were bent and a second adhesive drop was applied over each bent fiber end. (Fiber ends were bent so the fiber would not slip out of the adhesive instead of breaking when tested.) The adhesive was left to cure for 7 days before tensile testing the fiber.

The fibers on the tabs were then imaged using a Leica MZ16 optical microscope fitted with digital image capture to note the presence of any adhesive on the gauge length of the fiber or any other irregularities. The gauge length (between the adhesive drops on both sides of the center hole) was measured.

To tensile test a fiber, the tab was mounted in a DDL Tri 200Q Universal Tensile Tester (Figure 4). Each end of the tab was grasped in the clamps, which were 1 in. apart. Then the tab was cut on both sides of the center hole, taking care not to touch the fiber.

The tensile tester was set to a start threshold of 0.01 N, end test of 266 s, and log rate of 30.10 Hz. The pre-flight Bean fibers were pulled at a test rate of 203.2 mm/min. (Tensile tests on pristine FEP fibers indicated that a slower test rate may cause the fibers to slip out of the adhesive instead of breaking.) The post-flight Bean fibers were pulled at a test rate of 12.7 mm/min because they were more brittle so at higher test rates they would break before the tensile tester could register any data. The tensile test data and the average preflight and post-flight fiber diameters (obtained from FESEM photomicrographs by averaging the diameter in 10 positions on four fibers in each category) were used to calculate the ultimate tensile strength, elongation at failure, and Young's modulus for each fiber. The mean and standard deviation of each value was calculated for preflight and post-flight fibers.

3.0 Results and Discussion

3.1 Survey Photography

Upon return of the flight samples to the NASA Glenn Research Center, they were removed from the Kapron they were bagged in and photographed. Figure 5 compares the flight samples (right) with control samples (left) that were treated identically, but not flown in space. It can be seen in the photograph that space exposure darkened the fabrics and gave them a somewhat reddish tint. This will be explored quantitatively in the spectroscopy section of the study. A dark streak was noted in the space exposed sample (d) that stretches diagonally across the abraded Apollo-era FEP fabric. There was no evidence of this streak in the preflight photographs, and study of the flight environment around this sample did not yield a potential contamination source. No additional details were revealed when the samples were illuminated by ultraviolet (UV) light (Figure 6). More discussion of the streak appears in the sections on energy dispersive spectroscopy (EDS) and visible spectroscopy.

It was noted that the silver plated stainless steel hex nuts which were below the capscrews shown in Figure 5 turned black during the experiment. This was probably due to exposure to atomic oxygen (AO) in LEO during those periods when the ISS was reoriented such that the samples were exposed to the ram facing environment.

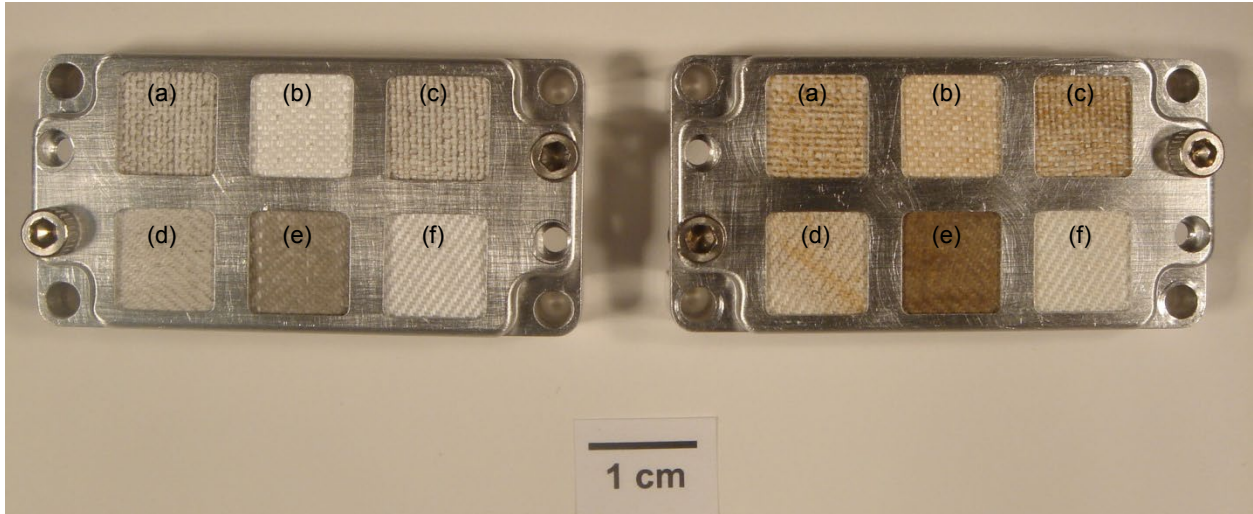


Figure 5.—Photograph of the control (left) and flown (right) MISSE-7 Spacesuit Fabric Exposure Experiment. Samples include abraded Ortho-fabric (a), pristine Ortho-fabric (b), double abraded Ortho-fabric (c), abraded Apollo era fabric (d), Alan Bean Apollo 12 fabric (e), and pristine Apollo era fabric (f).

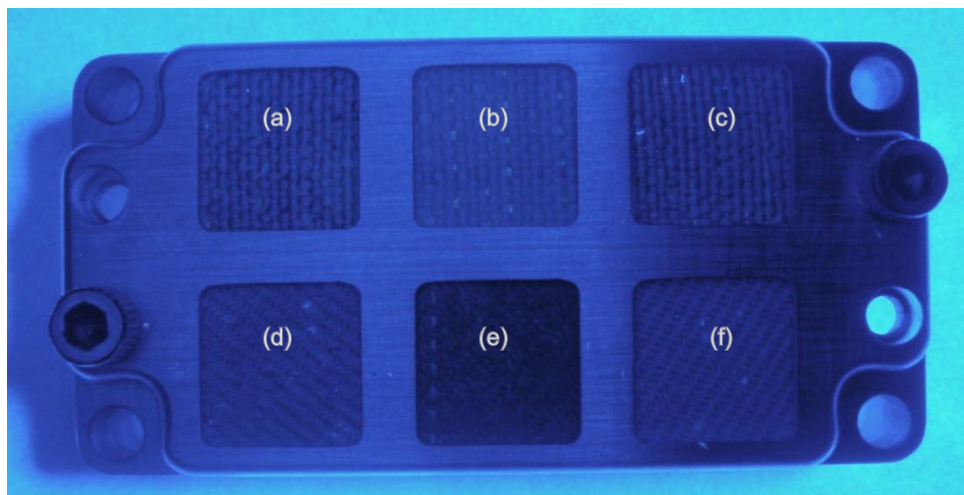


Figure 6.—Photograph of the MISSE-7 Spacesuit Fabric Exposure Experiment. Samples illuminated by ultraviolet light include abraded Ortho-fabric (a), pristine Ortho-fabric (b), double abraded Ortho-fabric (c), abraded Apollo era fabric (d), Alan Bean Apollo 12 fabric (e), and pristine Apollo era fabric (f).

After the initial photography, the flight samples were removed from the sample holder. After removing the assembly screws, the sample holder was placed face down on a Kapton surface and the base plate was removed, Figure 7(a). Then the aluminum shims were removed revealing the back of the samples, Figure 7(b). No indications of contamination were evident on the back of the samples. When the samples were removed from the flight holder, the perimeter area of the fabric that was trapped under the edge of the sample holder was readily visible in Figure 7(c). Space exposure darkened all of the samples. Each sample was immediately transferred to its own sample handler. These were the same sample handlers used in the preflight analysis, except that longer clamps were fabricated because the samples had been trimmed to fit into the flight sample holder. Figure 8 shows all six samples mounted in their sample handlers. Two unexposed edges are clearly visible for each sample.

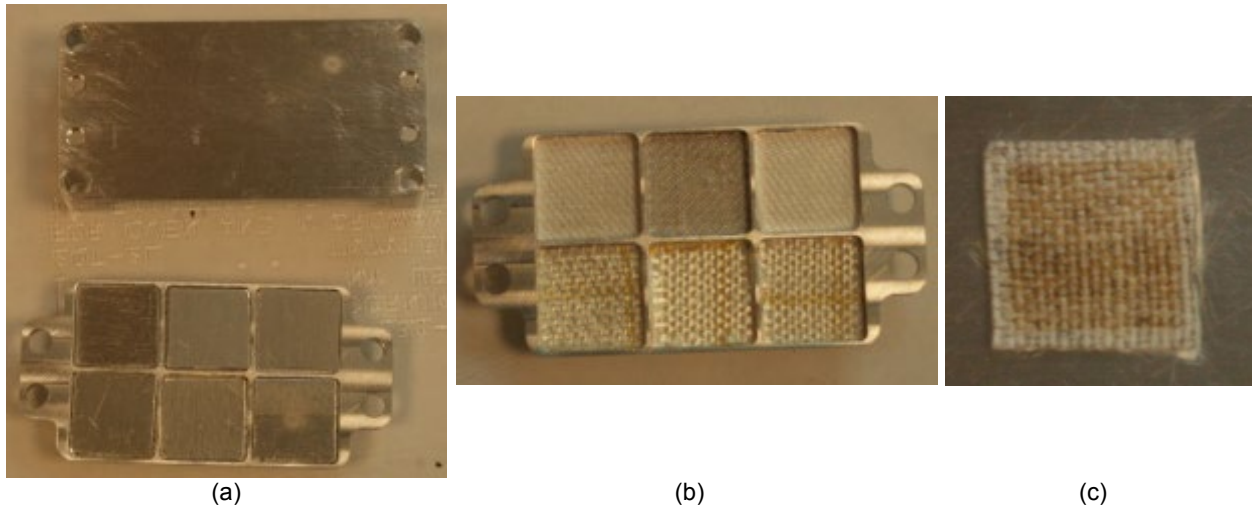


Figure 7.—Disassembly of the MISSE-7 Spacesuit Fabric Exposure Experiment showing the base removed (a), the backing plates removed (b), and the 2× dust-abraded Ortho-fabric sample after removal (c). Note that the fabric was darkened except in those regions covered by sample holder.

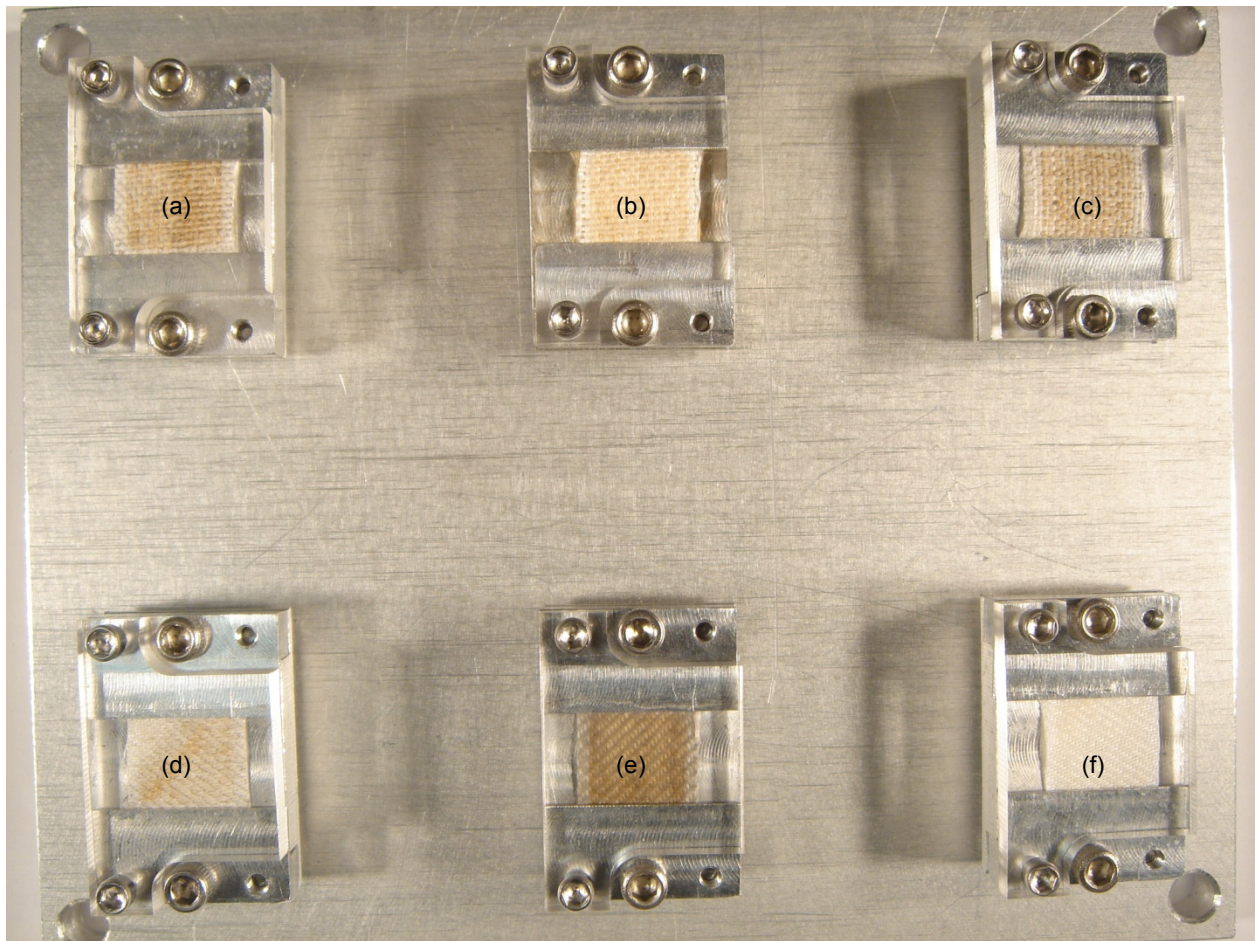


Figure 8.—MISSE-7 Spacesuit Fabric Exposure Experiment samples mounted in their sampler handlers: abraded Ortho-fabric (a), pristine Ortho-fabric (b), double abraded Ortho-fabric (c), abraded Apollo era fabric (d), Alan Bean Apollo 12 fabric (e), and pristine Apollo era fabric (f).

3.2 Microscopic Imaging

3.2.1 Pristine FEP Fabric

Images of the exposed pristine FEP fabric taken with the light microscope, the FESEM, and the AFM are collected in Appendix A. At low magnification optical microscopy showed that during exposure on the ISS the pristine FEP sample reddened in some places and darkened on the whole, perhaps due to UV radiation. Occasional dark specks in most of the images which occasionally reflect the light (Figure 9) suggesting these are metallic particles, most likely contamination debris which occurred during retrieval. Fabric near the edge of the sample holder, particularly in region B1f-3 (Appendix A) appear to be more reddened than the bulk of the fabric surface, though the source of the reddening has not been identified. There were no areas of obvious mechanical damage to the fiber up to 100× in magnification.

The most revealing images were obtained in the FESEM. The preflight inspection noted the existence of cracks in the individual fibers, with filaments observed within them. These same cracks are noted in the post-flight images, and their structure looks the same. Similarly, the scuff marks and holes noted in the sample preflight were located post flight with no noticeable change. At magnification > 1000× a new feature was seen (Figure 10). The entire surface has been textured with features ranging 1 to 4 μm long and about half as wide. The long part of the pit tends to run across the fiber width, rather than its length. These features are also clearly visible in the AFM, which shows that there is additional structure in the floor of the pits. FESEM images taken from the region protected by the samples holder (Section A.6 of Appendix A) show no such texture, confirming that the texturing is due to space exposure. The most likely cause of the texture is AO erosion.

Although the experiment was located on the wake face, and nominally did not see AO, there was AO exposure nonetheless. The largest AO dose occurred when the ISS was reoriented, such as happened when docking to the Space Shuttle. The AO fluence on the wake face was monitored by several other MISSE-7 experiments. For example, Finckenor has determined the wake side AO fluence to be $2.9 \pm 0.3 \times 10^{20}$ atoms/cm² using the method of erosion rate of Kapton HN (Ref. 8). This is about 7 percent of the ram-side fluence of $4.2 \pm 0.1 \times 10^{21}$ atoms/cm² (Ref. 8). Expressed another way, the wake-side samples experienced the equivalent of 38 days of ram AO exposure.

The AO erosion yield for FEP films has been determined previously to be 2.00×10^{-25} cm³/atom (Ref. 9). This predicts that about 0.6 μm should have been etched away from the surface. AFM imaging (Figure 11) suggests that the erosion pits have a depth consistent with that value.

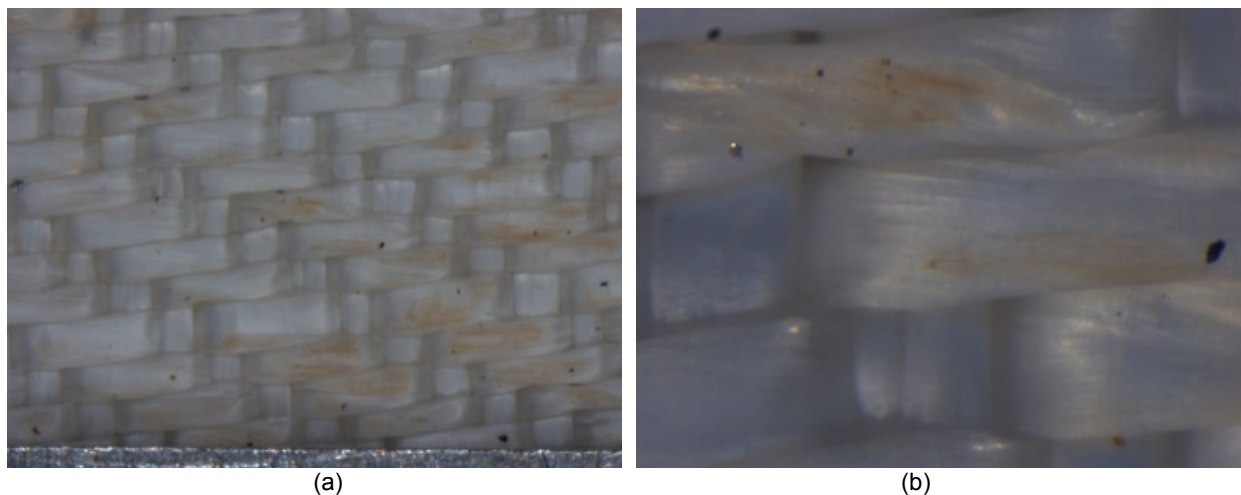


Figure 9.—Optical photomicrographs of pristine FEP at a magnification of 25× (a), and 100× (b) showing reddening of portions of the sample and debris.

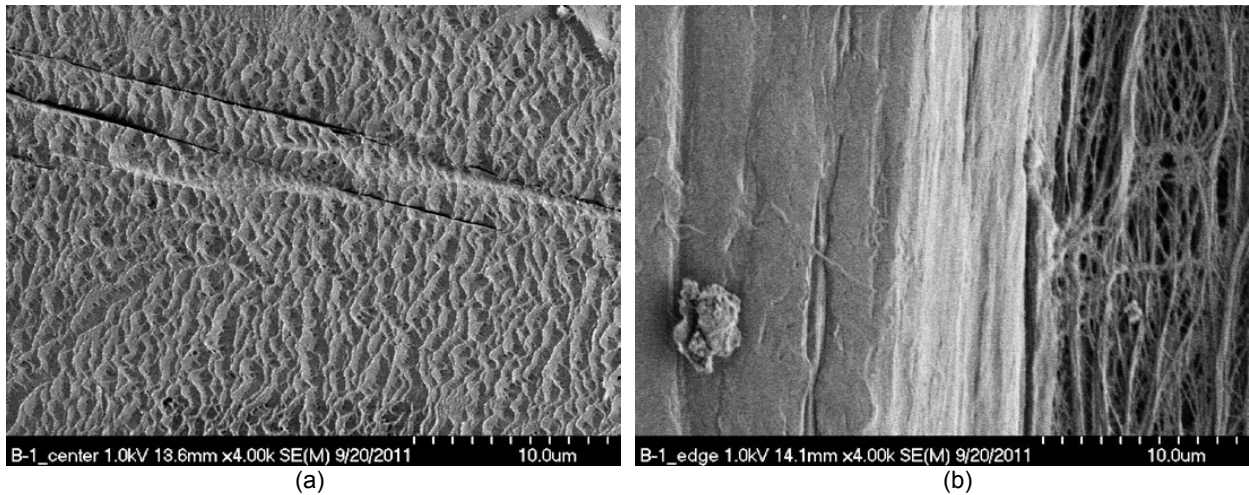


Figure 10.—FESEM photomicrographs of pristine FEP at a magnification of 4000× in the areas of the samples that were exposed (a), and protected by the samples holder (b).

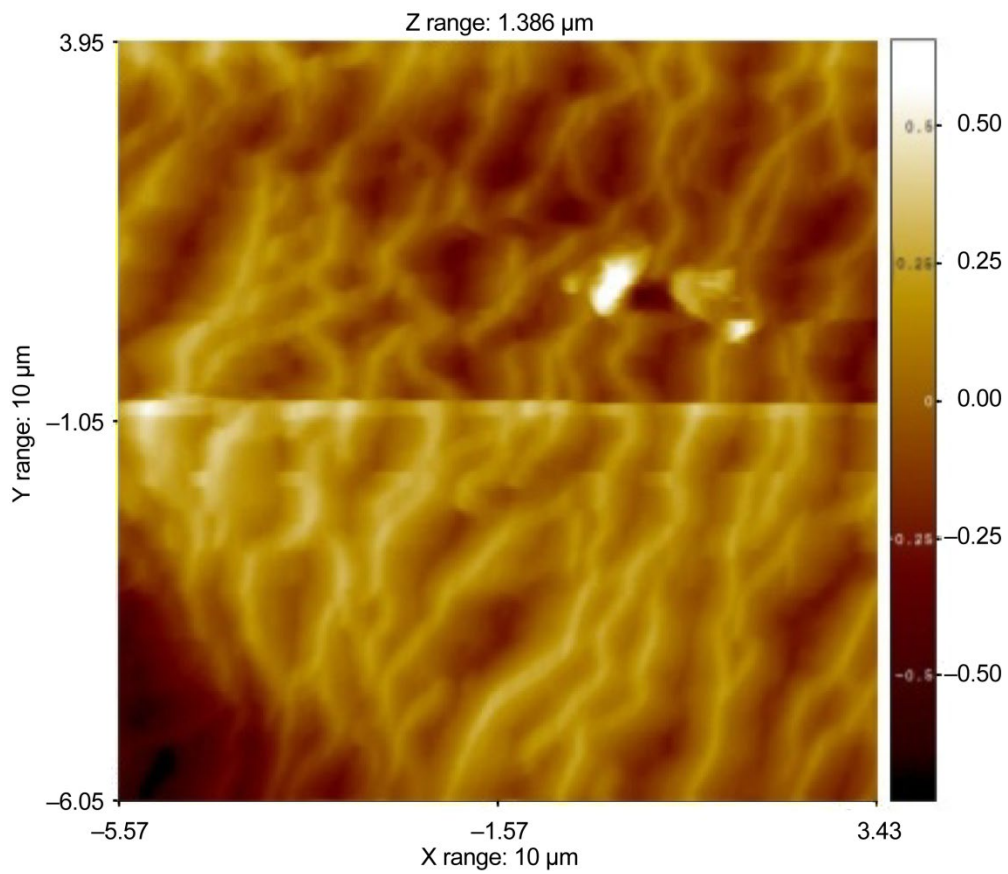


Figure 11.—AFM image of pristine FEP at a magnification of 10 μm square in an area of the samples exposed to AO. The pit depth was determined from scale on the right to be consistent with the 0.6 μm prediction of erosion. The line midway across the image is a raster imaging artifact.

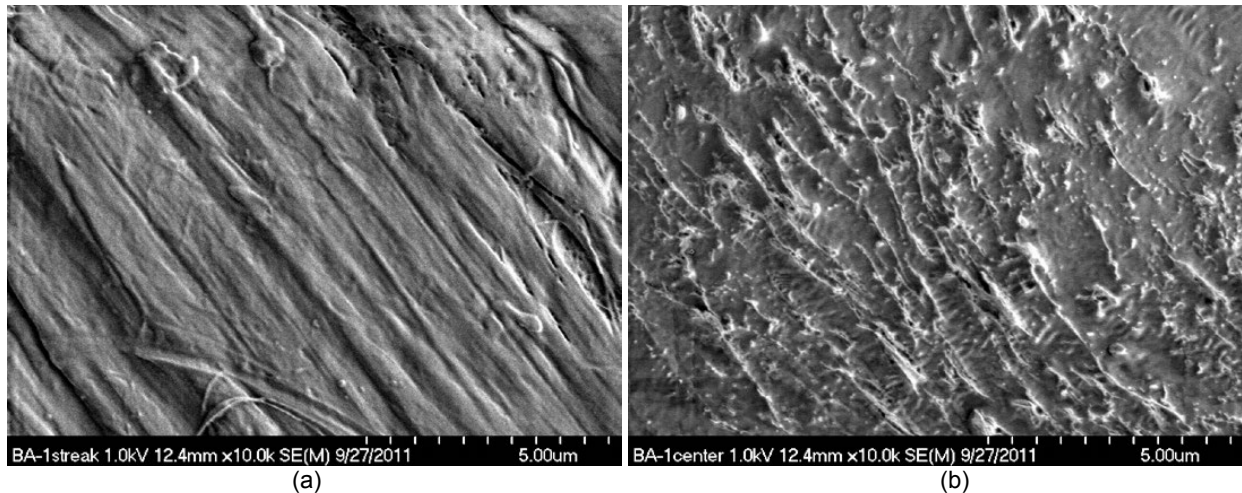


Figure 12.—FESEM photomicrographs of dust abraded FEP at 10000 \times in the areas of the samples that were exposed (a), and protected by the sample holder (b).

3.2.2 Dust Abraded FEP Fabric

Images of the exposed dust abraded FEP fabric taken with the light microscope, and the FESEM are collected in Appendix B. No usable images of this sample were obtained using the AFM. The plastic deformation and smearing of the fibers noted in the preflight characterization was clearly in evidence post-flight. So too were areas of scuffing and scribing. At high magnification in the FESEM, etch structures that were noted in the pristine fabric were observed in the abraded areas as well. However, their morphology was somewhat different. Whereas the pristine fiber exhibited closed ring pits, the abraded fabric exhibited a series of nearly parallel filaments (Figure 12). These appear to protrude high off of the surface, and it is speculated that these structures frustrated attempts to obtain AFM images.

As with the pristine sample, FESEM images taken from the region protected by the sample holder (Sections B.6 and B.7 of Appendix B) show no such texture, confirming that the texturing is most likely caused by atomic oxygen.

The outstanding feature of the abraded FEP sample is a dark streak that that is about 1 mm wide and extends at an angle of about 40 $^{\circ}$ from the corner near the Bean sample across nearly the entire sample. In the optical microscope the streak appeared to be produced by the same process that darkens the entire exposed sample of the surface. The color appeared to be the same and at higher magnification it can be seen that the streak is not at all continuous. The colorant merely covers a larger fraction of the fabric surface in that region. It does not extend into the region covered by the sample holder. No evidence of a different structure, texture, or composition for the region of the streak was observed under the FESEM.

3.2.3 Alan Bean Apollo FEP Fabric

Images of the exposed Alan Bean Apollo 12 fabric taken with the light microscope, and the FESEM are collected in Appendix C. As was the case in preflight imaging, no usable images of this sample were obtained using the AFM. The characteristic shredding of the fibers and embedded dust seen in the preflight samples was still present. However, as may be noted from Figure 13, there were many fewer places where shredded pieces of fiber stand up off of the fiber. Images at magnification > 1000 \times showed texturing that looks like that seen on the other Apollo-era FEP fabric samples. Interestingly, there are regions where the etch pattern looks more like the pristine fiber, and other areas that look more like the dust abraded fiber (Figure 14).

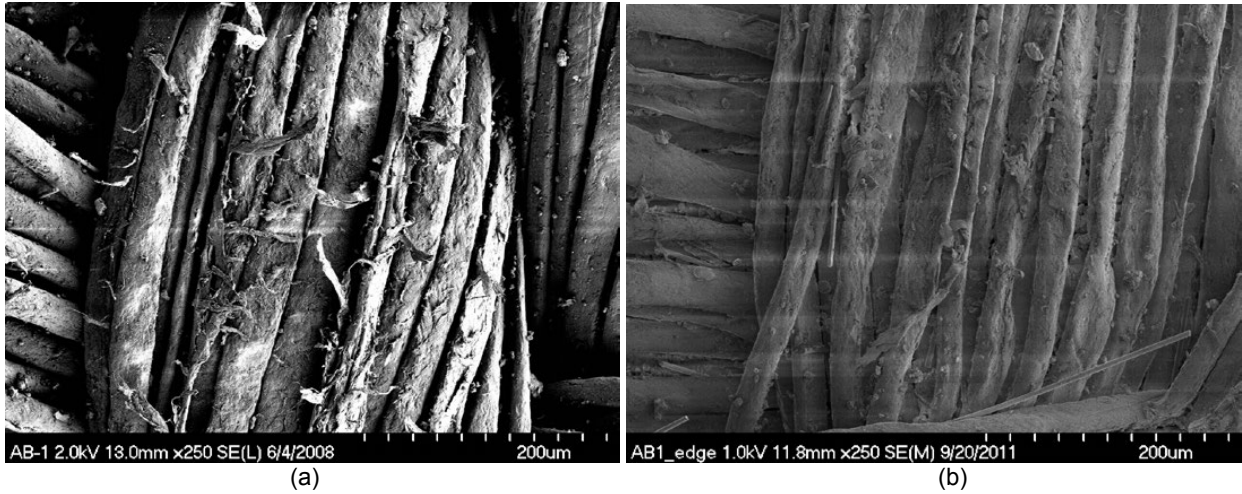


Figure 13.—Photomicrographs of the fabric from the left knee of Alan Bean’s Apollo 12 spacesuit as it was returned from the Moon (a), and after 18 months of LEO exposure in the wake side of MISSE-7 (b).

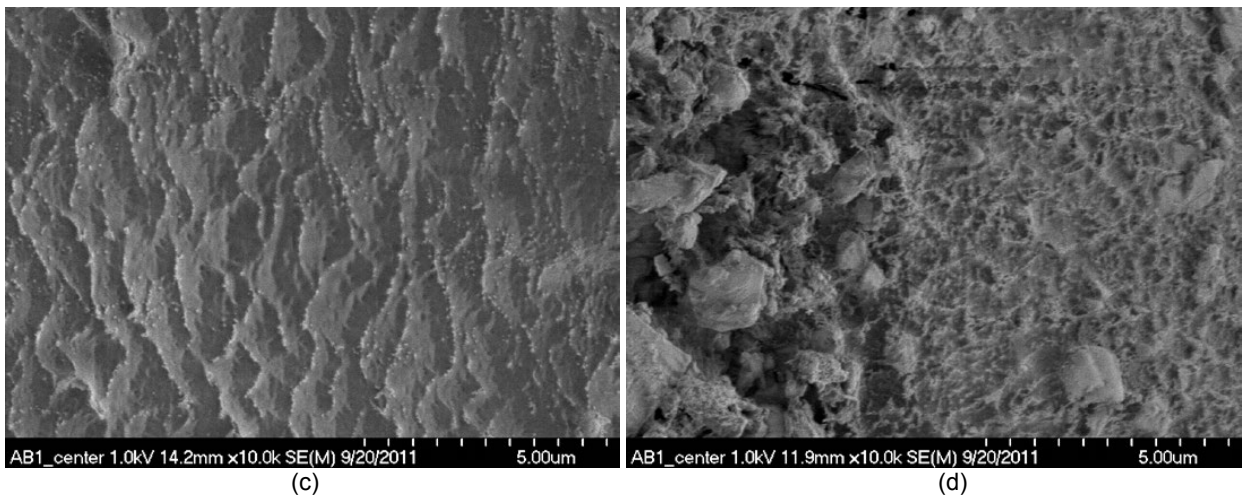
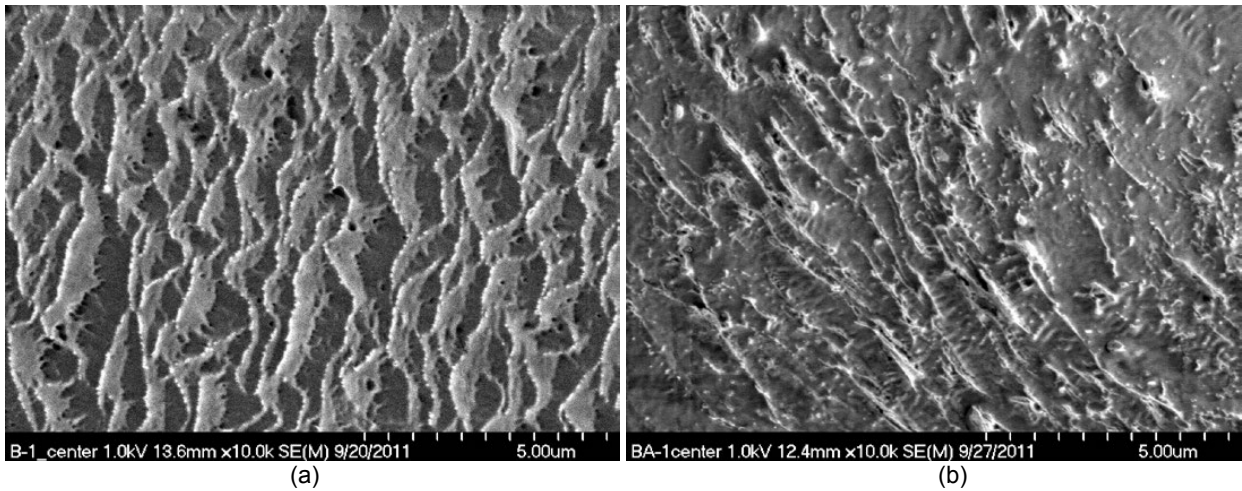


Figure 14.—Photomicrographs of pristine Apollo-era FEP (a), dust-abraded Apollo-era FEP (b) and fabric from the left knee of Alan Bean’s Apollo 12 spacesuit (c, d) after exposure on MISSE-7.

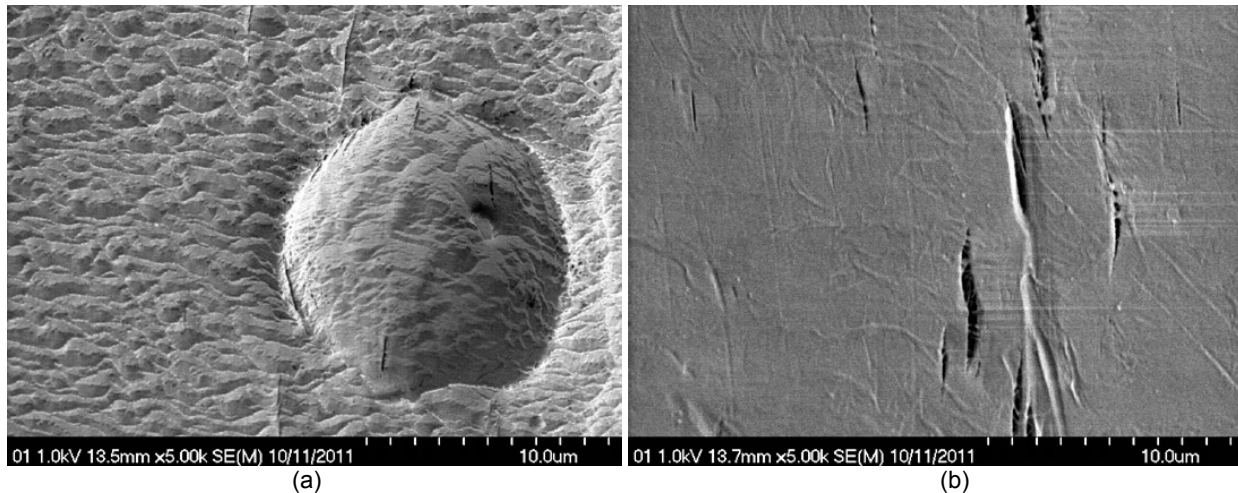


Figure 15.—FESEM photomicrographs of pristine Ortho-fabric at a magnification of 5000× in the areas of the samples that were exposed (a), and protected by the sample holder (b).

As before, FESEM images taken from the region protected by the sample holder (Section C.6 of Appendix C) show no etched texture, and shredded fiber pieces were also present in this region. This lends credence to the idea that both texturing and small shred removal are mostly caused by atomic oxygen.

3.2.4 Pristine Ortho-Fabric

Images of the space exposed pristine Ortho-fabric taken with the light microscope, the FESEM, and the AFM are collected in Appendix D. As with FEP, Ortho-fabric darkened and reddened upon space exposure. Interestingly, the weft had a much greater color change than the warp. In the pre-flight analysis, triangular indentations scattered throughout the sample were noted, most likely a result of the weaving process. There were some cracks on the surface and filaments in some of the cracks. There were a few impact sites on the sample. One that left a 12 μm wide crater is shown in Figure 15. No remnant of the projectile is seen. The texture seen within the crater implies that the impact occurred before the sample was exposed to a significant fluence of AO.

The post-flight fiber morphology is unchanged at low magnification, but at > 1000× the surface again appeared to have been etched by atomic oxygen. The dimensions and morphology of the pits are the same as that seen in the FEP fabric. Once again the edge where the sample was protected under the sample holder was also very similar to the preflight sample.

3.2.5 Abraded Ortho-Fabric

Images of the exposed dust-abraded Ortho-fabric taken with the light microscope, the FESEM, and the AFM are collected in Appendix E. In the samples preflight, the weft (top) fibers were plastically deformed and scored by the dust-abrasion process, and a considerable amount of dust remained trapped between the fibers. These features were also observed post-flight. Like the samples preflight, the weft (top) fibers were plastically deformed and scored by the dust-abrasion process. A considerable amount of dust remained trapped between the fibers. Like the pristine Ortho-fabric, it was darker and redder than preflight, with the color change being dominated by the weft. The fibers of this fabric were also etched, generally in patterns resembling the post-flight pristine Ortho-fabric. In some fibers, however, the damage was much more severe with a large fraction of the fiber being etched away through the entire volume of the fiber (Figure 16). Judging by the fiber diameter, these were probably Nomex fibers rather than PTFE. The atomic oxygen yield for Nomex is 10× that of PTFE, and so more than 4 μm of the fiber might have eroded (Ref. 9). As with the other samples, the edge where the sample was protected under the sample holder appeared very similar to the preflight sample.

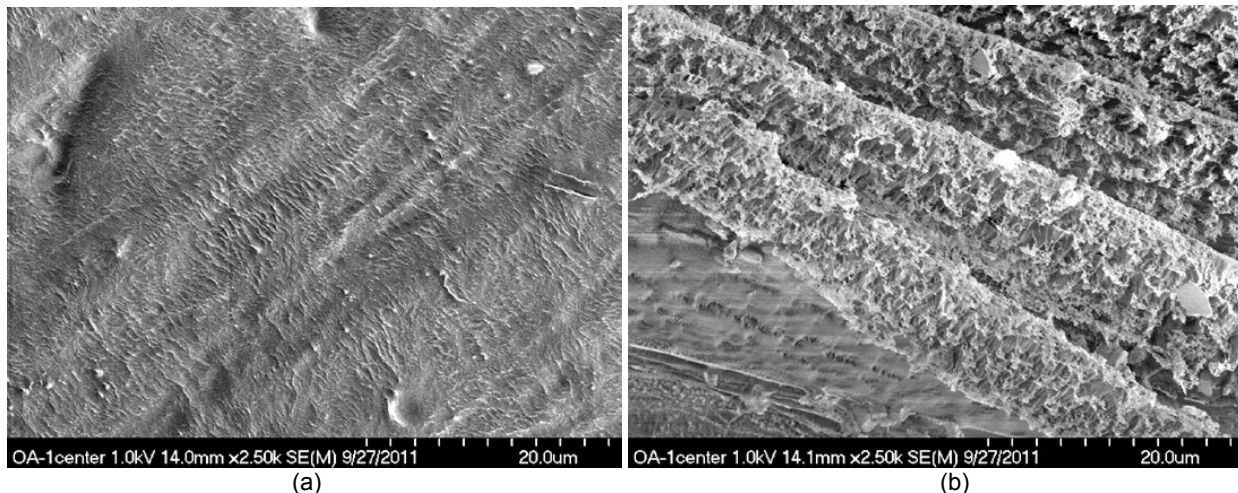


Figure 16.—FESEM photomicrographs of abraded Ortho-fabric at a magnification of 2500× in the areas of the samples that were exposed showing etching of the PTFE (a), and Nomex fibers (b).

3.2.6 Twice Abraded Ortho-Fabric

The post-flight appearance of the doubly abraded Ortho-fabric was virtually identical to that of the singly abraded Ortho-fabric. Thus, doubling the number of abrasion cycles from 8,000 to 16,000 had no measurable effect. Images of the exposed 2× dust-abraded Ortho-fabric taken with the light microscope, the FESEM, and the AFM are collected in Appendix F.

3.3 Energy Dispersive X-Ray Spectroscopy (EDS)

The EDS spectra of several samples were measured in order to determine whether the discoloration of the samples was due to radiation damage or contamination. Since EDS measures elemental composition of the samples, and FEP and PTFE signatures are simple and characteristic, containing only carbon and fluorine, contamination is easy to identify. EDS requires an electron beam of relatively high energy in order to excite inner shell electrons, so the samples were gold coated before the measurements were made. As a precaution, all samples were imaged thoroughly before the gold coating, and only a fraction of the samples were coated. None of the EDS spectra shown were taken in areas that contain dust particles.

The most obvious candidate for contamination was the dust-abraded FEP fabric which contained a dark streak across it. Figure 17 compares the EDS spectrum taken at the area where the streak was with a characteristic area where the sample was exposed to the space environment, and an area where the sample was protected from the environment. As can be seen, the spectra are virtually identical, with an approximate formula of CF_2 , characteristic of FEP.

Similar results were obtained for all three Ortho-fabric samples. This implies that the darkening was caused not by contamination, but by an interaction of the fabrics with the space environment, most likely UV radiation. Although this seems the most likely explanation, and is consistent with the even appearance of the discoloration on five of the samples, it is difficult to explain how the streak could appear in the abraded FEP sample.

3.4 Total Reflectance Spectroscopy

The results of space exposure on the FEP fabrics are shown in Figure 18. There was little change in the $\rho(\lambda)$ for wavelengths longer than 800 nm in the pristine fabric (Figure 18(a)). But there is a dramatic reduction in $\rho(\lambda)$ below 800 nm that becomes greater as λ becomes shorter, hence the reddening. This

darkening and reddening is in the visible region (400 to 700 nm) which is clearly shown in the optical photographs as discussed above. The α increased upon space exposure, as is shown in Table I.

The spectra of the pristine FEP can be used to help interpret the dust abraded FEP spectrum (Figure 18(b)). The functional form of the pre-flight and post-flight spectra for the dust abraded FEP sample above 500 nm is similar, except that the abraded sample is less reflective. In fact, Figure 18(a) shows that a simple rule of mixtures calculation, where the 64.2 percent of the spectrum is due to the JSC-1AF spectrum and the remainder is due to the FEP fabric, results in a reasonable fit to the measured dust-abraded FEP spectrum.

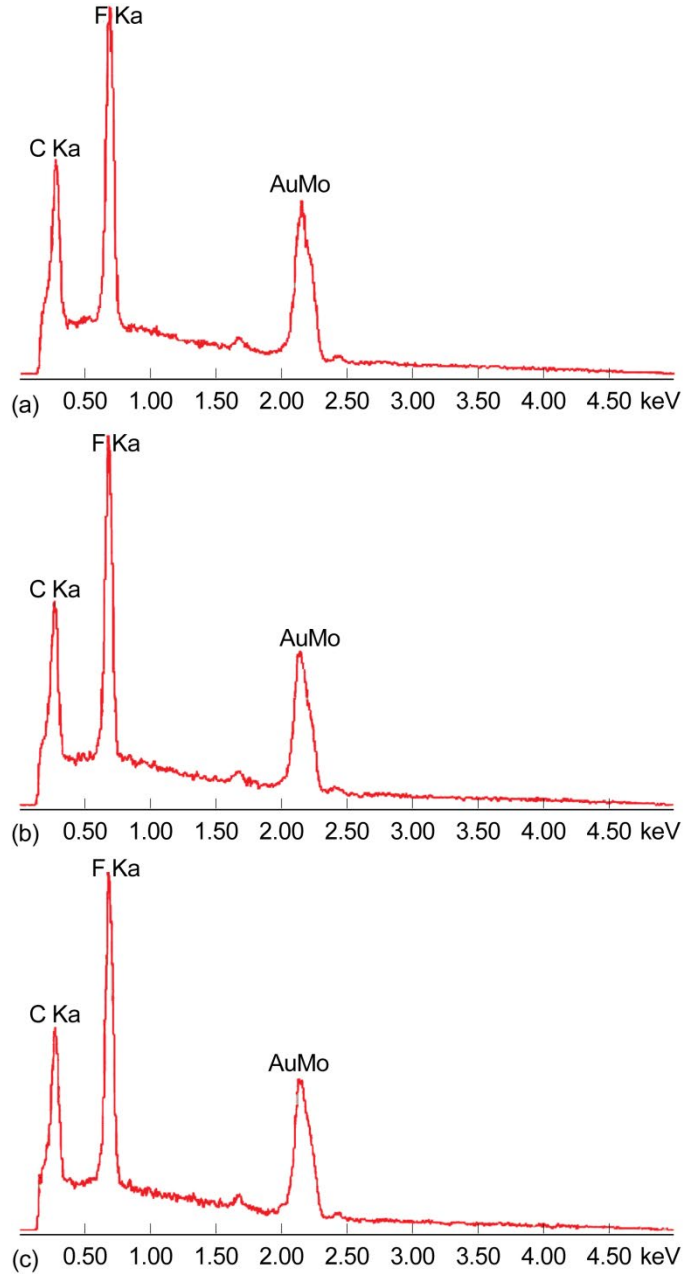


Figure 17.—EDS spectra of gold coated dust-abraded Apollo-era FEP fabric measured on the streak (see Figure 5) (a), on a space exposed area (b), and on protected area.

TABLE I.—INTEGRATED SOLAR ABSORPTANCE, α , FOR THE SIX MISSE-7 SAMPLES, BEFORE AND AFTER SPACE EXPOSURE

Absorptance (α)	Preflight	Post-flight	$\alpha_{\text{post-flight}}/\alpha_{\text{preflight}}$
Pristine FEP	0.22	0.28	1.27
Abraded FEP	0.41	0.44	1.07
A. Bean FEP	0.55	0.65	1.18
Ortho-fabric	0.24	0.33	1.38
Abraded Ortho-fabric	0.44	0.48	1.09
2x Abraded Ortho-fabric	0.45	0.49	1.09

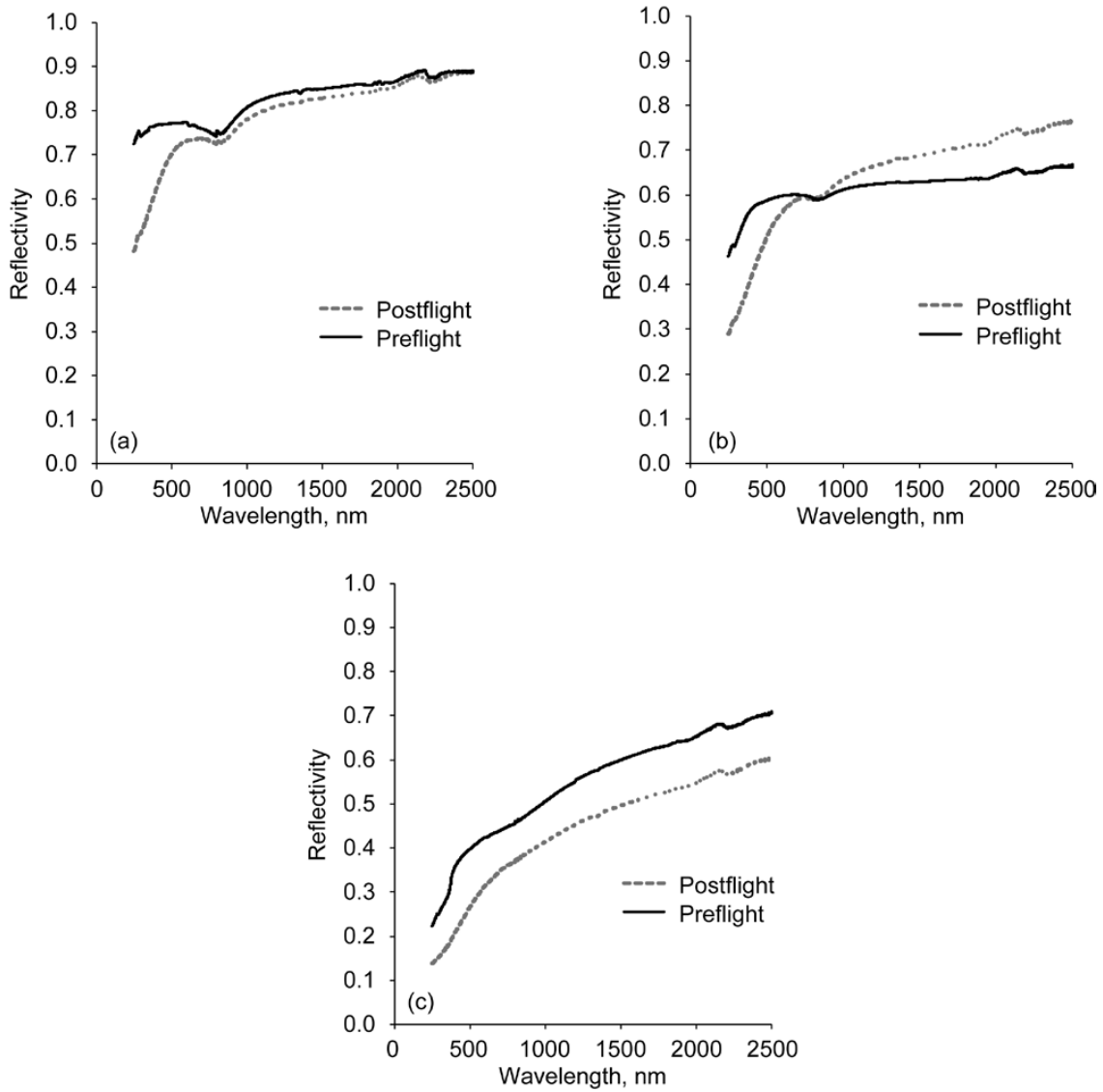


Figure 18.—Spectral $\rho(\lambda)$ of pre- and post-flight pristine FEP (a), dust abraded FEP (b), and Alan Bean suit (c).

However, this same rule of mixtures behavior clearly does not hold post-flight. The spectrum at λ longer than 800 nm becomes increasingly reflective with λ (Figure 18(b)). This is a spectral characteristic of lunar dust as well (Ref. 10). This spectral “reddening” can be seen in the Alan Bean suit spectrum shown in Figure 18(c), which was infused with lunar dust preflight. These data seem to indicate that UV radiation blocked by the Earth’s atmosphere is essential in the reddening mechanism. Note that the $\rho(\lambda)$ decreased on space exposure, but uniformly across the spectrum by about 0.10 (Figure 19(c)).

Taken together, it appears that space exposure has three $\rho(\lambda)$ effects on dust abraded FEP fabric. First, it apparently has little or no effect on FEP at $\lambda > 800$ nm, but darkens FEP increasingly at shorter λ down to 250 nm. Second, space exposure reddens the entrapped dust, with $\rho(\lambda)$ becoming increasing reflective at $\lambda > 800$ nm. Third, space exposure darkens the dust, as evidenced by the decrease in $\rho(\lambda)$ of the already reddened lunar dust in the Alan Bean spacesuit fabric.

The results of space exposure of the Ortho-fabric samples are shown in Figure 20. The behavior was considerably different from that of the FEP. Figure 20(a) shows that the effect of abrasion on the preflight samples was to darken the samples, but with change in $\rho(\lambda)$ becoming less as λ increases. Note that the Ortho-fabric has many more spectral features than the FEP, and those features are still visible after the dust abrasion. Doubling the number of abrasion cycles from 8,000 to 16,000 had virtually no effect on the spectrum.

Figure 19(b) shows that a simple rule of mixtures calculation where 66.9 percent of the spectrum is due to the JSC-1AF spectrum and the remainder is due to the Ortho-fabric results in a reasonable fit to the measured dust-abraded Ortho-fabric spectrum for $\lambda > 800$ nm. However, at $\lambda < 800$ nm the sample is darker and redder than predicted, with the difference in $\rho(\lambda)$ increasing as λ decreases. It is not clear why the rule of mixtures model does not work as well for the Ortho-fabric in the shorter λ region.

Figure 20(b) shows that the $\rho(\lambda)$ of Ortho-fabric slightly increases on space exposure for $\lambda > 800$ nm, but drops dramatically below 800 nm, and like the FEP the difference becomes greater as λ becomes shorter. As with the FEP this darkening and reddening in the visible region (400 to 700 nm) is also clearly shown in the optical photographs (Figure 5). The α of pristine Ortho-fabric increases by 38 percent upon space exposure (Table I).

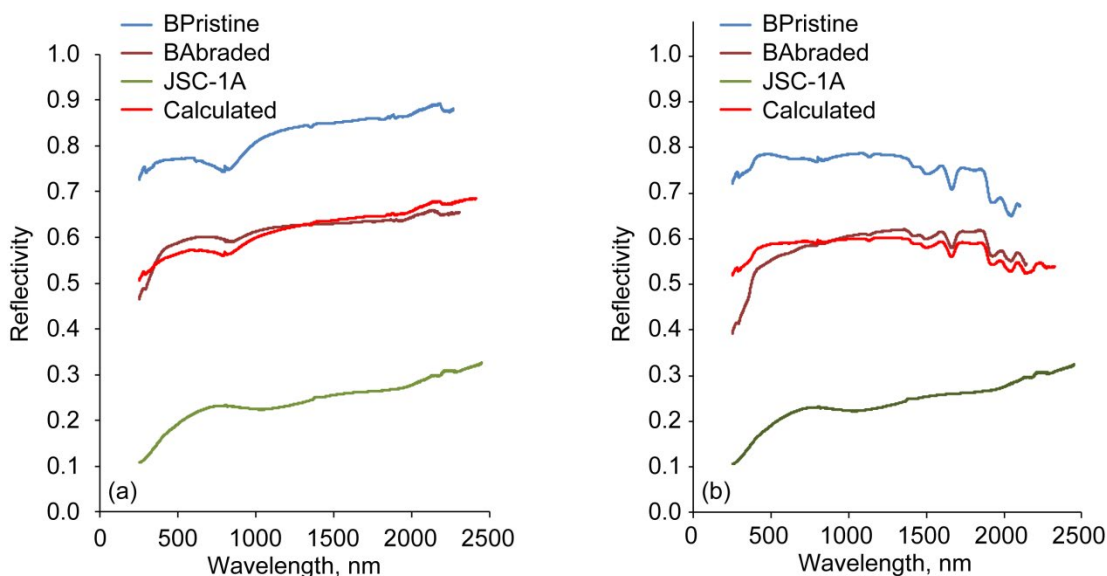


Figure 19.—Spectra of pre-flight $\rho(\lambda)$ of pristine fabric, lunar simulant JSC-1A, a linear combination of the two, and JSC-1A abraded fabric for FEP (a), and Ortho-fabric (b), shows that the simulant-abraded fabric spectra are reasonably well predicted by the linear combination of pristine fabric and lunar simulant.

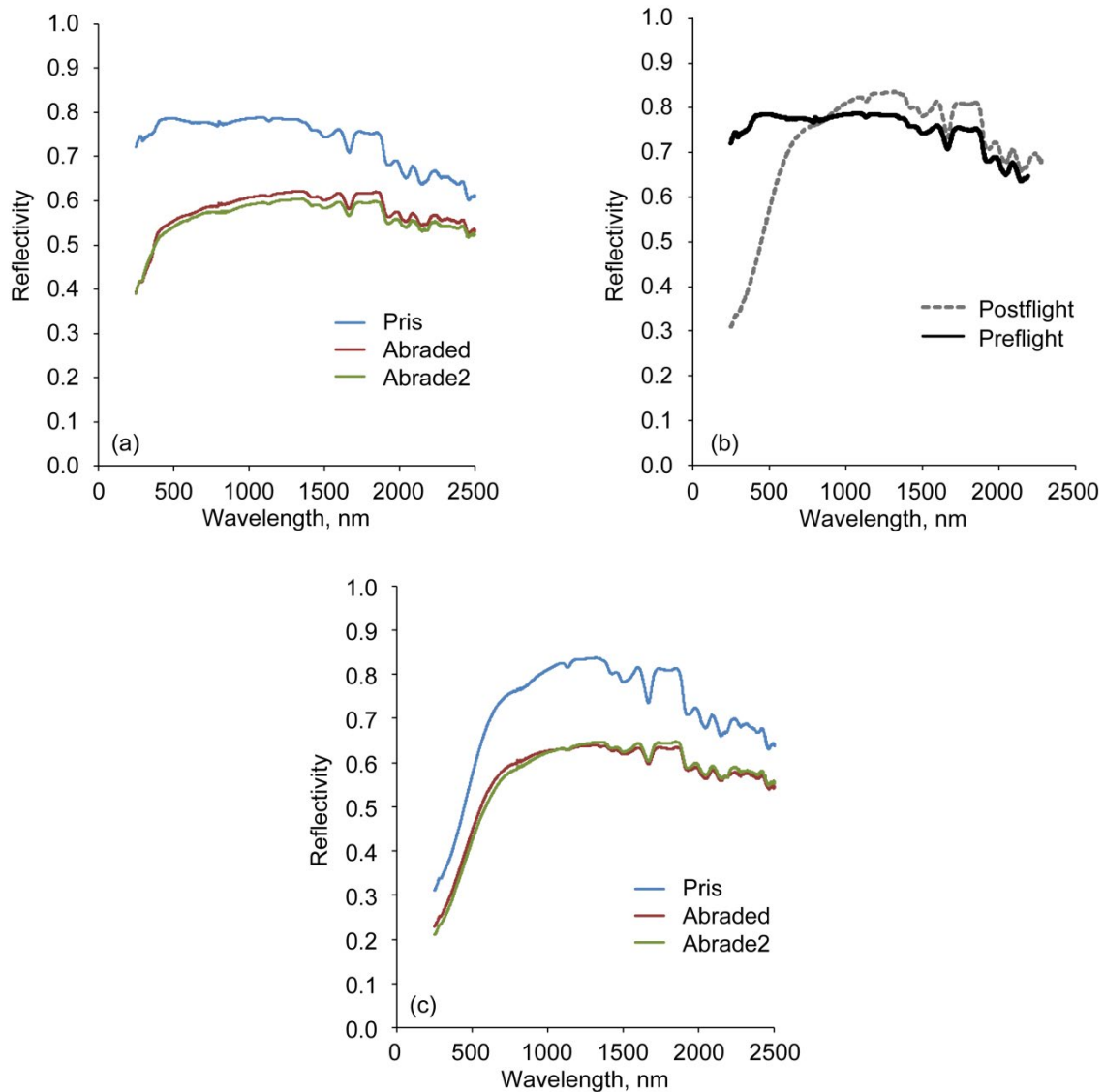


Figure 20.—Spectral $\rho(\lambda)$, of the three Ortho-fabric samples pre-flight (a), preflight compared to post-flight spectrum for pristine Ortho-fabric (b), and the three Ortho-fabric samples post-flight (c).

Figure 20(c) shows the post-flight spectra of the pristine, abraded, and 2× abraded Ortho-fabric. The reddening at $\lambda > 800$ nm that was so striking in the FEP spectrum does not appear in the Ortho-fabric spectrum. There is only a darkening of the spectrum on abrasion. The dust appears to have little if any effect on the spectrum, implying that the dust-abraded spectrum is dominated by abrasion damage, rather than by dust particles.

3.5 Tensile Test

Tensile testing of single fibers from the fabrics was problematic. Since the flight specimens were so small, the length of fiber available for gripping was limited to 2 to 3 mm on each end. And since the fibers were FEP it was difficult to sufficiently grip the fibers over such a small length to exert a force large enough to break the fibers. Both the Ortho-fabric and the FEP had fibers much too large (200 to

600 μm) to break using our protocol. Only the fibers from the Alan Bean suit were sufficiently thin. The average fiber diameters were measured to be $23 \pm 3 \mu\text{m}$, and did not measurably change during exposure. This indicates that the AO etching observed in the microscopy was a surface effect and likely did not contribute significantly to mechanical degradation of the fibers.

The results of tensile testing of fibers from the Alan Bean sample are shown in Table II. The ultimate tensile strength of the fibers decreased by a factor of 4.1 ± 1.4 , the elongation to failure decreased by 4.3 ± 2.0 , and the modulus increased by a factor of 2.2 ± 1.0 . Since there was limited AO exposure damage, as evidenced by the fiber diameters being constant before and after exposure, the degradation was likely caused by exposure to radiation.

TABLE II.—CHANGE IN TENSILE PROPERTIES OF ALAN BEAN FABRIC SAMPLES AFTER 18 MONTHS EXPOSURE TO THE LEO WAKE ENVIRONMENT

	Ultimate tensile strength, Pa	Elongation at failure	Young's modulus, Pa
Pre-flight Bean Fibers	226 ± 39	1.03 ± 0.24	229 ± 58
Post-flight Bean Fibers	55 ± 17	0.24 ± 0.10	492 ± 199

Nevertheless, the degradation in tensile properties of lunar dust abraded spacesuit fabric when exposed to the space environment was substantial. This must be taken into account when planning for long term missions to the lunar surface. The fabric had been exposed to light wear, only being worn on the lunar surface for 7.8 hr, yet that combined with 18 months of space exposure decreased the tensile strength by a factor of four. Clearly, during a long mission, the integrity of the fabric would benefit from shielding it from solar radiation when it is not being worn. It is unfortunate that data were unable to be obtained for pristine fabrics in order to determine how much the dust abrasion changed the degradation properties. Somewhat larger samples including pristine FEP fabric are currently being exposed on MISSE-8, and may shed light on this.

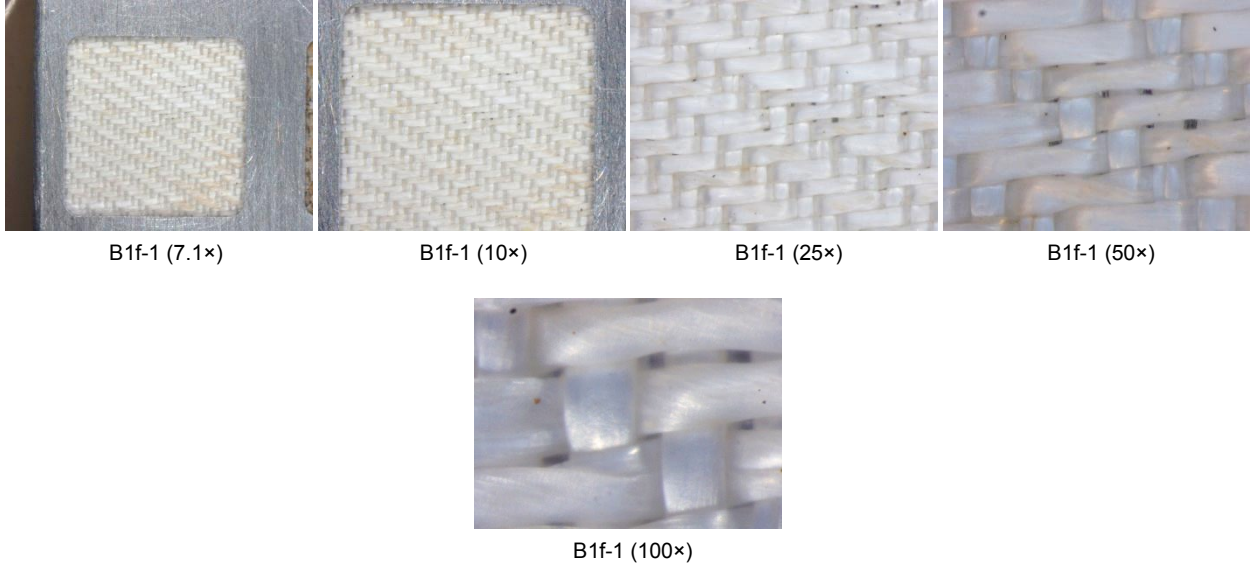
4.0 Conclusions

Six samples of pristine and dust abraded outer layer spacesuit fabrics were included on MISSE-7 as the Spacesuit Fabric Exposure Experiment. They were exposed to the wake LEO environment on the ISS for 18 months in order to determine whether abrasion by lunar dust increases radiation degradation. The fabric samples were characterized using optical microscopy, FESEM, EDS, optical spectroscopy and tensile testing after exposure on the ISS. Comparison of pre- and post-flight characterizations showed that ultraviolet radiation darkened and reddened all six fabrics. On space exposure, the α of the FEP fabric increased by 27 percent, and that of the Ortho-fabric increased by 38 percent. The α of FEP fabric abraded with JSC-1A increased by 7 percent, and JSC-1A abraded Ortho-fabric increased 9 percent. In both cases most of their spectra could be explained as a linear addition of the fabric and the dust, though the correlation did not hold in the visible and UV wavelengths for the Ortho-fabric. Spectroscopically, the lunar dust laden Apollo 12 sample darkened, but did not appreciably redden. No evidence of contamination was seen in the EDS results, suggesting that the discoloration was due to radiation damage. Even though the samples were positioned on the wake side, because the ISS periodically reorients, the samples were exposed to the equivalent of about 38 days of ram AO. Evidence for this was seen in the oxidation of silver-coated fasteners and the etching of fabric fibers. The erosion seen in the fibers was quantitatively consistent with previously reported values for the erosion yields of the materials. Space exposure decreased the ultimate tensile strength and elongation to failure of the Apollo space suit fibers by a factor of four and increased the elastic modulus by a factor of two. The severity of the degradation of the fabric samples over the eighteen month exposure period demonstrates the necessity to find ways to prevent or mitigate radiation damage to spacesuits when planning extended missions to the Moon.

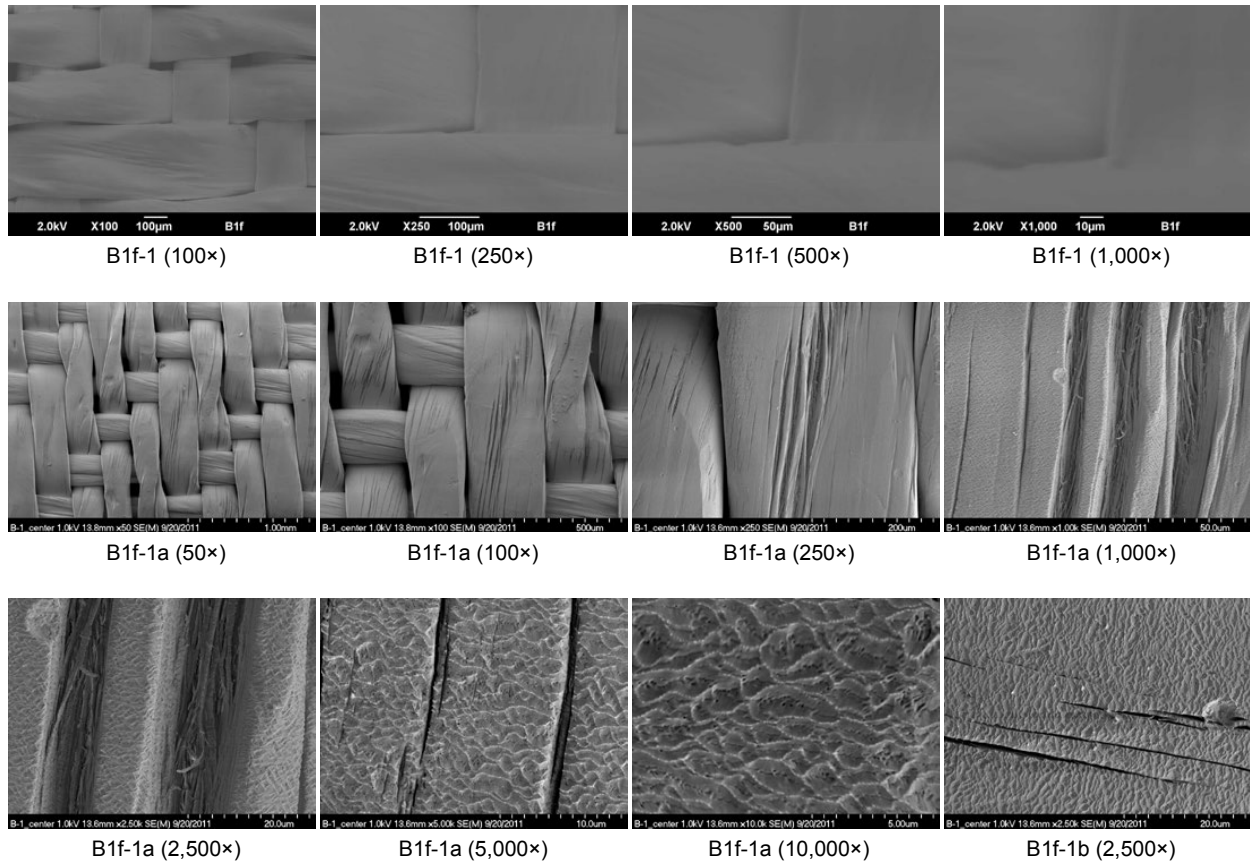
Appendix A.—Post-Flight Pristine Apollo Fabric

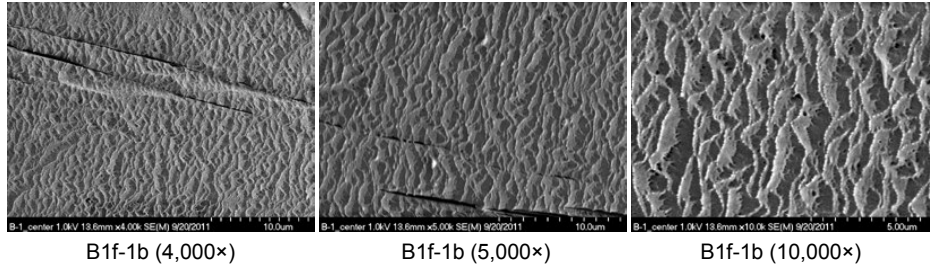
A.1 B1f-1

A.1.1 Optical Microscopy

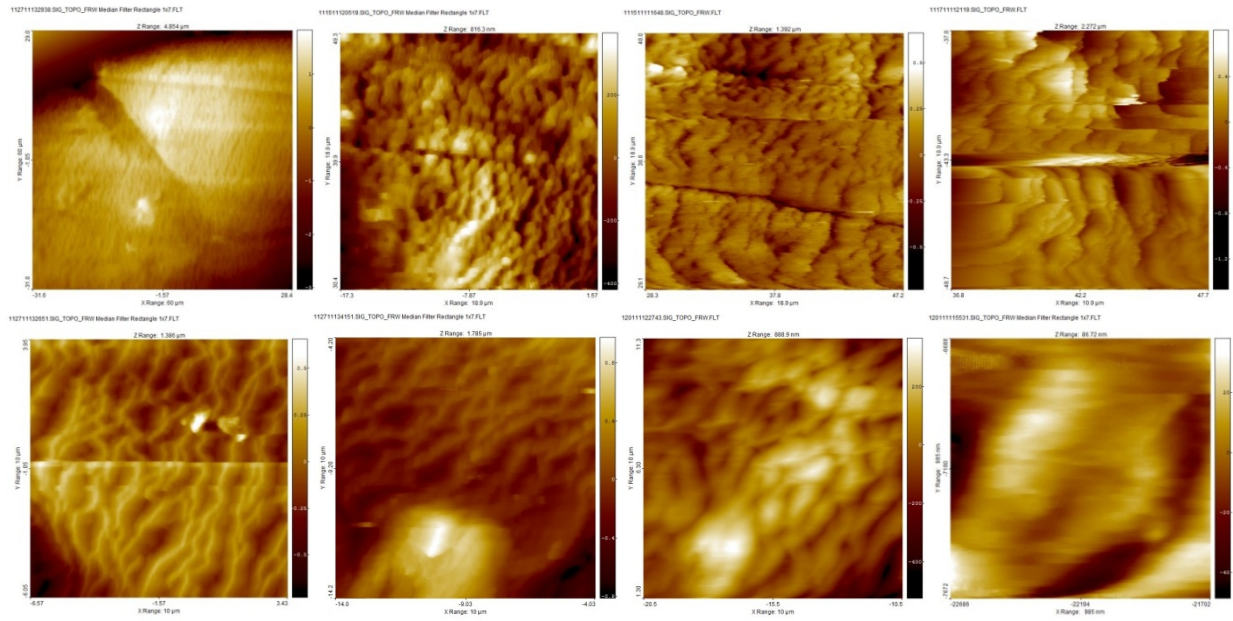


A.1.2 Electron Microscopy



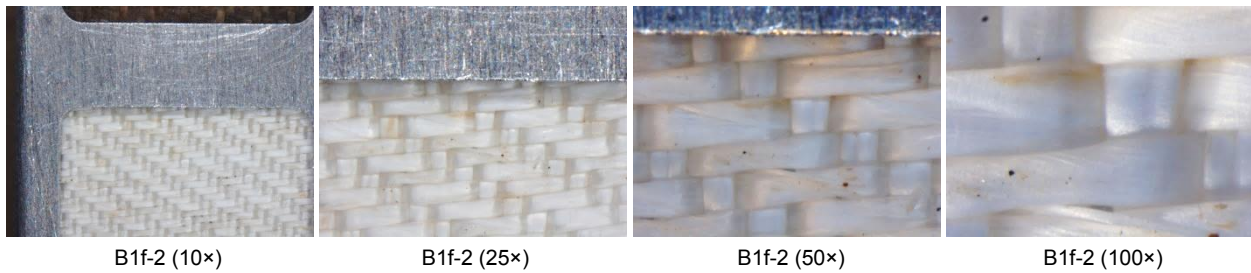


A.1.3 Atomic Force Microscopy

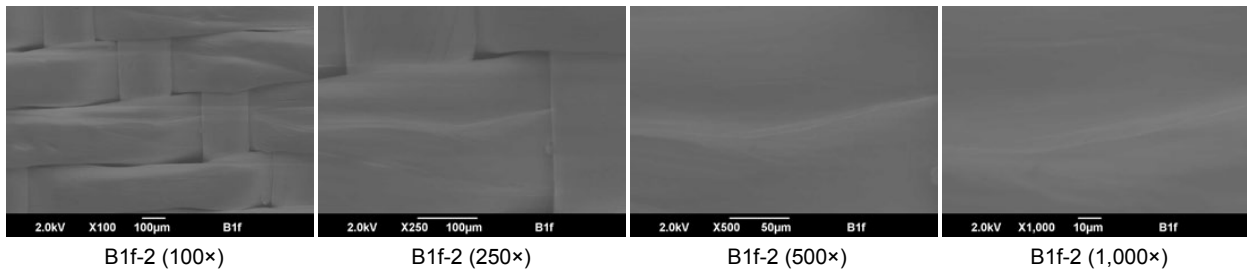


A.2 B1f-2

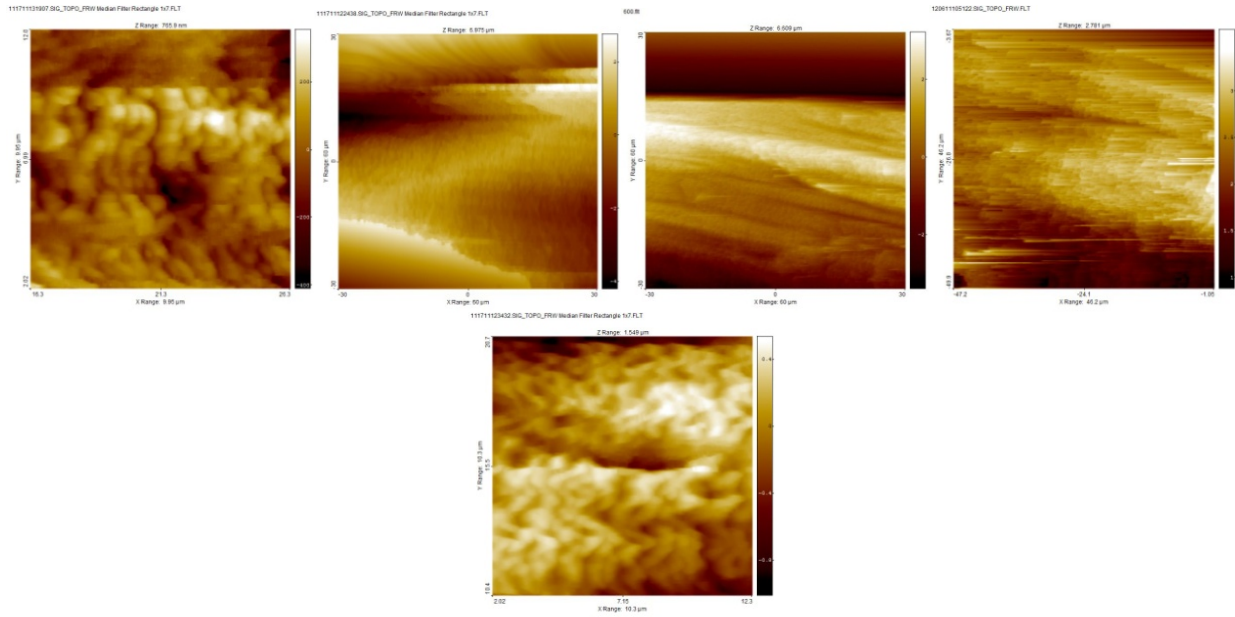
A.2.1 Optical Microscopy



A.2.2 Electron Microscopy



A.2.3 Atomic Force Microscopy



A.3 B1f-3

A.3.1 Optical Microscopy



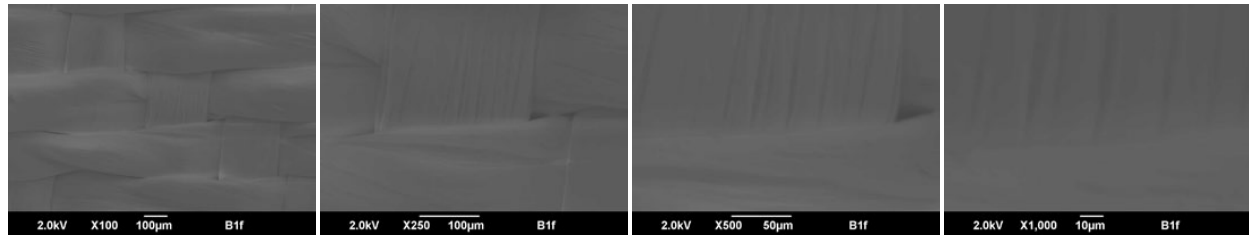
B1f-3 (10×)

B1f-3 (25×)

B1f-3 (50×)

B1f-3 (100×)

A.3.2 Electron Microscopy



B1f-3 (100×)

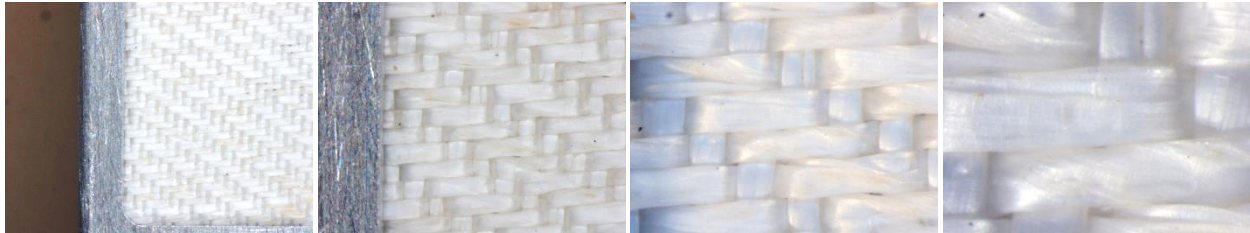
B1f-3 (250×)

B1f-3 (500×)

B1f-3 (1,000×)

A.4 B1f-4

A.4.1 Optical Microscopy



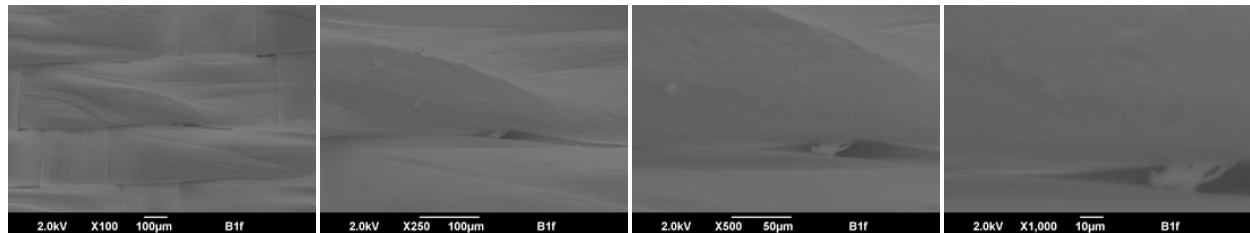
B1f-4 (10×)

B1f-4 (25×)

B1f-4 (50×)

B1f-4 (100×)

A.4.2 Electron Microscopy



B1f-4 (100×)

B1f-4 (250×)

B1f-4 (500×)

B1f-4 (1,000×)

A.5 B1f-5

A.5.1 Optical Microscopy



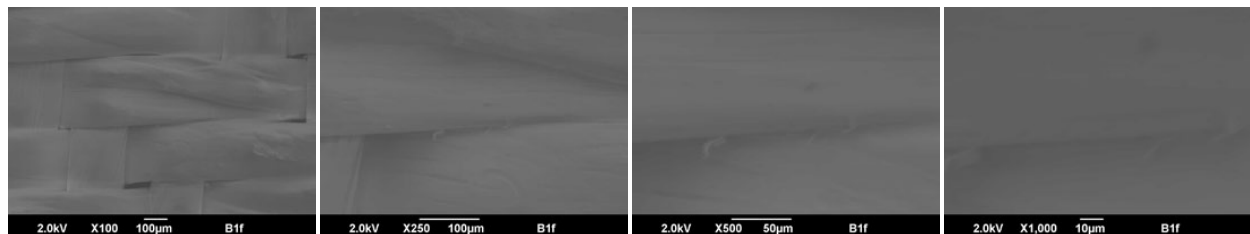
B1f-5 (10×)

B1f-5 (25×)

B1f-5 (50×)

B1f-5 (100×)

A.5.2 Electron Microscopy



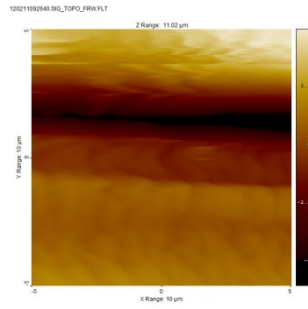
B1f-5 (100×)

B1f-5 (250×)

B1f-5 (500×)

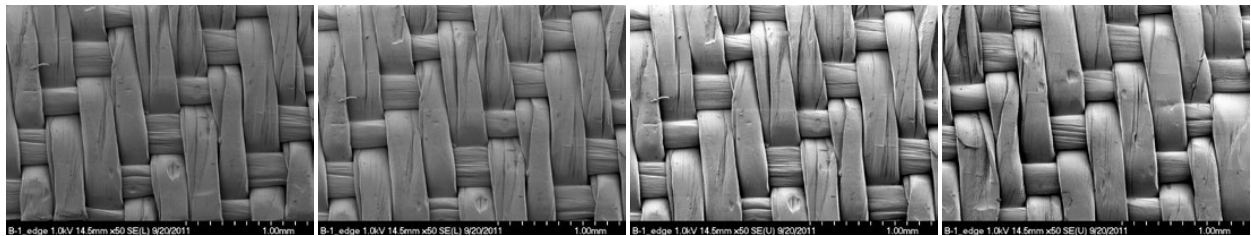
B1f-5 (1,000×)

A.5.3 Atomic Force Microscopy



A.6 B1f-6

A.6.1 Electron Microscopy

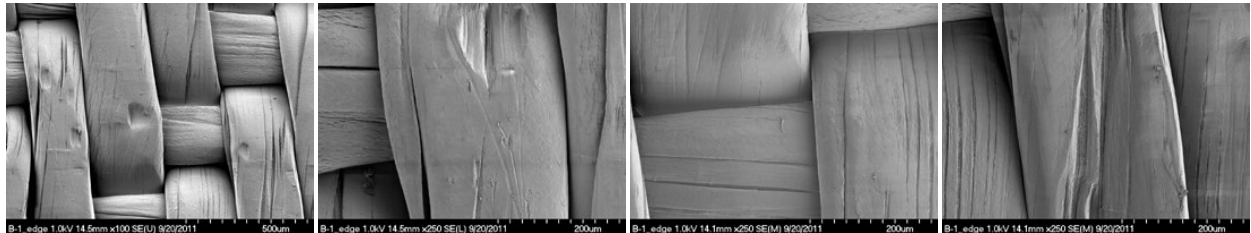


B1f-6 (50×)

B1f-6a (50×)

B1f-6a (50×)

B1f-6b (50×)

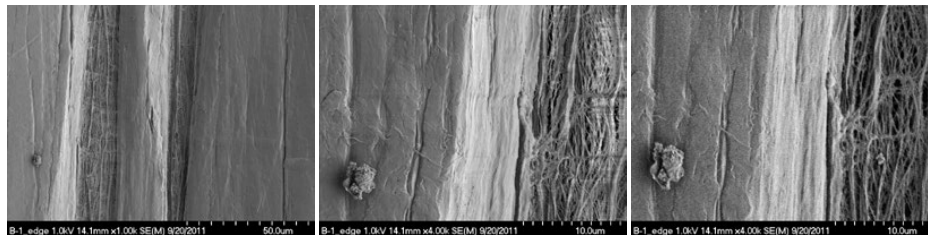


B1f-6b (100×)

B1f-6c (250×)

B1f-6d (250×)

B1f-6e (250×)



B1f-6e (1,000×)

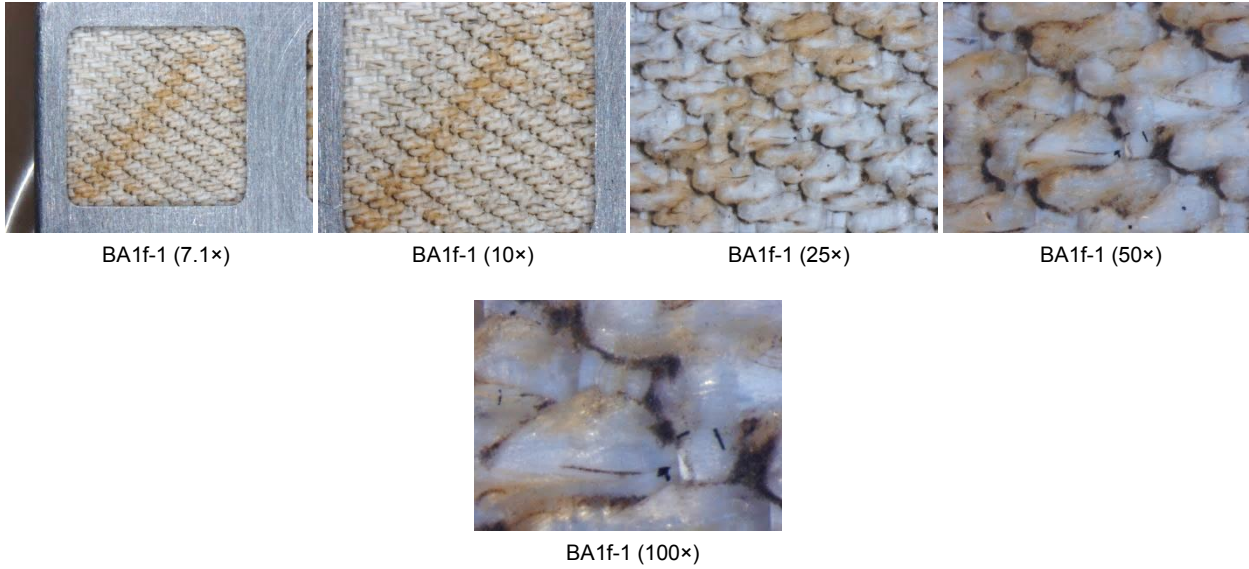
B1f-6e (4,000×)

B1f-6e (4,000×)

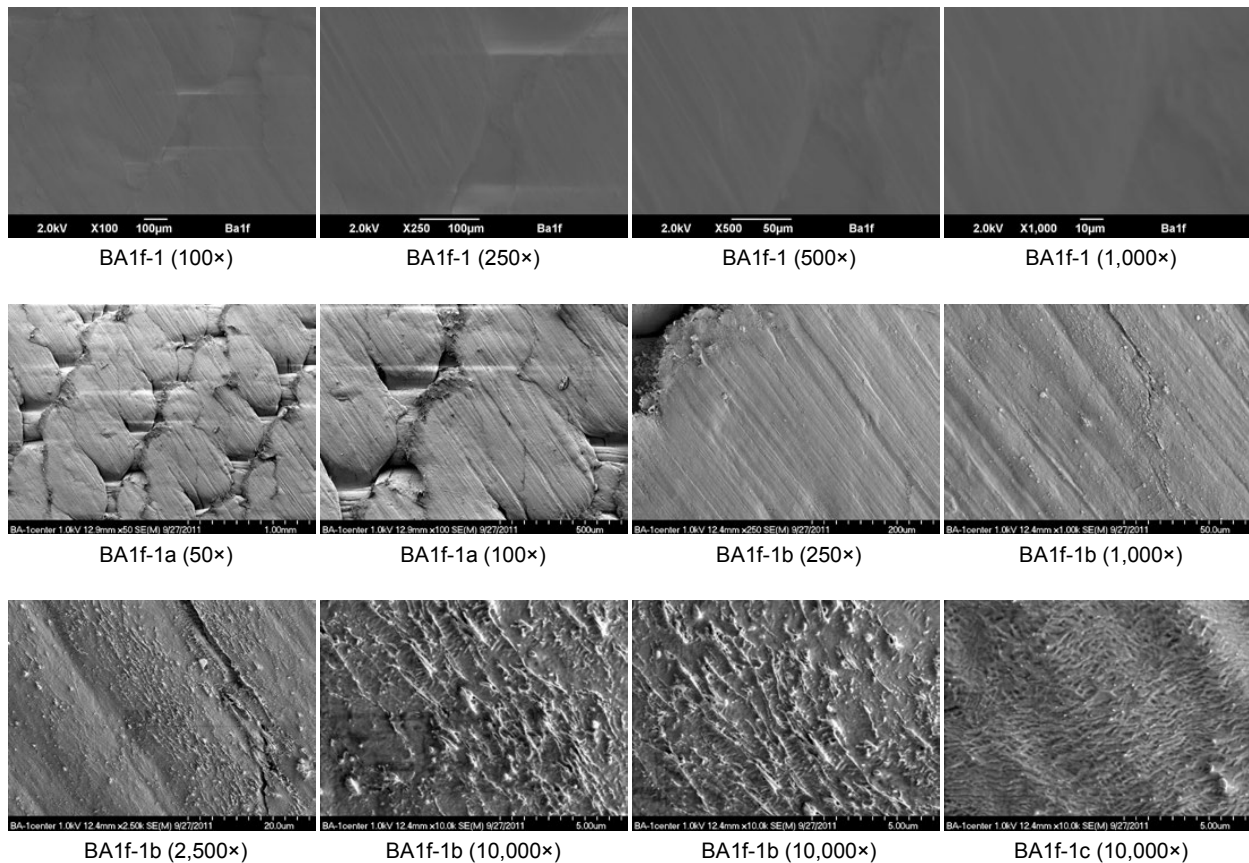
Appendix B.—Post-Flight Abraded Apollo Fabric

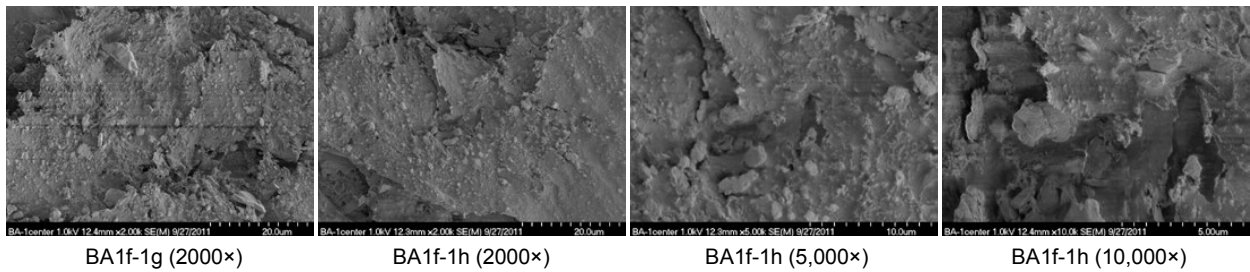
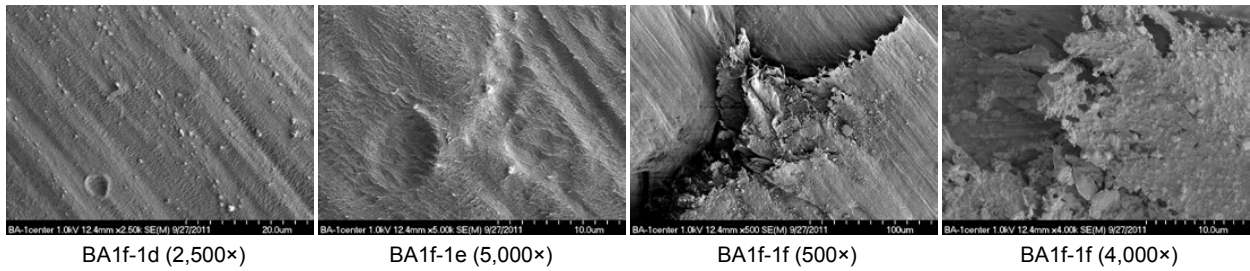
B.1 BA1f-1

B.1.1 Optical Microscopy



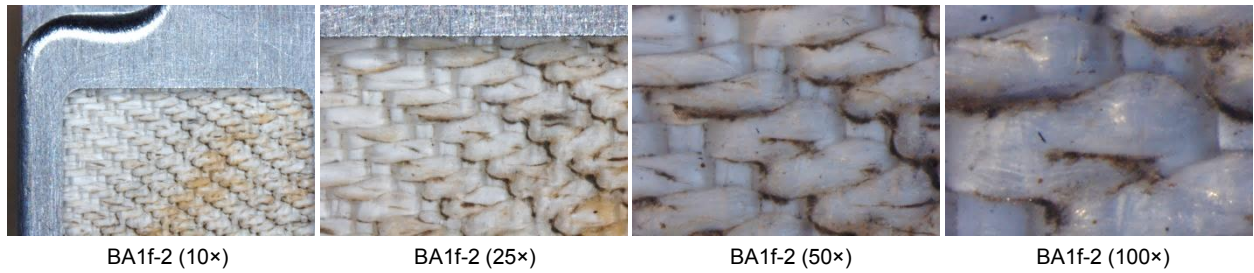
B.1.2 Electron Microscopy



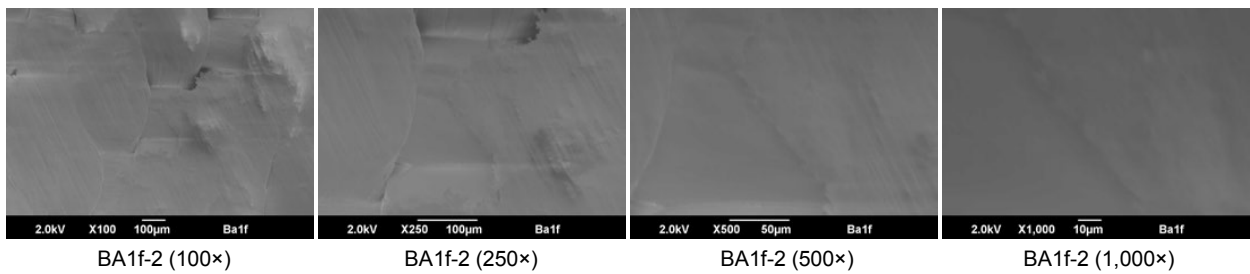


B.2 BA1f-2

B.2.1 Optical Microscopy

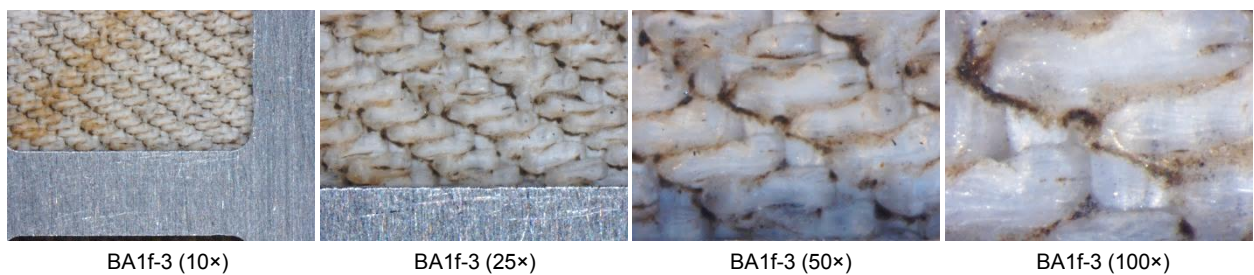


B.2.2 Electron Microscopy

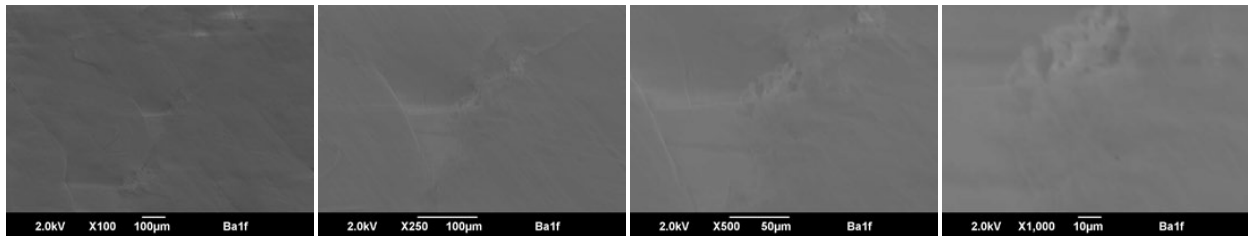


B.3 BA1f-3

B.3.1 Optical Microscopy



B.3.2 Electron Microscopy



BA1f-3 (100×)

BA1f-3 (250×)

BA1f-3 (500×)

BA1f-3 (1,000×)

B.4 BA1f-4

B.4.1 Optical Microscopy



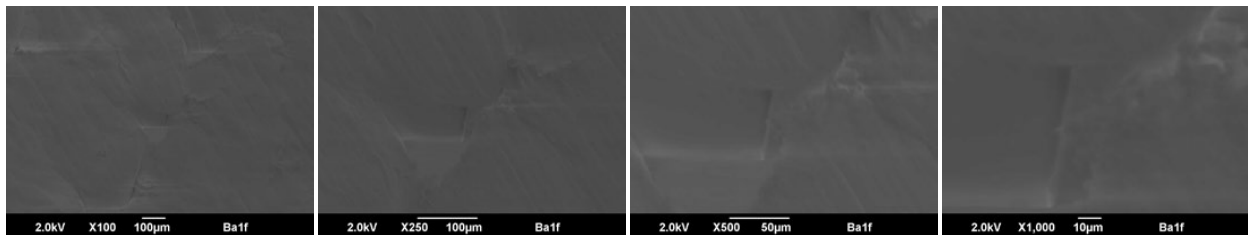
BA1f-4 (10×)

BA1f-4 (25×)

BA1f-4 (50×)

BA1f-4 (100×)

B.4.2 Electron Microscopy



BA1f-4 (100×)

BA1f-4 (250×)

BA1f-4 (500×)

BA1f-4 (1,000×)

B.5 BA1f-5

B.5.1 Optical Microscopy



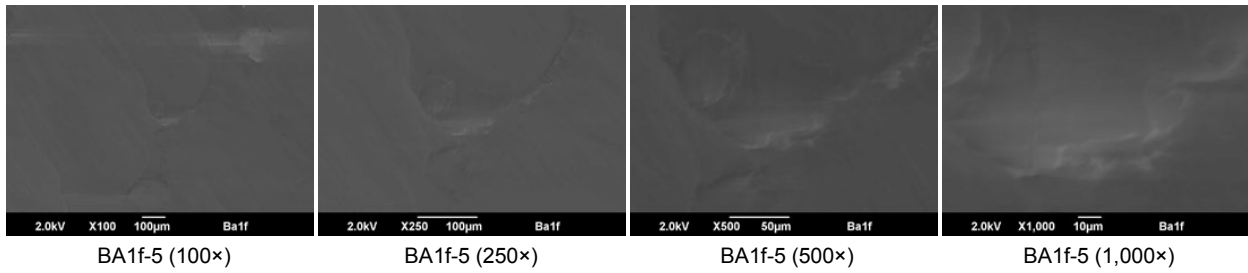
BA1f-5 (10×)

BA1f-5 (25×)

BA1f-5 (50×)

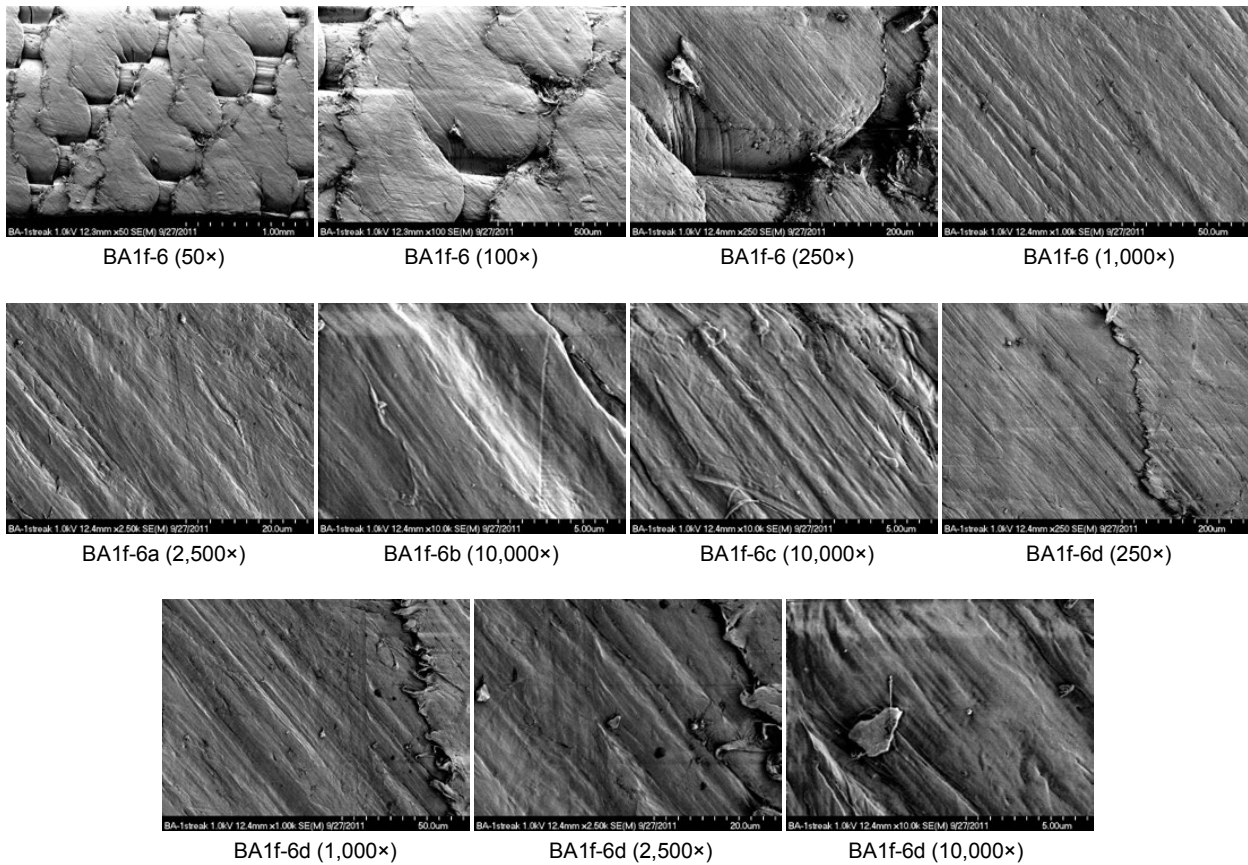
BA1f-5 (100×)

B.5.2 Electron Microscopy



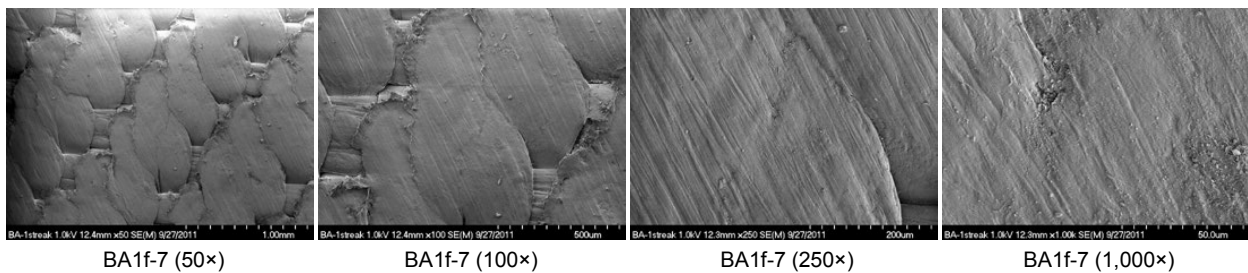
B.6 BA1f-6 (Edge Under Holder)

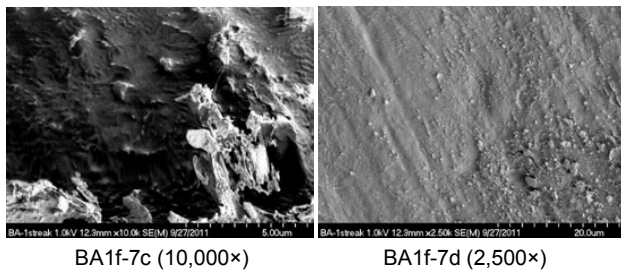
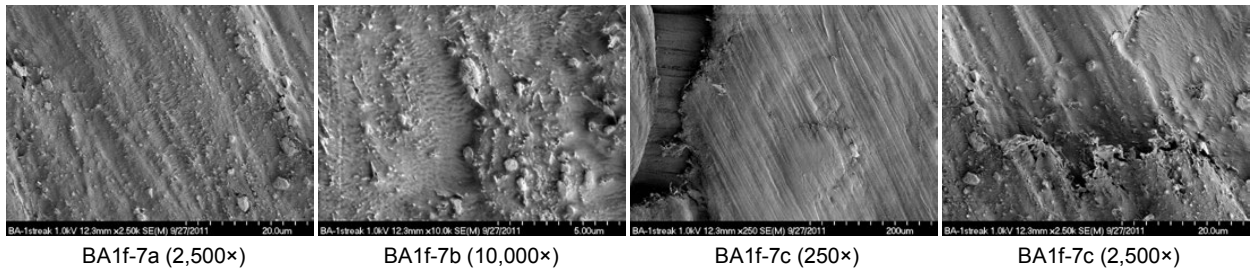
B.6.1 Electron Microscopy



B.7 BA1f-7 (Streak—Upper Left)

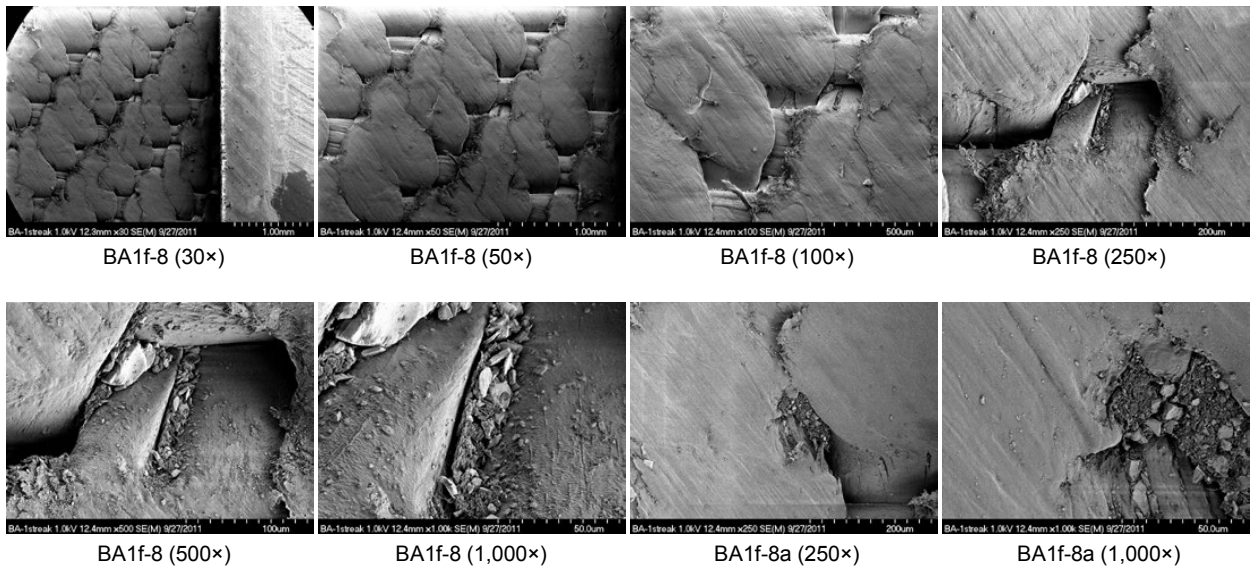
B.7.1 Electron Microscopy





B.8 BA1f-8 (Streak—Lower Right)

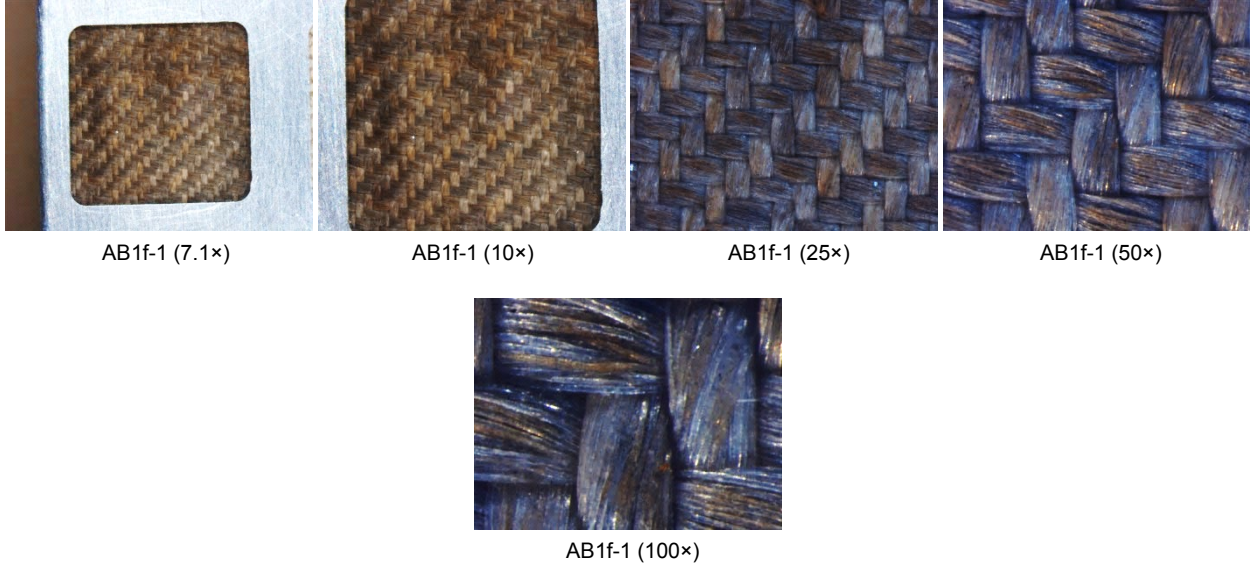
B.8.1 Electron Microscopy



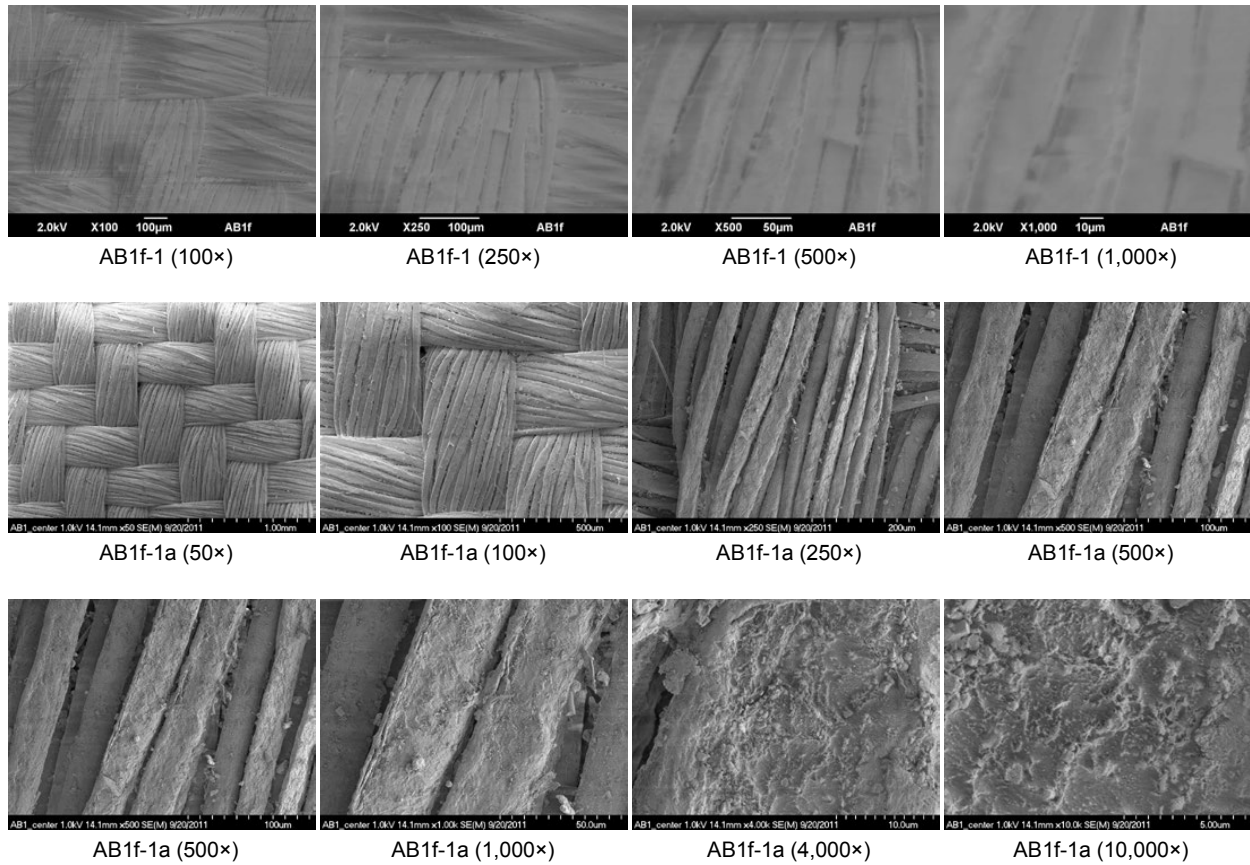
Appendix C.—Post-Flight Alan Bean Apollo 12 Fabric

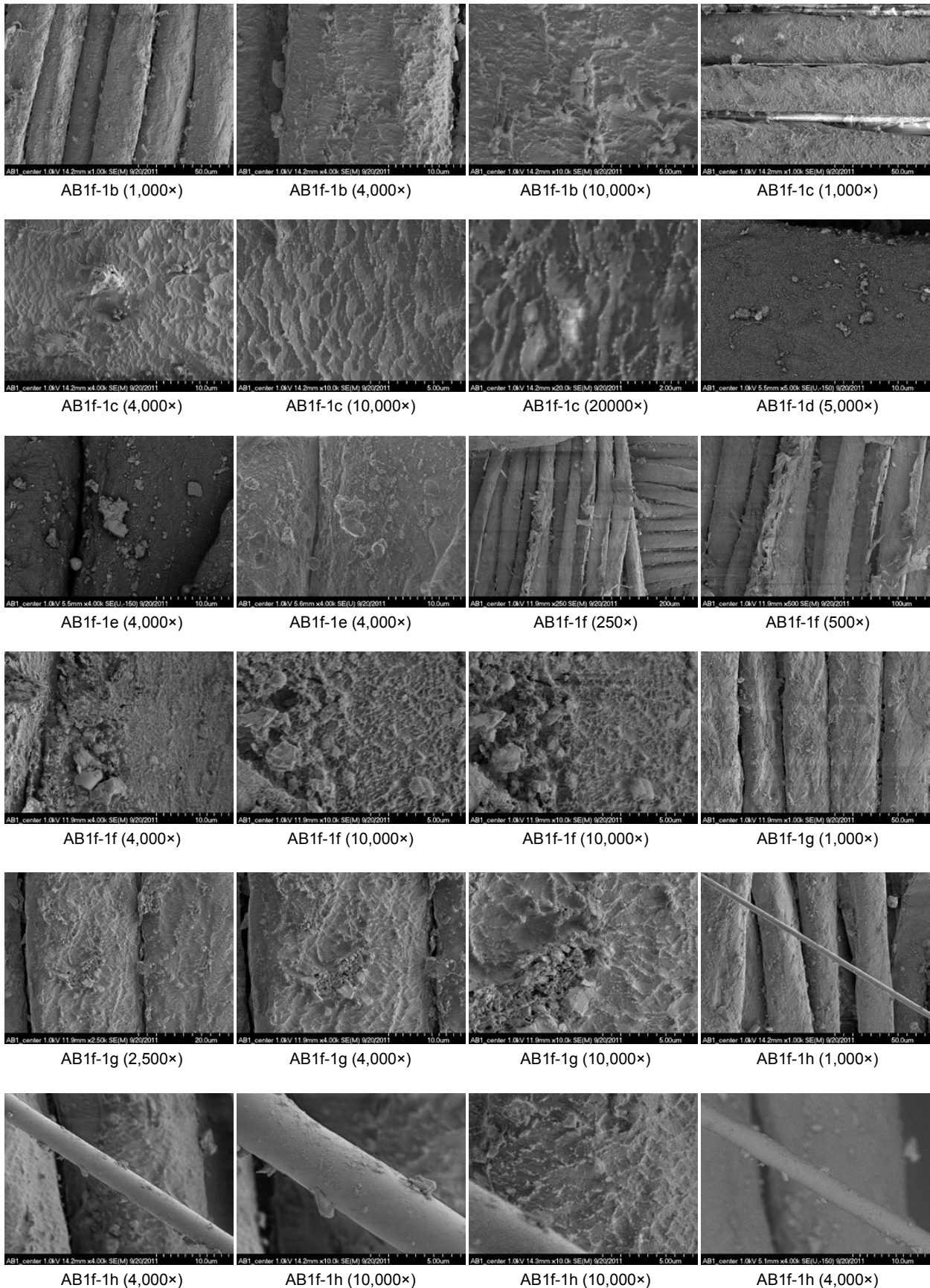
C.1 AB1f-1

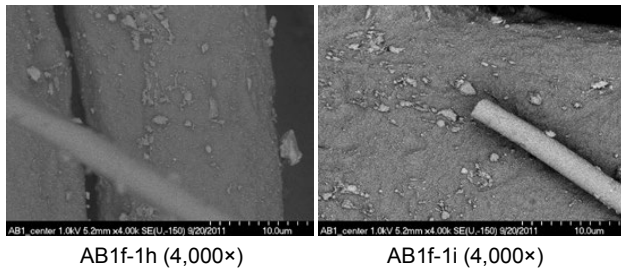
C.1.1 Optical Microscopy



C.1.2 Electron Microscopy

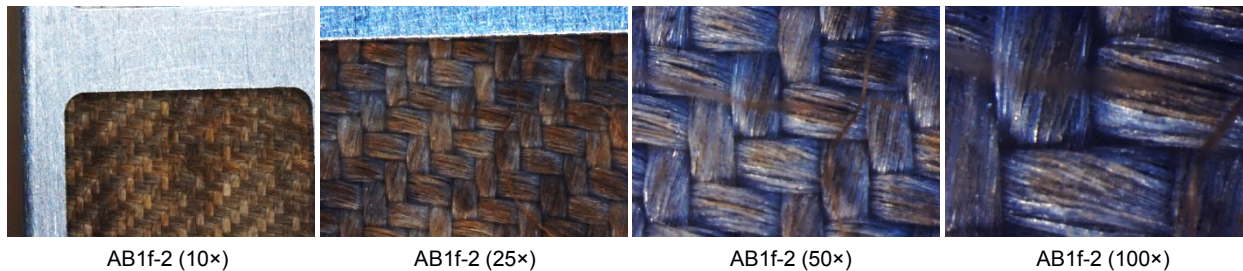




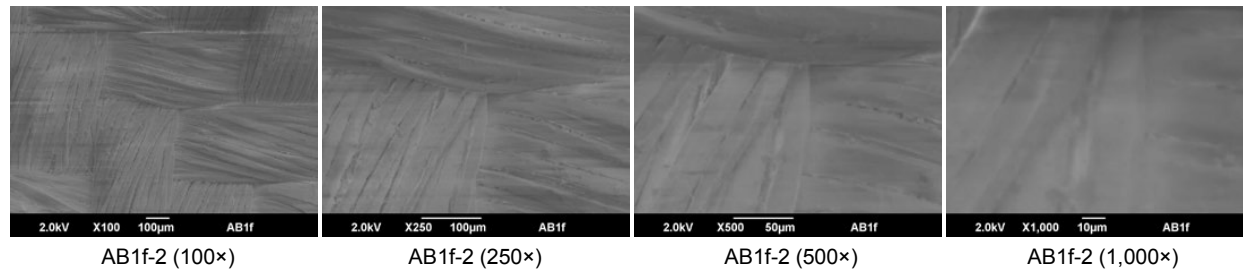


C.2 AB1f-2

C.2.1 Optical Microscopy

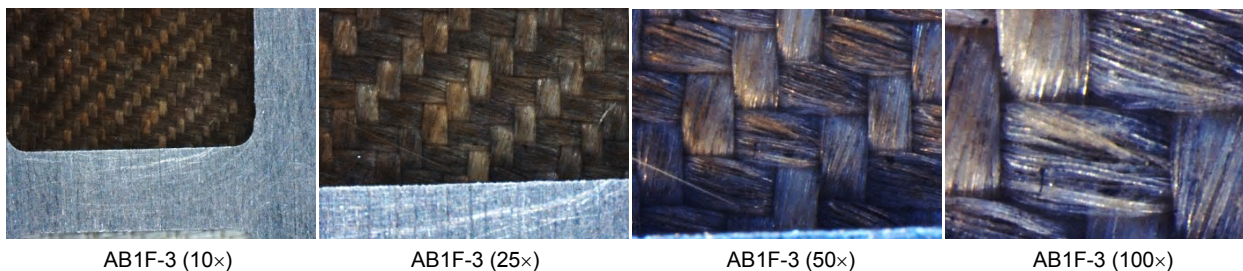


C.2.2 Electron Microscopy

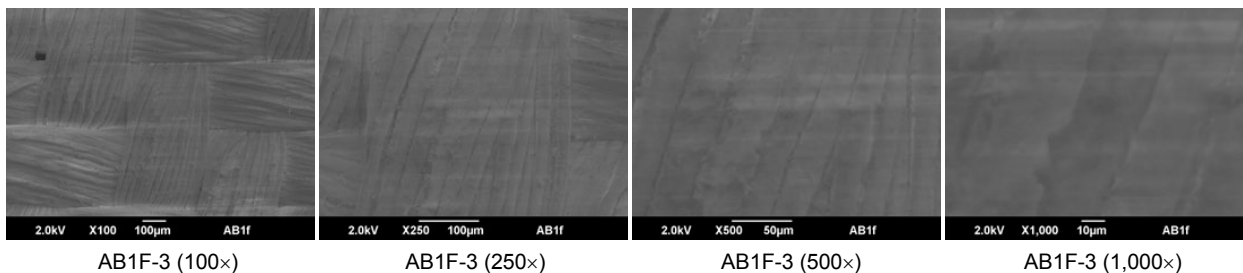


C.3 AB1f-3

C.3.1 Optical Microscopy



C.3.2 Electron Microscopy



C.4 AB1f-4

C.4.1 Optical Microscopy



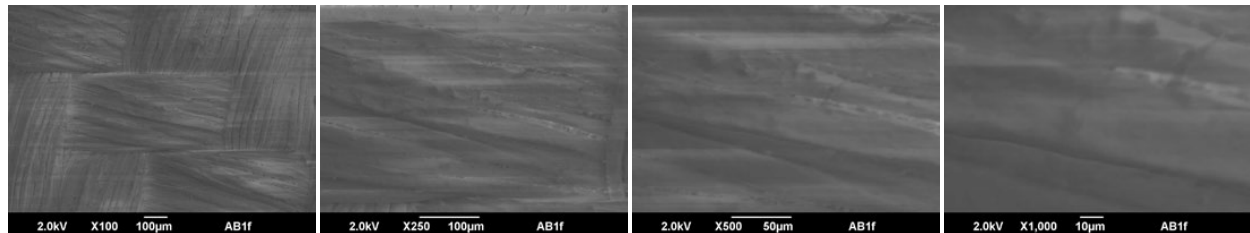
AB1f-4 (10×)

AB1f-4 (25×)

AB1f-4 (50×)

AB1f-4 (100×)

C.4.2 Electron Microscopy



AB1f-4 (100×)

AB1f-4 (250×)

AB1f-4 (500×)

AB1f-4 (1,000×)

C.5 AB1f-5

C.5.1 Optical Microscopy



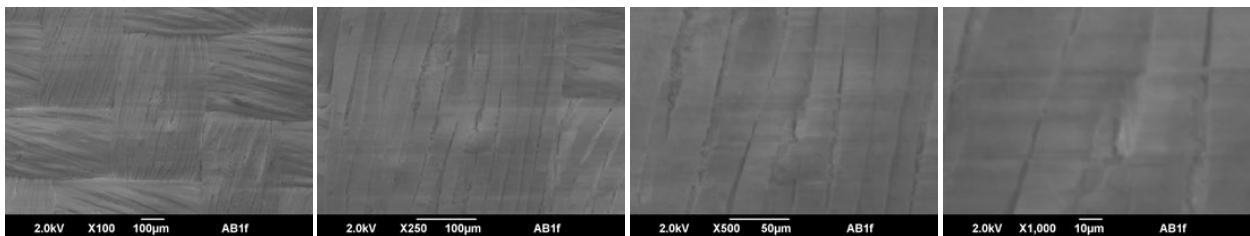
AB1F-5 (10×)

AB1F-5 (25×)

AB1F-5 (50×)

AB1F-5 (100×)

C.5.2 Electron Microscopy



AB1F-5 (100×)

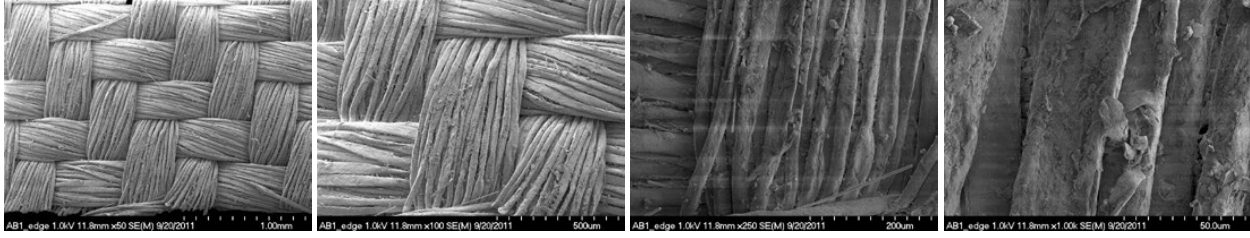
AB1F-5 (250×)

AB1F-5 (500×)

AB1F-5 (1,000×)

C.6 AB1f-6 (Edge Under Holder)

C.6.1 Electron Microscopy

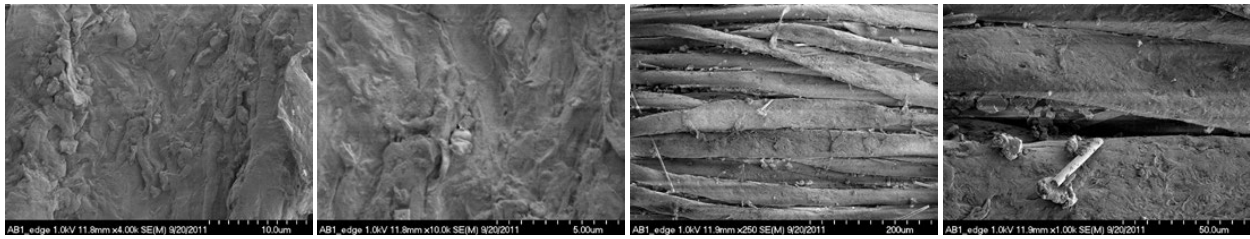


AB1F-6 (50×)

AB1F-6 (100×)

AB1F-6 (250×)

AB1F-6 (1,000×)

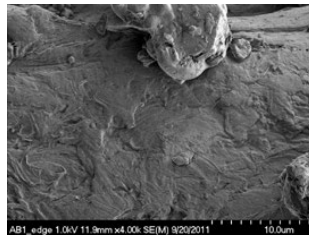


AB1F-6 (4,000×)

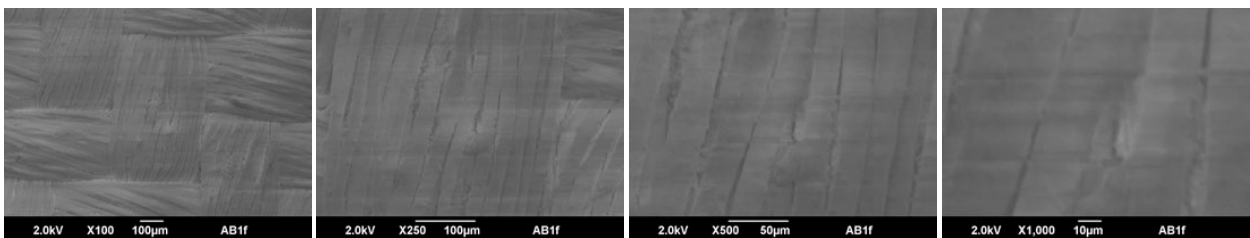
AB1F-6 (10,000×)

AB1F-6a (250×)

AB1F-6a (1,000×)



AB1F-6a (4,000×)



AB1F-6b (100×)

AB1F-6b (250×)

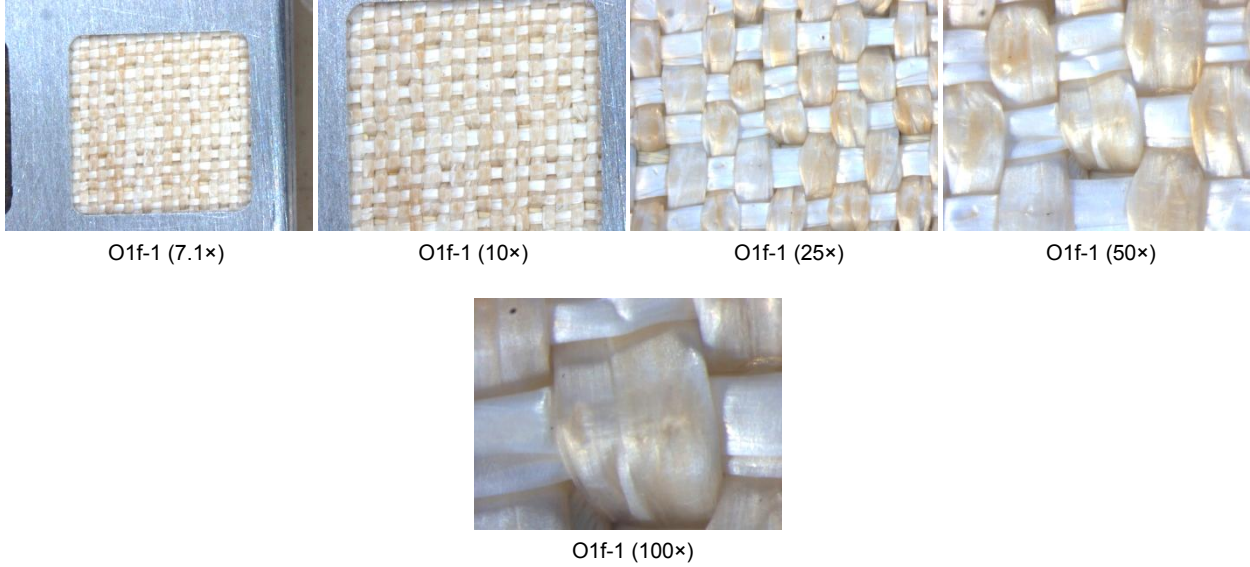
AB1F-6b (500×)

AB1F-6b (1,000×)

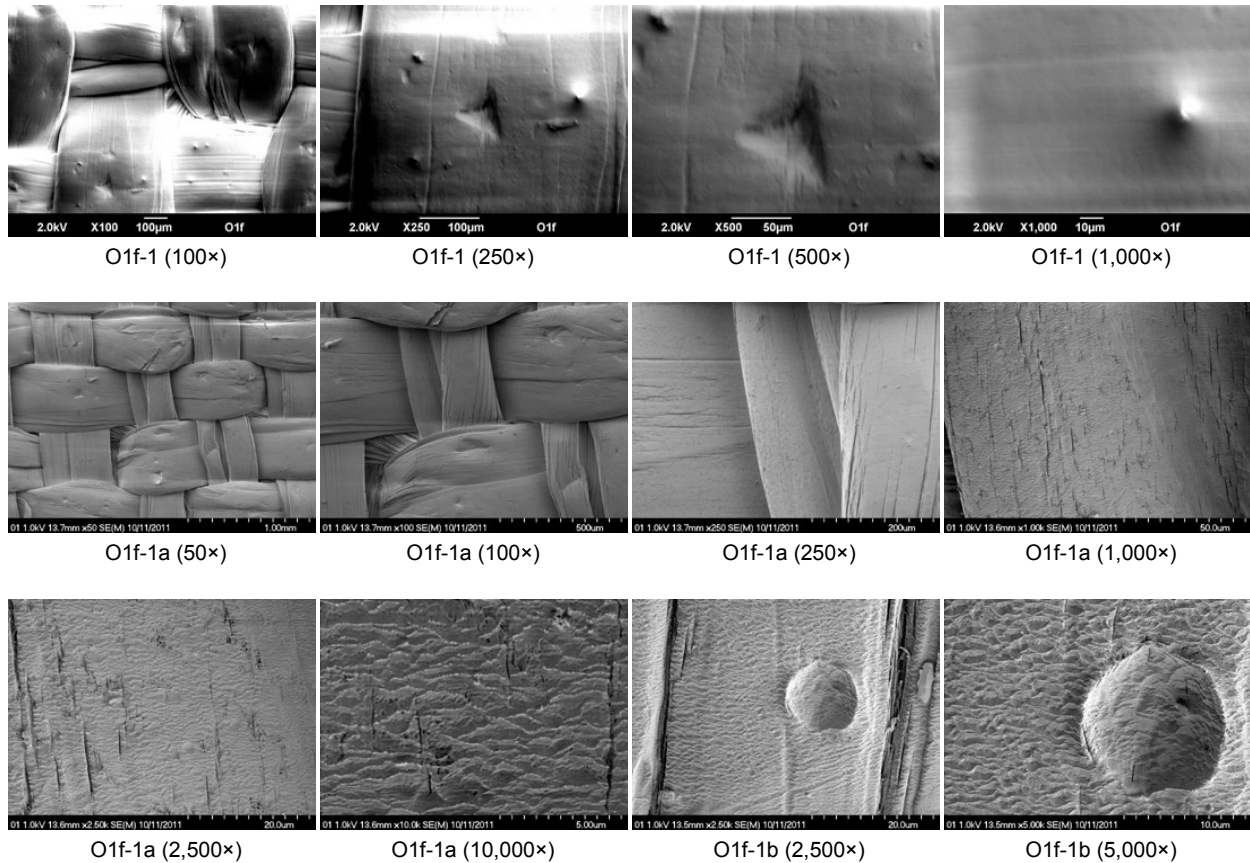
Appendix D.—Post-Flight Pristine Ortho-Fabric

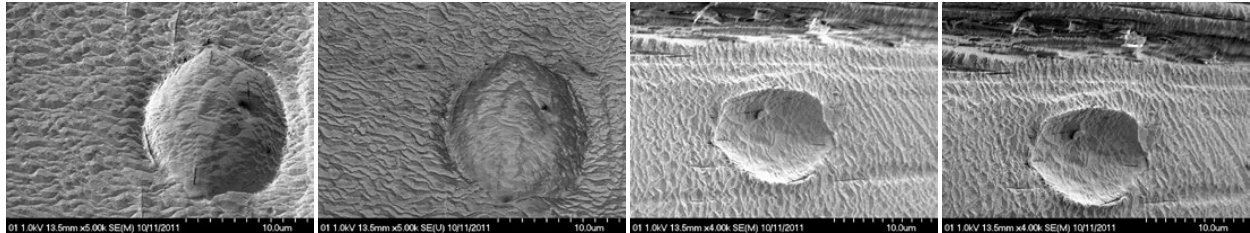
D.1 O1f-1

D.1.1 Optical Microscopy



D.1.2 Electron Microscopy



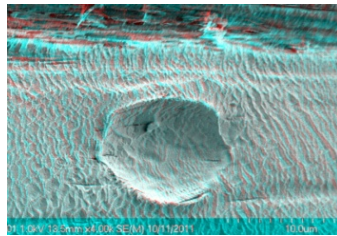


O1f-1b (5,000×)

O1f-1b (5,000×)

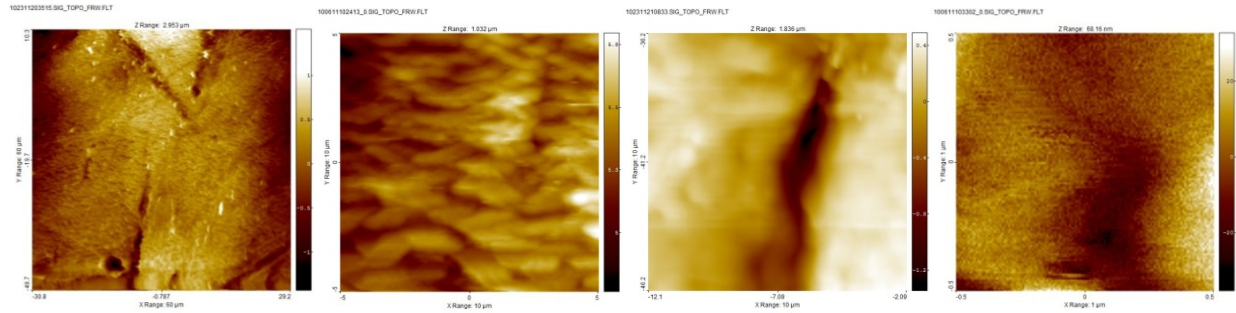
O1f-1b (4,000×)

O1f-1b (4,000×)



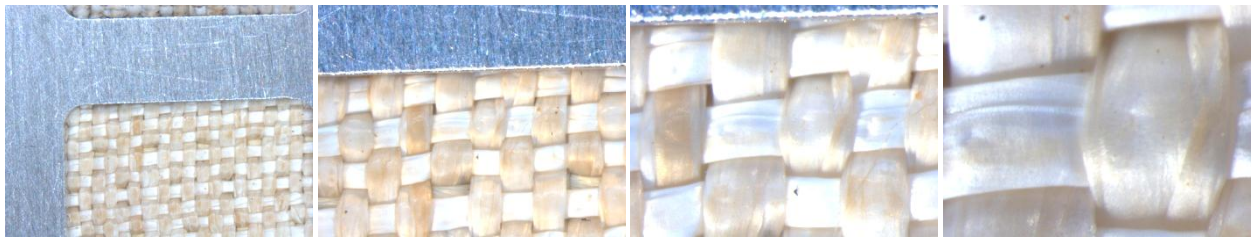
O1f-1b (4,000×)

D.1.3 Atomic Force Microscopy



D.2 O1f-2

D.2.1 Optical Microscopy



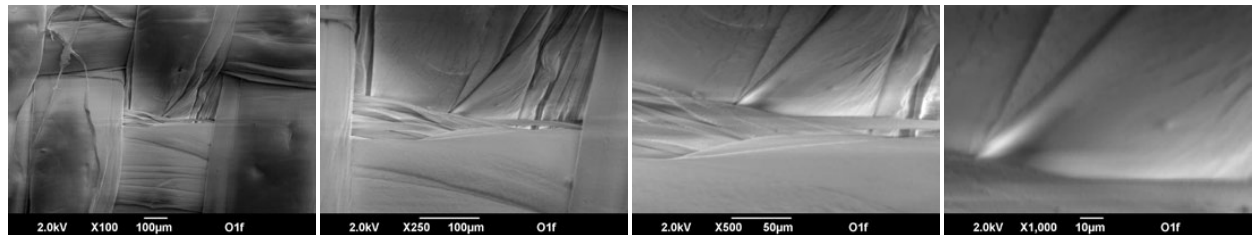
O1f-2 (10×)

O1f-2 (25×)

O1f-2 (50×)

O1f-2 (100×)

D.2.2 Electron Microscopy

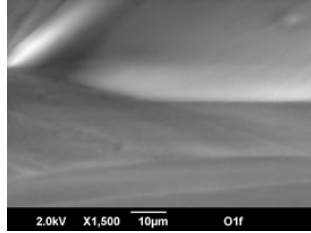


O1f-2 (100×)

O1f-2 (250×)

O1f-2 (500×)

O1f-2 (1,000×)



O1f-2 (1,500×)

D.3 O1f-3

D.3.1 Optical Microscopy



O1f-3 (10×)



O1f-3 (25×)

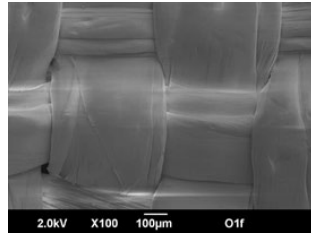


O1f-3 (50×)

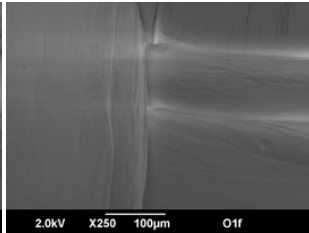


O1f-3 (100×)

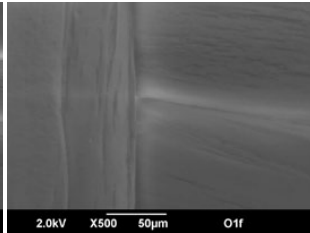
D.3.2 Electron Microscopy



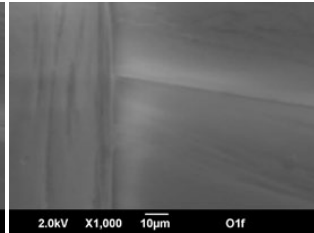
O1f-3 (100×)



O1f-3 (250×)



O1f-3 (500×)



O1f-3 (1,000×)

D.4 O1f-4

D.4.1 Optical Microscopy



O1f-4 (10×)



O1f-4 (25×)

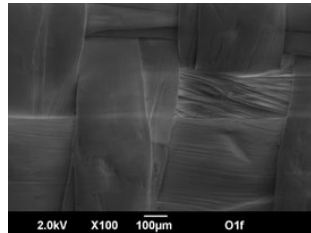


O1f-4 (50×)

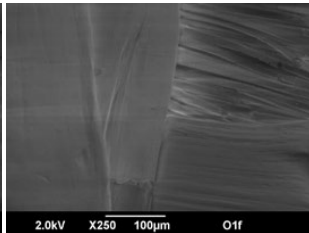


O1f-4 (100×)

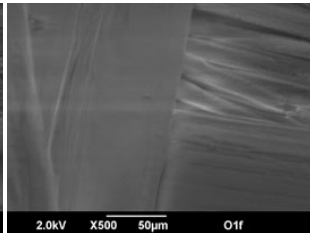
D.4.2 Electron Microscopy



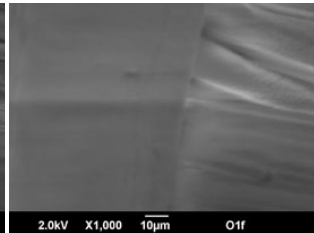
O1f-4 (100×)



O1f-4 (250×)

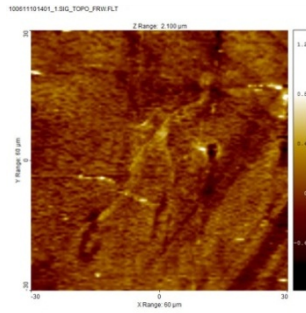


O1f-4 (500×)



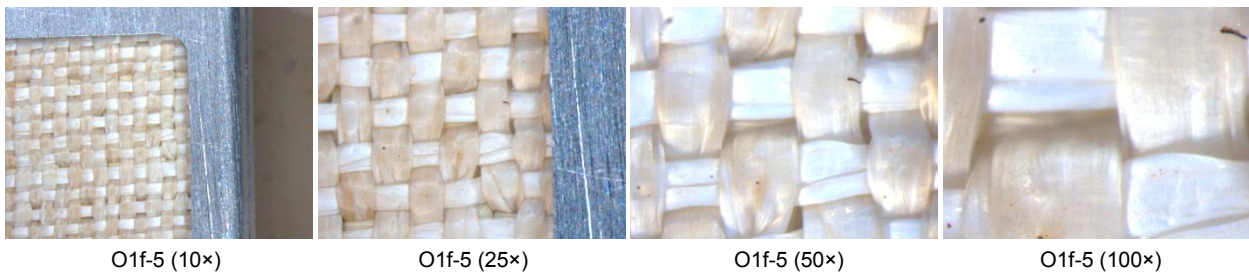
O1f-4 (1,000×)

D.4.3 Atomic Force Microscopy

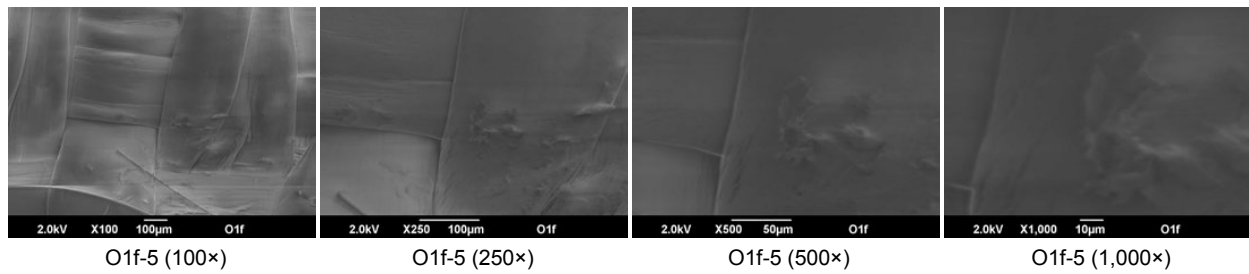


D.5 O1f-5

D.5.1 Optical Microscopy

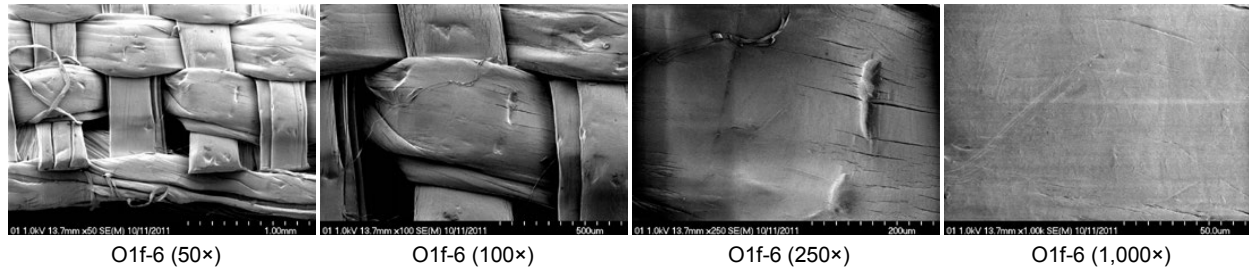


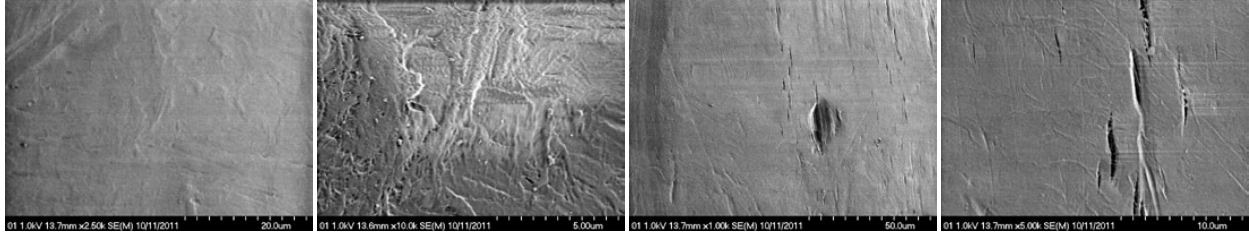
D.5.2 Electron Microscopy



D.6 O1f-6 (Edge Under Holder)

D.6.1 Electron Microscopy



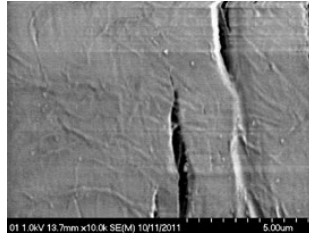


O1f-6 (2,500×)

O1f-6 (10,000×)

O1f-6a (1,000×)

O1f-6a (5,000×)

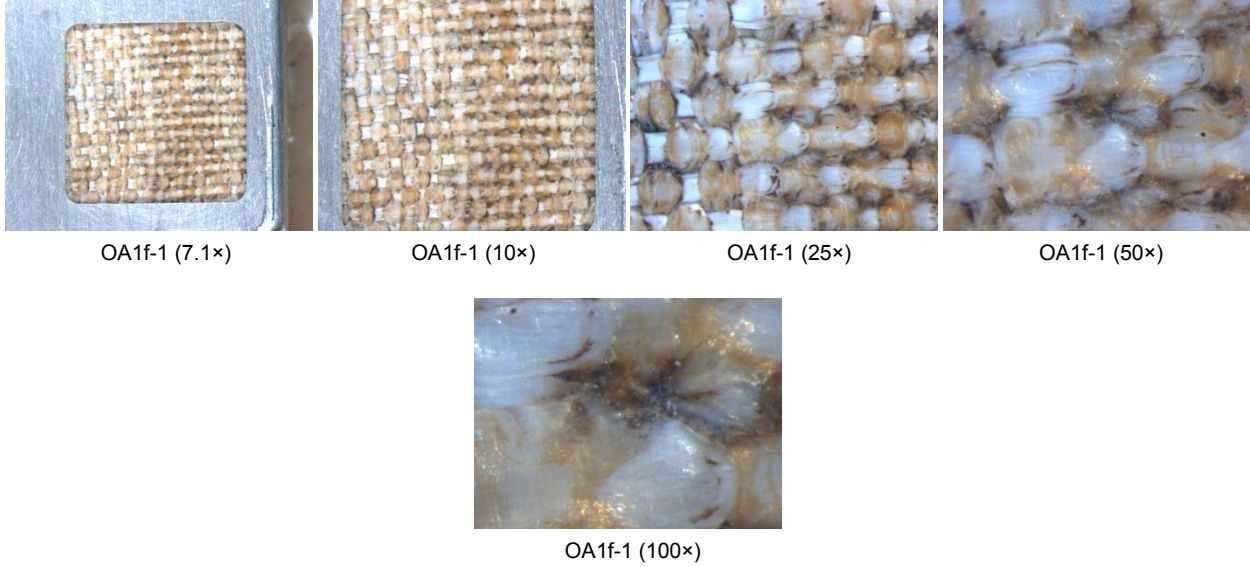


O1f-6a (10,000×)

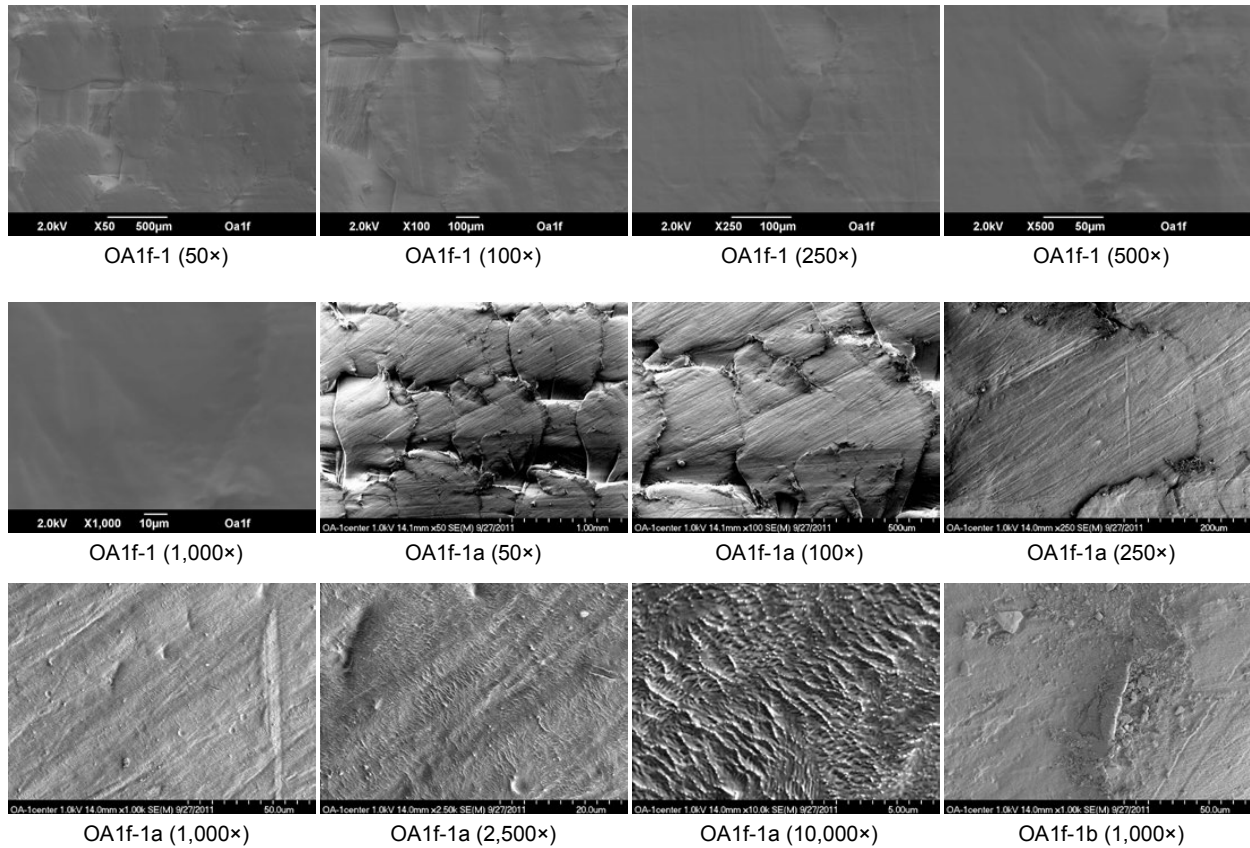
Appendix E.—Post-Flight Abraded Ortho-Fabric

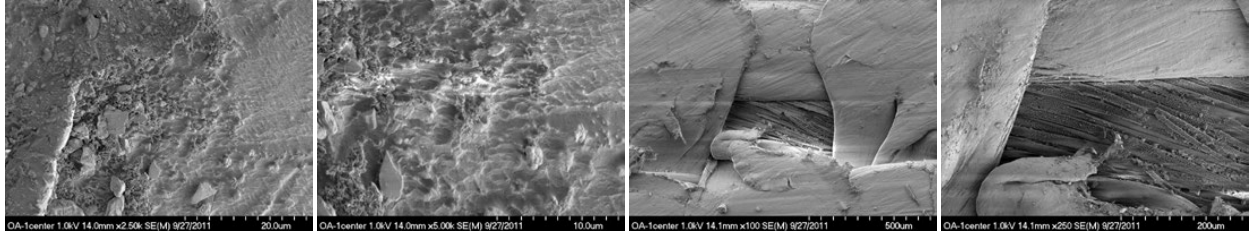
E.1 OA1f-1

E.1.1 Optical Microscopy



E.1.2 Electron Microscopy



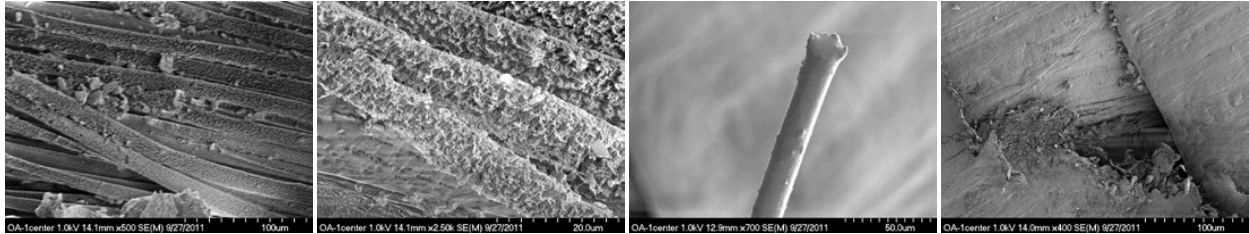


OA1f-1b (2,500×)

OA1f-1b (5,000×)

OA1f-1c (100×)

OA1f-1c (250×)

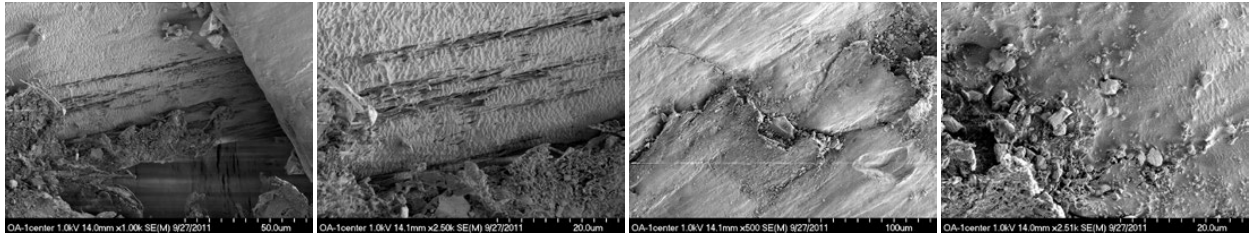


OA1f-1c (500×)

OA1f-1c (2,500×)

OA1f-1d (700×)

OA1f-1e (400×)

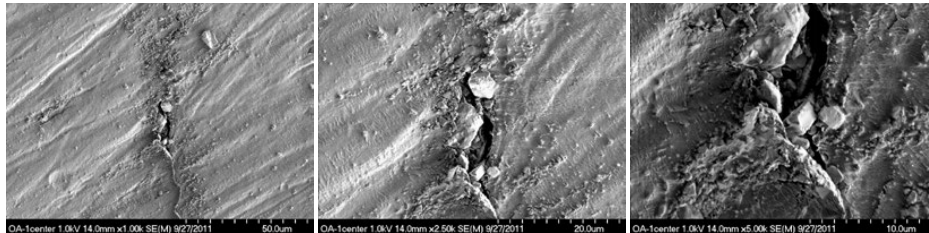


OA1f-1e (1,000×)

OA1f-1e (2,500×)

OA1f-1f (500×)

OA1f-1f (2,510×)

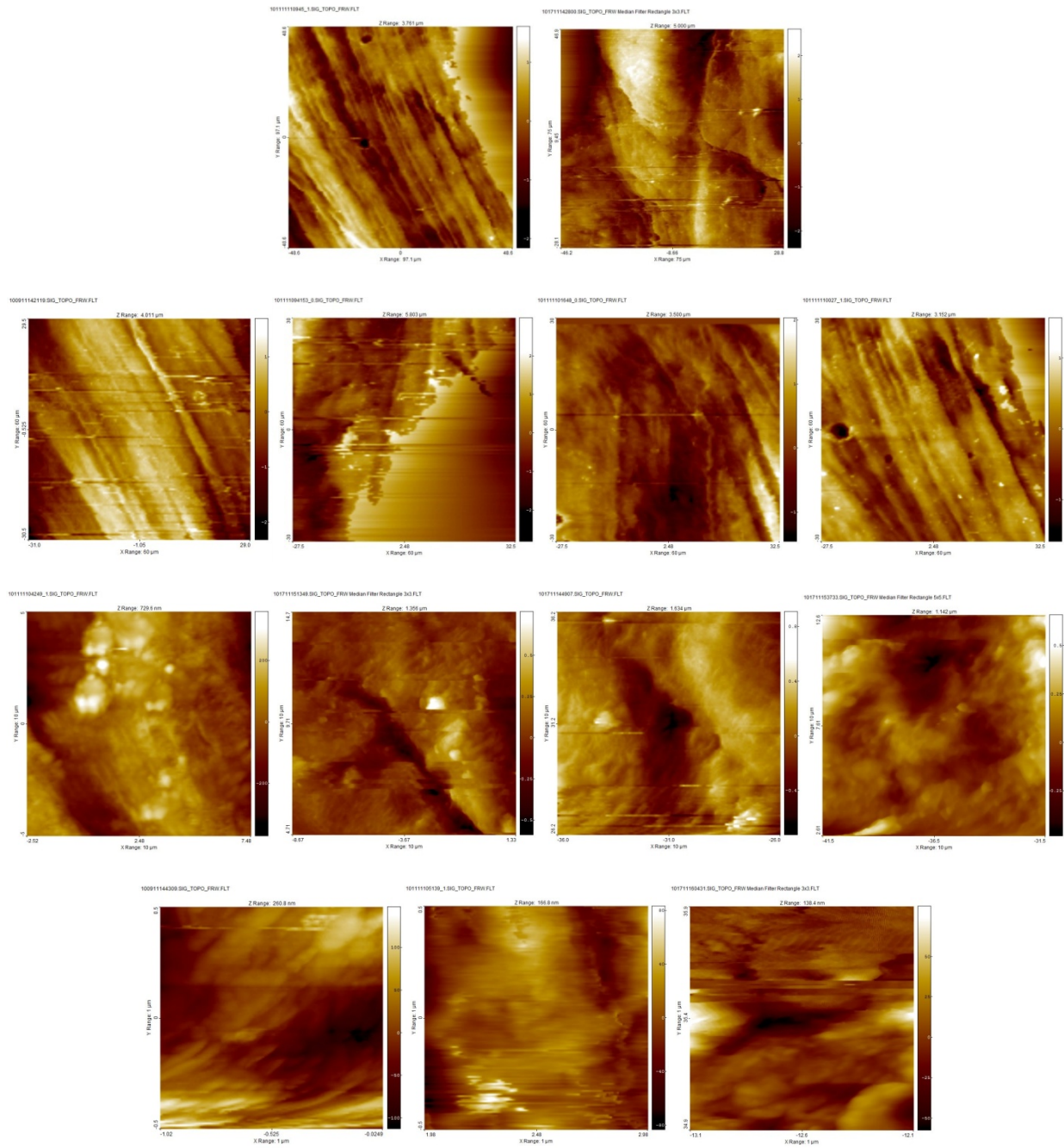


OA1f-1g (1,000×)

OA1f-1g (2,500×)

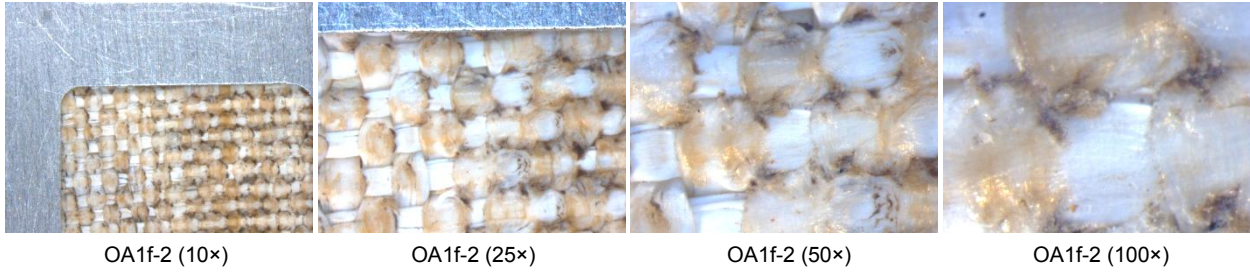
OA1f-1g (5,000×)

E.1.3 Atomic Force Microscopy

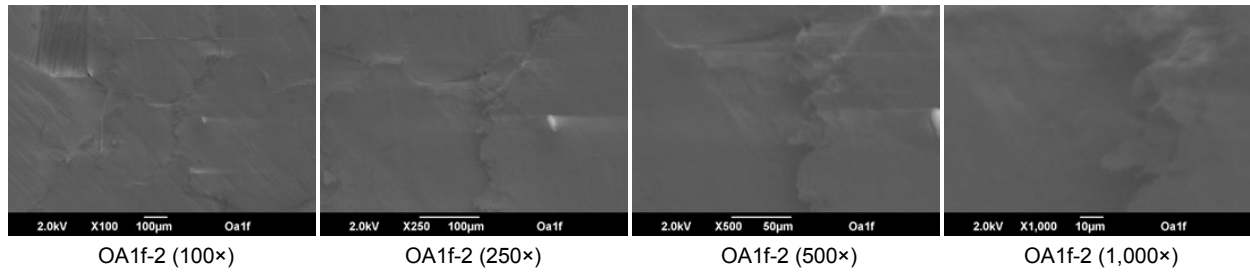


E.2 OA1f-2

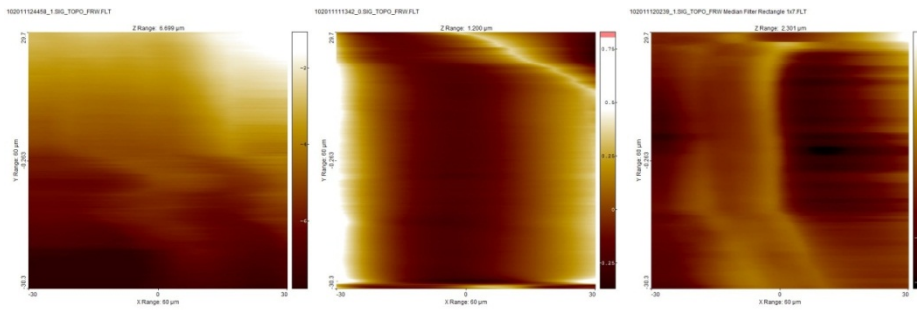
E.2.1 Optical Microscopy



E.2.2 Electron Microscopy

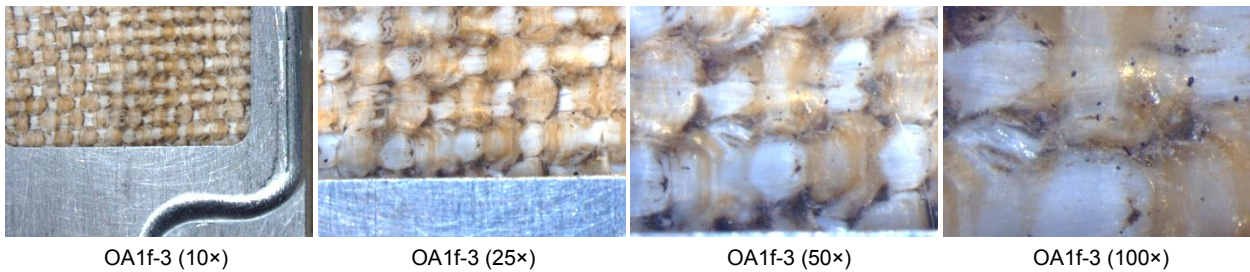


E.2.3 Atomic Force Microscopy

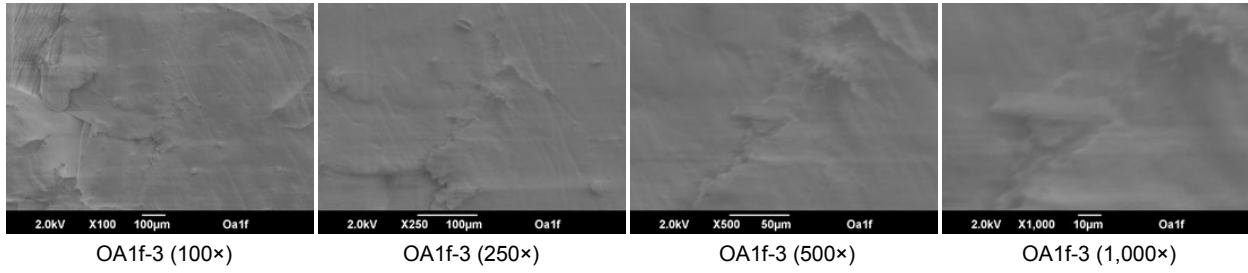


E.3 OA1f-3

E.3.1 Optical Microscopy

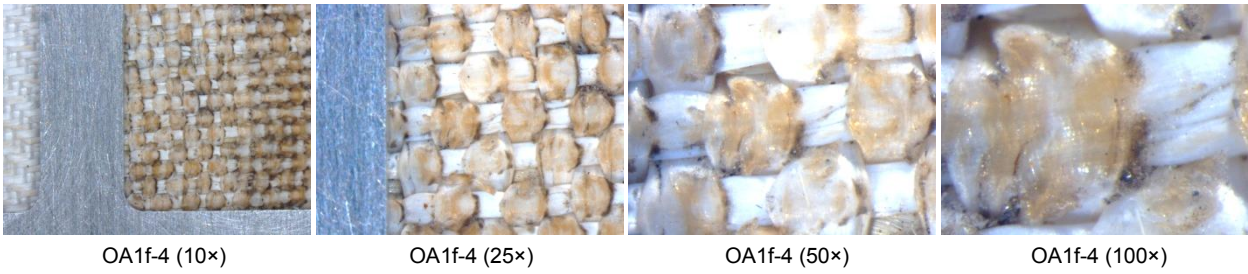


E.3.2 Electron Microscopy

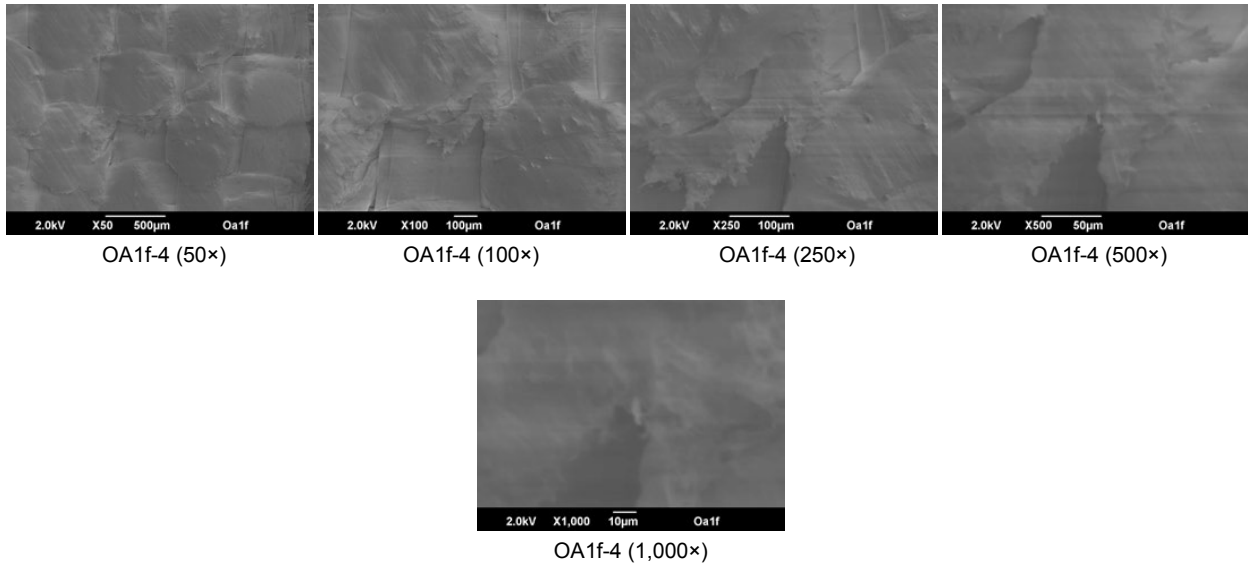


E.4 OA1f-4

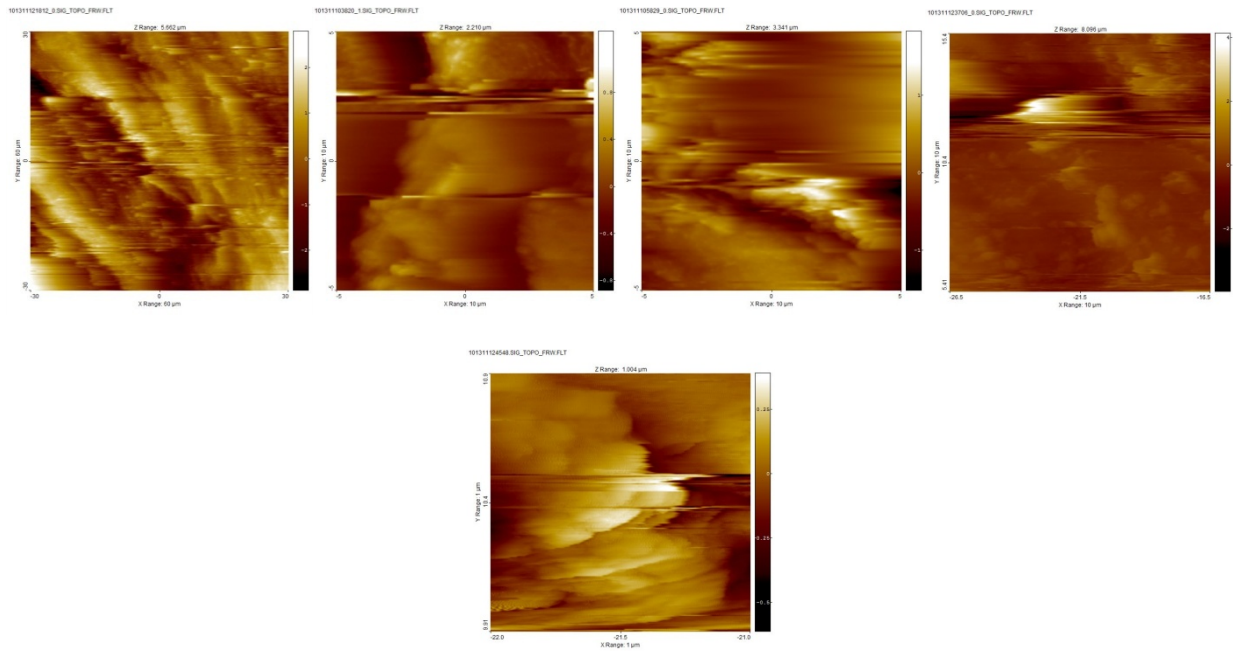
E.4.1 Optical Microscopy



E.4.2 Electron Microscopy

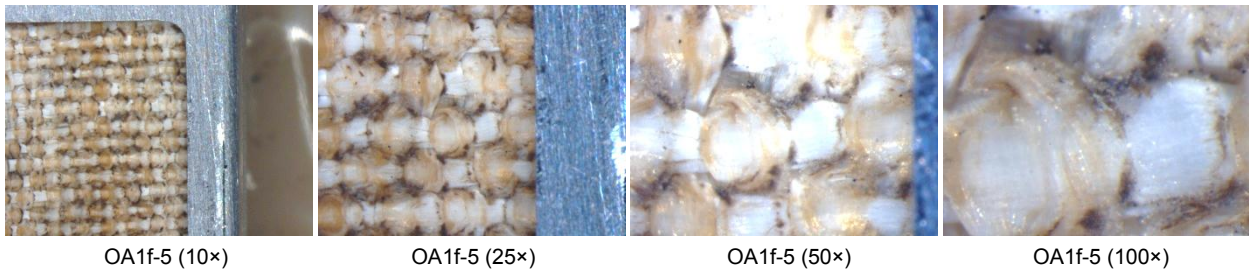


E.4.3 Atomic Force Microscopy

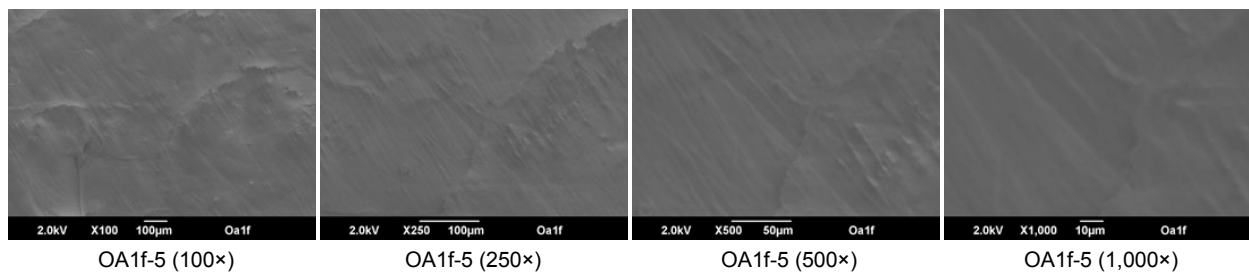


E.5 OA1f-5

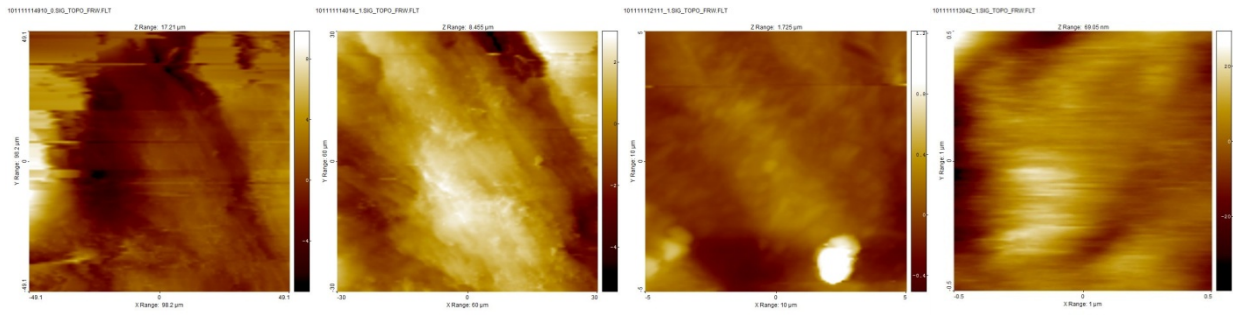
E.5.1 Optical Microscopy



E.5.2 Electron Microscopy

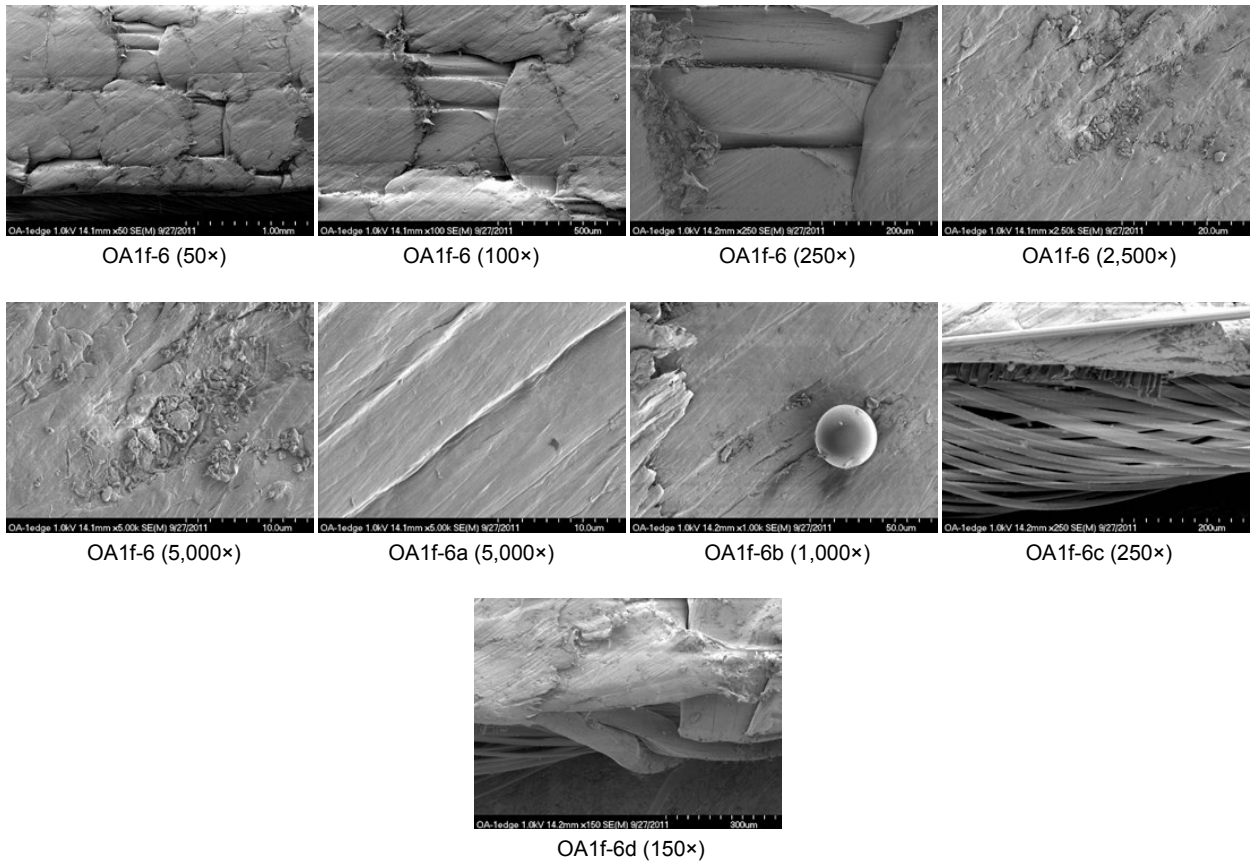


E.5.3 Atomic Force Microscopy



E.6 OA1f-6 (Edge Under Holder)

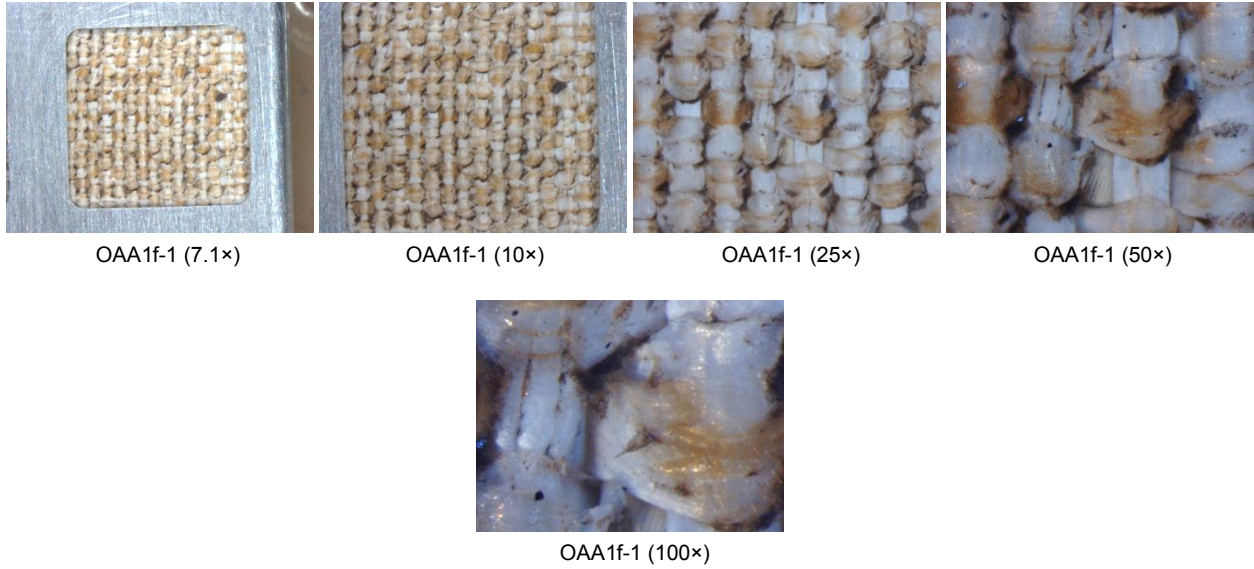
E.6.1 Electron Microscopy



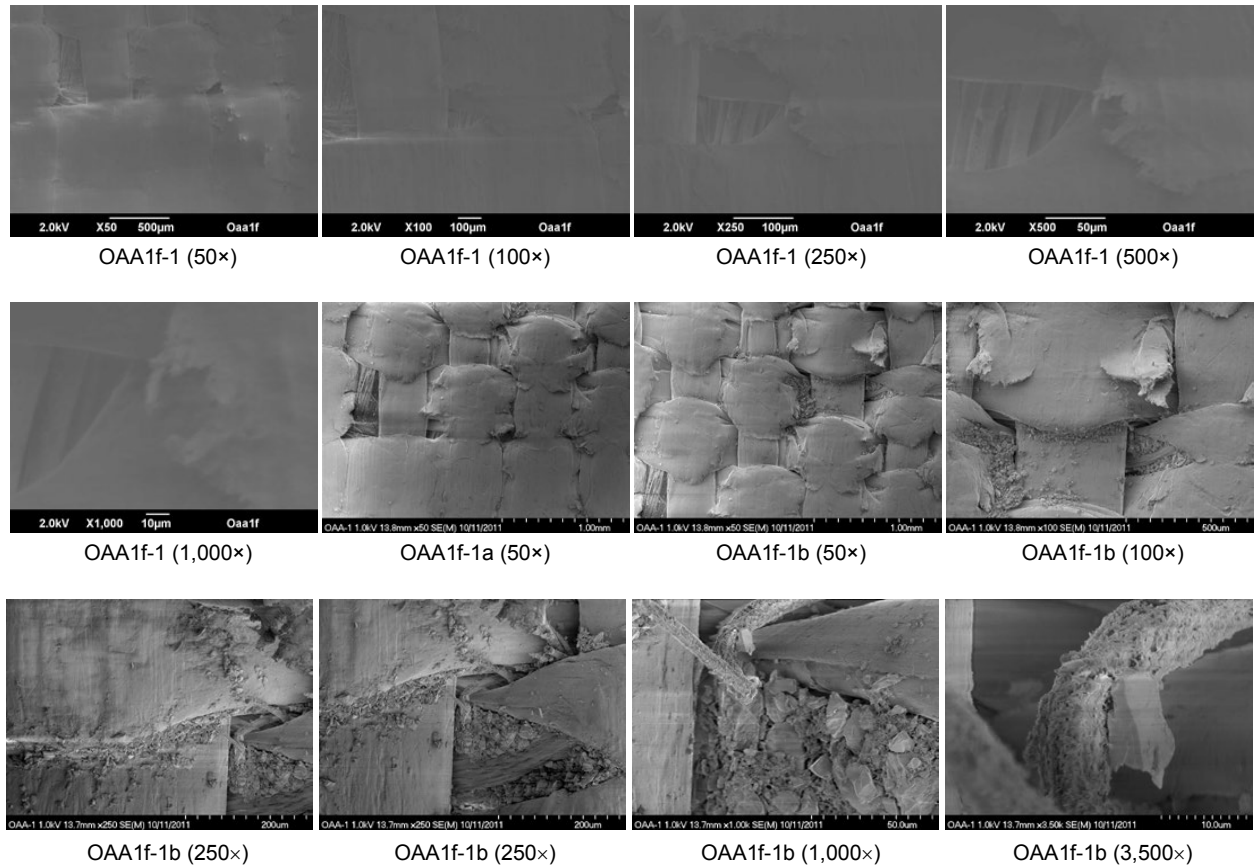
Appendix F.—Post-Flight Doubly Abraded Ortho-Fabric

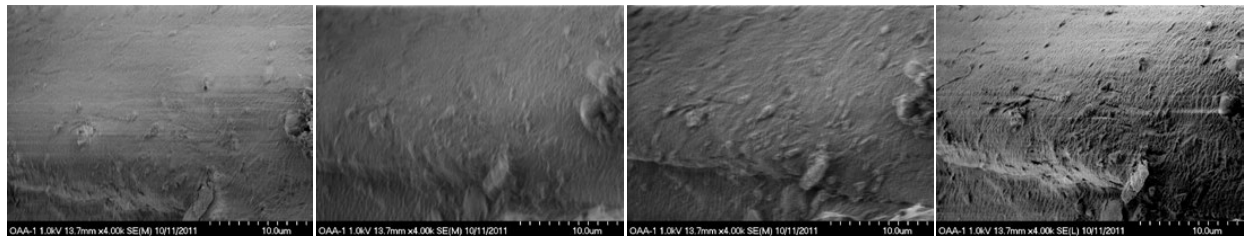
F.1 OAA1f-1

F.1.1 Optical Microscopy



F.1.2 Electron Microscopy



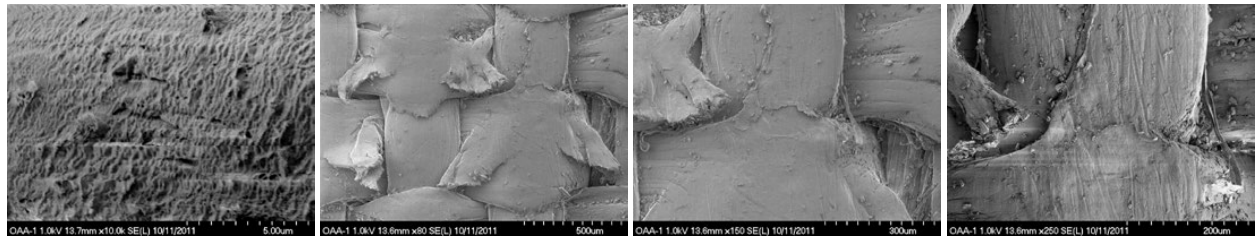


OAA1f-1c (4,000×)

OAA1f-1c (4,000×)

OAA1f-1c (4,000×)

OAA1f-1c (4,000×)

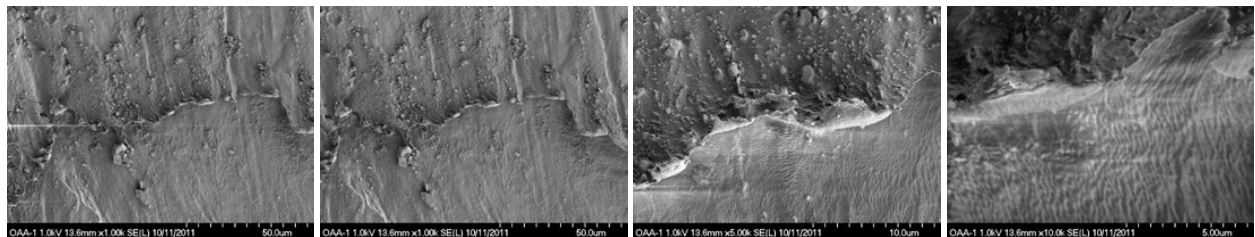


OAA1f-1c (10,000×)

OAA1f-1d (80×)

OAA1f-1d (150×)

OAA1f-1d (250×)



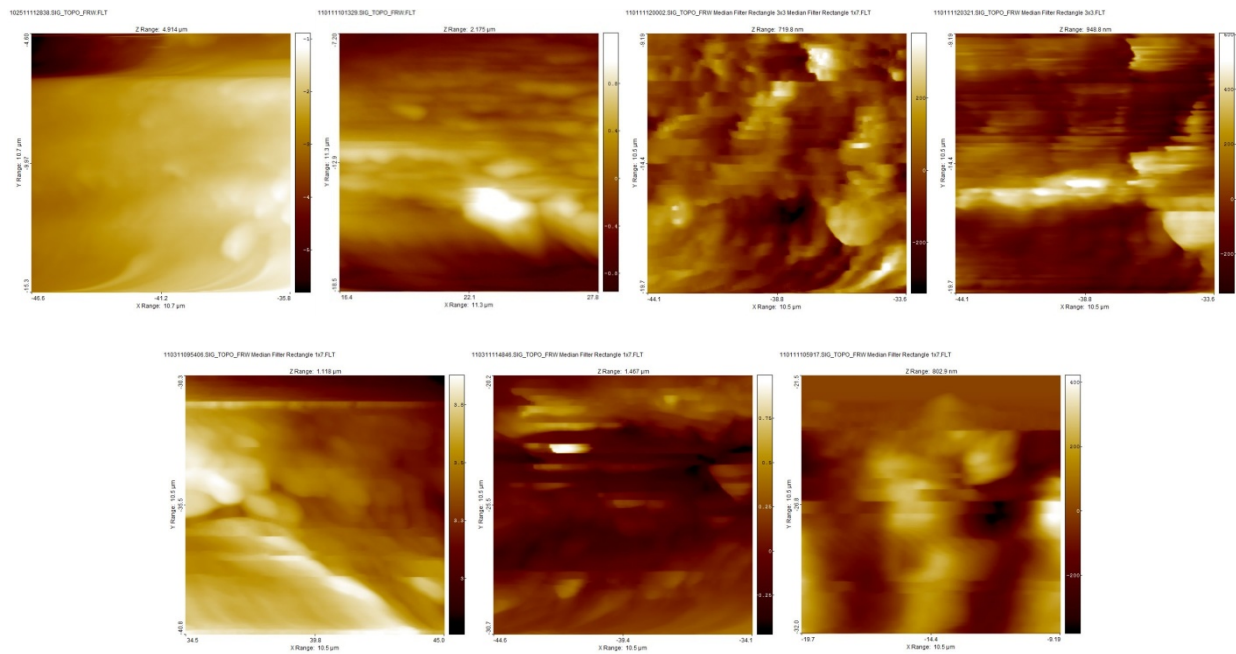
OAA1f-1d (1,000×)

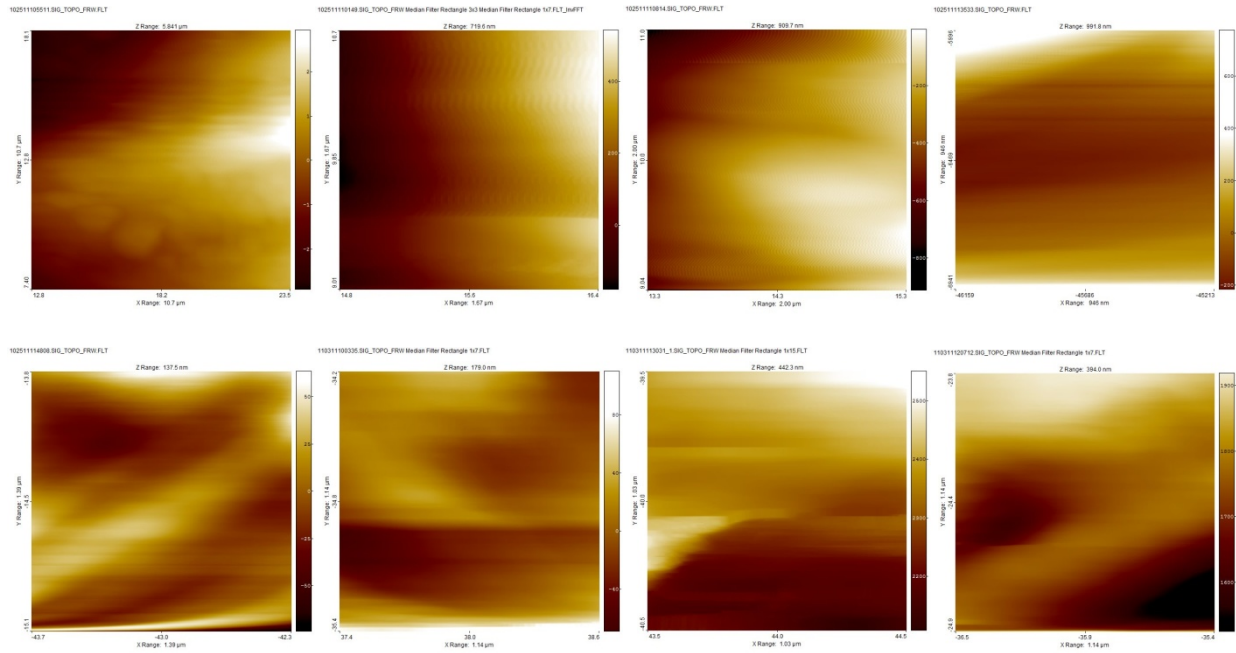
OAA1f-1d (1,000×)

OAA1f-1d (5,000×)

OAA1f-1d (10,000×)

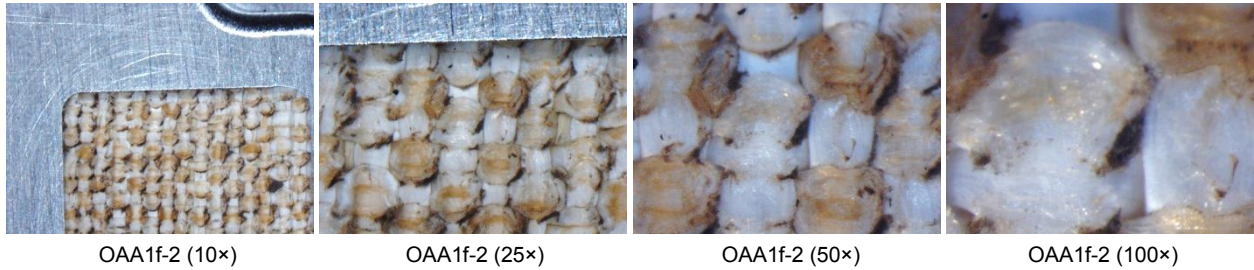
F.1.3 Atomic Force Microscopy



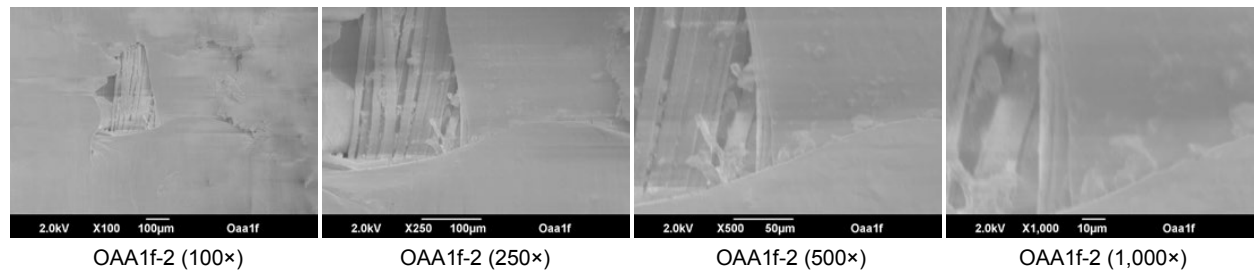


F.2 OAA1f-2

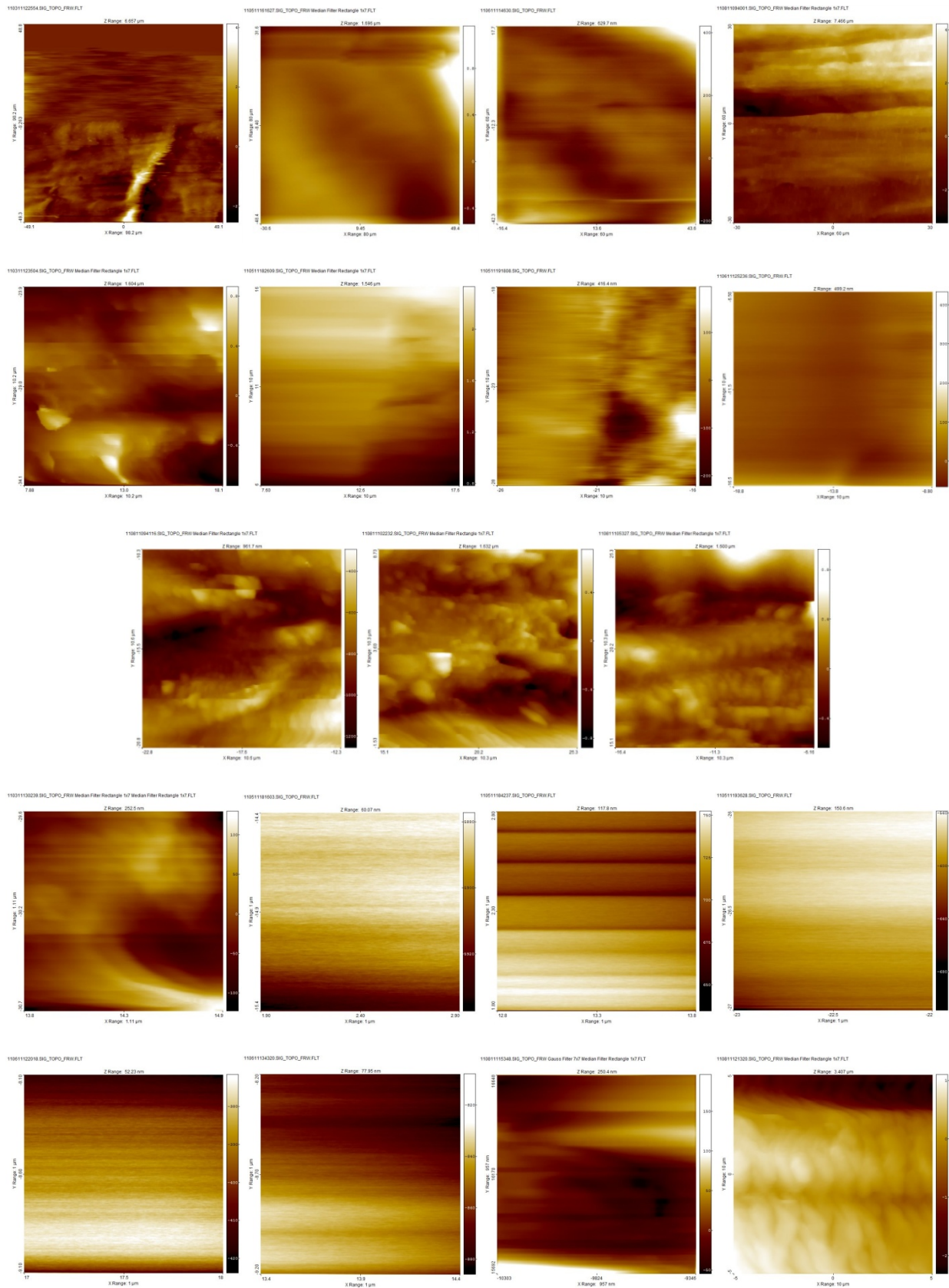
F.2.1 Optical Microscopy



F.2.2 Electron Microscopy

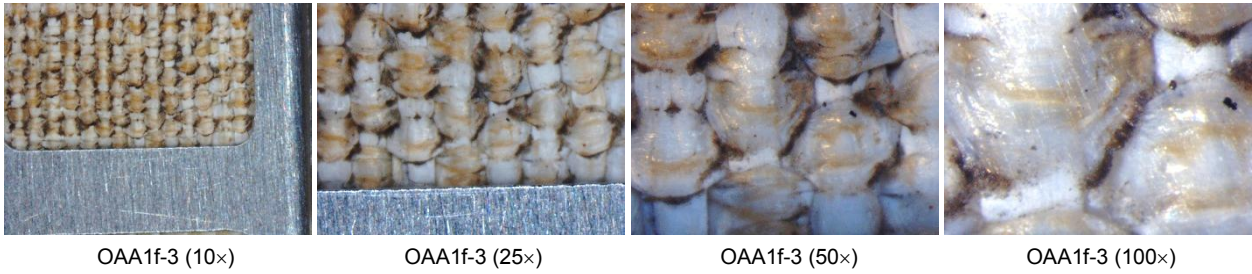


F.2.3 Atomic Force Microscopy

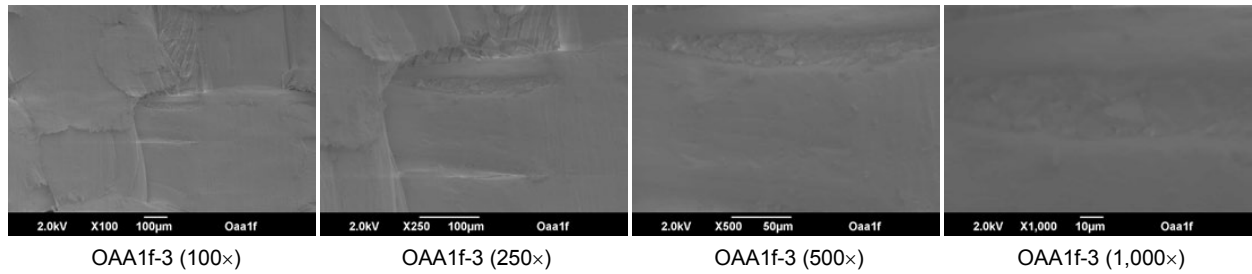


F.3 OAA1f-3

F.3.1 Optical Microscopy

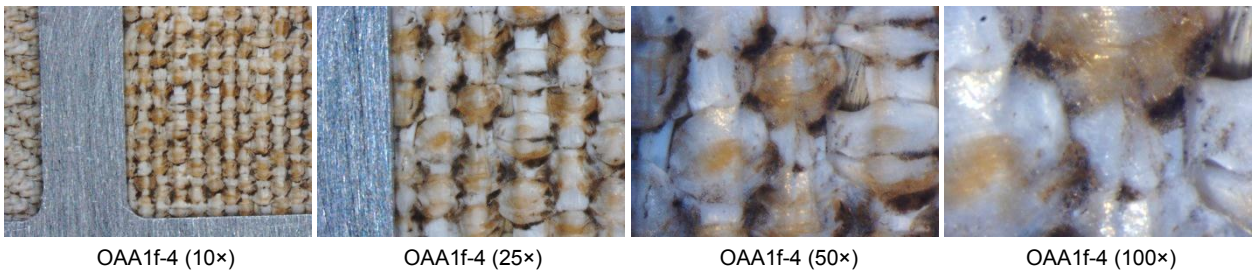


F.3.2 Electron Microscopy

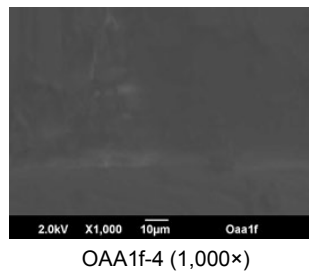
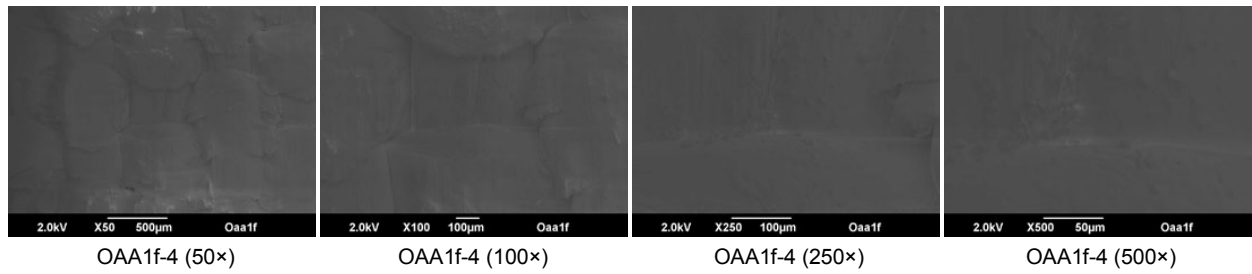


F.4 OAA1f-4

F.4.1 Optical Microscopy

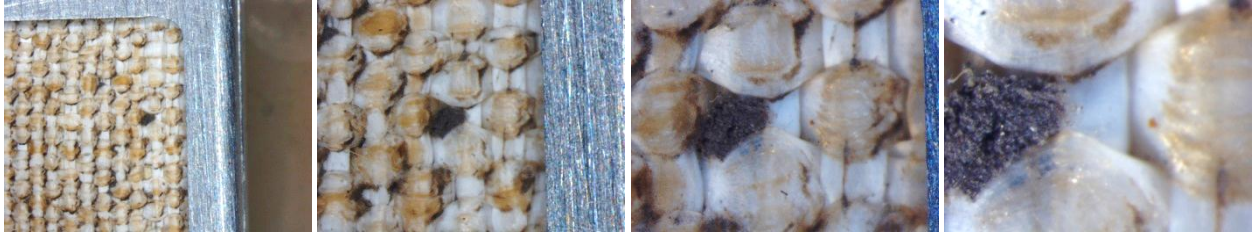


F.4.2 Electron Microscopy



F.5 OAA1f-5

F.5.1 Optical Microscopy



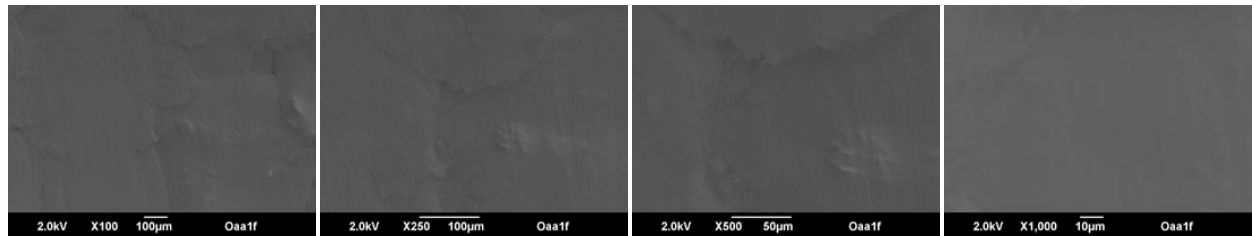
OAA1f-5 (10×)

OAA1f-5 (25×)

OAA1f-5 (50×)

OAA1f-5 (100×)

F.5.2 Electron Microscopy



OAA1f-5 (100×)

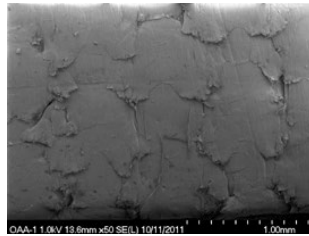
OAA1f-5 (250×)

OAA1f-5 (500×)

OAA1f-5 (1,000×)

F.6 OAA1f-6 (Edge Under Holder)

F.6.1 Electron Microscopy



OAA1f-6 (50×)

References

1. J.R. Gaier, "The Effects of Lunar Dust on EVA Systems During the Apollo Missions," NASA/TM—2005-213610/REV1, 2005.
2. Apollo 12 Technical Crew Debriefing, December 1, 1969, pp. 10-54.
3. J.A. Townsend, et al., "Hubble Space Telescope metalized Teflon[®] FEP thermal control materials: on orbit degradation and post-retrieval analysis", High Performance. Polymers **11(1)** (1999) pp. 81-99.
4. J.A. Dever, et al., "Effects of Radiation and Thermal Cycling of Teflon[®] FEP", High Perf. Polymers **11(1)** (1999) pp. 123-140.
5. J.R. Gaier, et al., "Pre-Flight Characterization of Samples for the MISSE-7 Spacesuit Fabric Exposure Experiment," NASA/TM—2009-215810, 2009.
6. NASA Solicitation Number NNJ09289992R (2009).
7. ASTM Standard Test Method for Tensile Strength and Young's Modulus of Fibers, C 1557-03, Reapproved 2008.
8. M.M. Finckenor (NASA MSFC) *personal communication*.
9. K.K. de Groh, et al., "MISSE 2 PEACE Polymers Atomic Oxygen Erosion Experiment on the International Space Station", Special Issue: High Performance Polymers 20 (2008) pp. 388-409.
10. Lunar Soil Characterization Consortium. Bidirectional reflectance spectra for lunar soils. Available at <http://www.planetary.brown.edu/relabdocs/LSCCsoil.html>, accessed April 2010.

REPORT DOCUMENTATION PAGE			Form Approved OMB No. 0704-0188		
<p>The public reporting burden for this collection of information is estimated to average 1 hour per response, including the time for reviewing instructions, searching existing data sources, gathering and maintaining the data needed, and completing and reviewing the collection of information. Send comments regarding this burden estimate or any other aspect of this collection of information, including suggestions for reducing this burden, to Department of Defense, Washington Headquarters Services, Directorate for Information Operations and Reports (0704-0188), 1215 Jefferson Davis Highway, Suite 1204, Arlington, VA 22202-4302. Respondents should be aware that notwithstanding any other provision of law, no person shall be subject to any penalty for failing to comply with a collection of information if it does not display a currently valid OMB control number.</p> <p>PLEASE DO NOT RETURN YOUR FORM TO THE ABOVE ADDRESS.</p>					
1. REPORT DATE (DD-MM-YYYY) 01-08-2012		2. REPORT TYPE Technical Memorandum		3. DATES COVERED (From - To)	
4. TITLE AND SUBTITLE Post-Flight Characterization of Samples for the MISSE-7 Spacesuit Fabric Exposure Experiment			5a. CONTRACT NUMBER		
			5b. GRANT NUMBER		
			5c. PROGRAM ELEMENT NUMBER		
6. AUTHOR(S) Gaier, James, R.; Waters, Deborah, L.; Jaworske, Donald, A.; McCue, Terry, R.; Folz, Angela; Baldwin, Sammantha; Clark, Gregory, W.; Batman, Brittany; Bruce, John			5d. PROJECT NUMBER		
			5e. TASK NUMBER		
			5f. WORK UNIT NUMBER WBS 368185.01.03.04.04		
7. PERFORMING ORGANIZATION NAME(S) AND ADDRESS(ES) National Aeronautics and Space Administration John H. Glenn Research Center at Lewis Field Cleveland, Ohio 44135-3191			8. PERFORMING ORGANIZATION REPORT NUMBER E-18329		
9. SPONSORING/MONITORING AGENCY NAME(S) AND ADDRESS(ES) National Aeronautics and Space Administration Washington, DC 20546-0001			10. SPONSORING/MONITOR'S ACRONYM(S) NASA		
			11. SPONSORING/MONITORING REPORT NUMBER NASA/TM-2012-217651		
12. DISTRIBUTION/AVAILABILITY STATEMENT Unclassified-Unlimited Subject Categories: 91, 54, and 27 Available electronically at http://www.sti.nasa.gov This publication is available from the NASA Center for AeroSpace Information, 443-757-5802					
13. SUPPLEMENTARY NOTES					
14. ABSTRACT Six samples of pristine and dust-abraded outer layer spacesuit fabrics were included in the Materials International Space Station Experiment-7, in which they were exposed to the wake side low Earth orbit environment (LEO) on the International Space Station (ISS) for 18 months in order to determine whether abrasion by lunar dust increases radiation degradation. The fabric samples were characterized using optical microscopy, field emission scanning electron microscopy, and tensile testing before and after exposure on the ISS. Comparison of pre- and post-flight characterizations showed that wake side LEO environment darkened and reddened all six fabrics, increasing their integrated solar absorptance by 7 to 38 percent. There was a decrease in the ultimate tensile strength and elongation to failure of lunar dust abraded Apollo spacesuit fibers by a factor of four and increased the elastic modulus by a factor of two. The severity of the degradation of the fabric samples over this short exposure time demonstrates the necessity to find ways to prevent or mitigate radiation damage to spacesuits when planning extended missions to the Moon.					
15. SUBJECT TERMS Space suit; Degradation; Low Earth orbits; Lunar dust					
16. SECURITY CLASSIFICATION OF:			17. LIMITATION OF ABSTRACT UU	18. NUMBER OF PAGES 70	19a. NAME OF RESPONSIBLE PERSON STI Help Desk (email:help@sti.nasa.gov)
a. REPORT U	b. ABSTRACT U	c. THIS PAGE U			19b. TELEPHONE NUMBER (include area code) 443-757-5802

